AN INVESTIGATION INTO THE ACTIVATED CARBON-CATALYZED ARSENIC OXIDATION PROCESS

by

Rebecca Lynn Radzinski

A thesis submitted to the Robert M. Buchan Department of Mining

In conformity with the requirements for

the degree of Master of Applied Science

Queen's University

Kingston, Ontario, Canada

(January, 2017)

Abstract

Arsenic is a highly toxic element that is becoming an increasingly more prevalent issue for mining and metallurgical operations. Arsenic is an abundant element in the earth's crust and is commonly associated with metals such as gold, silver, copper, nickel and many others. Arsenic is often oxidized prior to its removal from process streams because the higher oxidation state of arsenic typically offers a more stable solid product. A novel and robust process to oxidize arsenic is activated carbon-catalyzed arsenic oxidation which is a process which uses oxygen, as the only consumable reagent, and activated carbon.

The arsenic oxidation mechanism was explored via cyclic voltammetry, zeta potential measurements, X-ray photoelectric spectroscopy, shake tests, batch tests and continuous column tests. It was determined that hydrogen peroxide is formed on the surface of activated carbon and this aids in the oxidation of arsenic. Adsorption of arsenic species on the activated carbon was a large factor in the investigation. Two mechanisms of arsenic oxidation were theorized and it is believed that they occur simultaneously. The first hypothesized reaction pathway is that As (III) is oxidized when it contacts hydrogen peroxide on the activated carbon surface and is then instantly adsorbed as an As (V) compound. The second hypothesized reaction pathway is that As (III) adsorbs onto the surface of activated carbon and is then oxidized by hydrogen peroxide present in close proximity in the solution to the activated carbon surface. Activated alumina was used instead of carbon during a batch test experiment in order to verify that it is the functional groups of carbon that perform the catalytic ability of activated carbon to oxidize arsenic and not the porous nature of its surface. It was concluded that activated alumina had no ability to oxidize arsenic and therefore it is the functional groups on the carbon surface that provide the oxidative capabilities.

Acknowledgements

I would like to thank my supervisor, Dr. Ahmad Ghahreman, for his guidance throughout my time in graduate studies. His patience, support and advice was greatly appreciated. I would also like to thank Larissa Smith, Larry Steele, Perry Ross and Maritza Bailey for their technical assistance in the laboratory, Gabriele Schatte for her help conducting X-ray photoelectron spectroscopy and Graham Cairns and the Analytical Services Unit for the ICP analysis. Financial support for this work was provided by the Natural Sciences and Engineering Research Council of Canada through a Discovery Grant RGPIN-2015-05718.

A special thanks goes to the Hydrometallurgy Group in the Robert M. Buchan Department of Mining for their unwavering support, valuable discussions and assistance.

Finally, a huge thank you goes to my family and friends who always offered support and encouragement over the course of my research; I couldn't have done it without you!

Table of Contents

List of Figures

List of Tables

Chapter 1

Introduction

1.1 General Overview

The purpose of this thesis is to investigate a novel process for the treatment of acidic arsenical process streams resulting from mining and metallurgical operations. The process studied in this thesis uses oxygen gas in the presence of activated carbon to catalyze the oxidation of arsenite to arsenate with high oxidation efficiencies. This process was developed and patented by Barrick Gold Corporation in 2014 (Choi, Ghahremaninezhad, & Ahern, 2014a).

Arsenic is a toxic element that is found in abundance throughout the earth's crust. Arsenic is often found in sulphide orebodies with elements rich in copper and/or gold. The two most commonly found oxidation states of arsenic are the trivalent (arsenite) and pentavalent (arsenate) state. For the purpose of remediation and arsenic removal it is most often necessary to oxidize arsenic to its pentavalent form.

Arsenic can enter water aquifers due to geogenic and anthropogenic causes. The World Health Organization guidelines state that levels in drinking water should not exceed 10 µg/L arsenic (Basha, Selvi, Ramasamy, & Chellammal, 2008; Bora, Gogoi, Baruah, & Dutta, 2016; Leist, Casey, & Caridi, 2000; Smedley & Kinniburgh, 2002). Many technologies to remove arsenic at low concentrations have been studied, but they do not necessarily apply to the mining industry as arsenic concentrations in metallurgical process streams can exceed 20 g/L in smelter operations. Canada has strict regulations which govern the concentration of hazardous materials in mining effluents. According to the Metal Mining Effluent Regulations in Canada the maximum monthly average of arsenic in an effluent stream is 0.50 mg/L, the maximum concentration in a composite sample is 0.75 mg/L and the maximum concentration in a grab sample is 1.00 mg/L (Canada, 2015).

The process that Barrick has developed and patented is now in use in industry. The use of activated carbon as a catalyst for arsenic oxidation for a large-scale operation is novel because in the past and present activated carbon was used as an adsorbent to remove impurities in drinking water.

Activated carbon-catalyzed arsenic oxidation is an effective method to oxidize arsenic but there continues to be a lack of information on the exact mechanisms of how the activated carbon and oxygen work together to oxidize arsenic. It was hypothesized that a strong oxidant is formed on the activated carbon surface when oxygen is present. This thesis investigates the activated carbon surface during the process as well as the factors affecting the oxidation and adsorption of arsenic in the system specified.

1.2 Research Objectives

The main objective of this research is to investigate how the activated carbon, oxygen and arsenic interact together to oxidize arsenic at a high efficiency. Topics studied include the catalytic abilities of activated carbon, oxidant formation, activated carbon surface chemistry, adsorption isotherm models and factors affecting the initial arsenic oxidation, arsenic adsorption and oxidant formation.

1.3 Thesis Organization

This thesis is divided into seven chapters with Chapter 1 being a brief and general introduction to this thesis. This chapter outlines and emphasizes the significance and need for the research conducted.

Chapter 2 is a literature review which gives an understanding of the importance of oxidizing arsenic to remove it from mining and metallurgical effluent streams. Topics in Chapter 2 include: the effect of arsenic speciation on toxicity, mobility, solubility and stability of arsenic compounds, activated carbon and its chemistry, previous work completed on the topic of activated carbon-assisted arsenic oxidation and industrially employed arsenic immobilization strategies.

Chapter 3 explains the main experimental methods and apparati used throughout the test work. Raw material preparation is described in regards to pretreating activated carbon for each test and creating solutions from the reagents required for the respective tests.

Chapter 4 presents the fundamental studies conducted for the thesis and discusses the preliminary findings. This chapter is focused on learning more about the surface chemistry of activated carbon when in contact with an acidic arsenite solution and oxygen. Cyclic voltammetry is used to highlight the catalytic properties of activated carbon. The surface of carbon is explored via studying oxidant formation on the carbon surface and its desorption as well as investigating the speciation of arsenic that has adsorbed on the activated carbon surface. X-ray photoelectron spectroscopy experiments are discussed in regards to the nitrogen, oxygen, carbon, sulphur and arsenic present in the system. Finally, arsenic adsorption is modeled to fit two adsorption isotherms.

Chapter 5 details the findings of the batch tests conducted. The first part of the chapter focuses on how changing the arsenic concentration and activated carbon pulp density affects the oxidation of arsenic. Next, the effect of oxygen flow rate and oxygen concentration is presented. Finally, the oxidizing effectiveness and adsorbent capacity of activated carbon is compared against another industrial adsorbent: activated alumina.

Chapter 6 presents preliminary findings on the effect of introducing ferrous and cupric ions into the system. This chapter focuses solely on continuous column tests.

Chapter 7 includes concluding remarks about the findings presented throughout the thesis and presents recommendations for future studies in this research area.

Chapter 2

Literature Review

2.1 Introduction

Arsenic, chemical symbol "As," is the 33rd element on the periodic table and is classified as a metalloid. Arsenic, which has a large history of past uses, is one of the world's prevalent contamination issues. Arsenic chemistry is quite complex due to a variety of factors such as its various oxidation states, metalloid properties and interactions with other species.

In the past arsenic trioxide (As_2O_3) was used for wood preservation; however, its usage was stopped in 2003 due to public health concerns. Global arsenic industrial consumption has declined as a result of agricultural industries no longer using arsenic-based pesticides, herbicides and fungicides (Fujita, Taguchi, Kubo, Shibata, & Nakamura, 2009). Current uses for arsenic include: gallium-arsenide semi-conductors, an additive to lead car batteries and an anti-friction agent in bearings (Long, Peng, & Bradshaw, 2012). As global arsenic consumption for niche industries decreased the arsenic production increased; between the years of 2000 to 2012 arsenic production had risen by 20 tonnes/year to 60 tonnes/year and between the years of 2004-2012 arsenic consumption had decreased by 20 tonnes/year to 5 tonnes/year (González-Contreras, Weijma, & Buisman, 2012). Due to the small commercial demand for arsenic, the majority of arsenic removed from mining and metallurgical operations must be stabilized and stored in a safe manner in order to decrease the environmental risks associated with arsenic mobilization and toxicity (D. Zhang, Yuan, Wang, Jia, & Demopoulos, 2015).

Arsenic is an abundant element in the earth's crust and is found in more than 300 minerals. The average concentration of arsenic on earth is approximately 5 ppm (Riveros, Dutrizac, & Spencer, 2001). Toxic and mobile forms of arsenic can be liberated from minerals due to geogenic or anthropogenic activities. The scope of this review is limited to the discussion of arsenic chemistry and speciation, activated carbon

and related properties, arsenic mobilization in the mining and metallurgical industries, and arsenic immobilization methods.

2.1.1 Sources of Arsenic

Arsenic is the 20th most abundant element in the earth's crust and is typically found in conjunction with sulphur-rich rocks and minerals. Arsenic can be found as part of various mineral groups such as arsenides, sulphides, oxides and arsenates (Riveros et al., 2001).

The breakdown of the known arsenic compounds is approximately: 60% arsenates, 20% sulphides/sulphosalts, 10% oxides, and the remainder are arsenite, arsenides, native arsenic and/or metal alloys (Drahota & Filippi, 2009).

Table 1: The most common arsenic-containing minerals (Riveros et al., 2001)

Type	Mineral	Formula
Arsenides	Nickeline	$NiAs_2$
	Safflorite	$(Co,Fe,Ni)As_2$
	Skutterudite	$CoAs_3$
Arsenates	Oliverite	$Cu_2(AsO_4)OH$
	Scorodite	$FeAsO_4{\cdot}2H_2O$
Oxides	Arsenolite	As_2O_3
	Claudite	As_2O_3
Sulfides and Sulfosalts	Arsenopyrite	FeAsS
	Arsenical pyrite	$Fe(As,S)_2$
	Cobaltite	CoAsS
	Enargite	Cu_3AsS_4
	Orpiment	As_2S_3
	Realgar	As_4S_4
	Tennantite	$(Cu,Fe)_{12}As_4S_{13}$

The most commonly found arsenic mineral is arsenopyrite. Other common arsenic-bearing minerals include orpiment (As_2S_3), realgar (As_4S_4), niccolite (NiAs), cobaltite (CoAsS), tennantite ($Cu12As_4S_{13}$)

and enargite (Cu_3AsS_4). High concentrations of arsenic-bearing minerals are often located with transition metals and cadmium, lead, silver, gold, antimony, phosphorus, tungsten and molybdenum (Smedley & Kinniburgh, 2002). Enargite and tennantite are minerals which are processed for copper and contain arsenic (Long et al., 2012). Due to similar flotation characteristics of the two minerals to other sulphide minerals, the arsenic-containing stream from the flotation cells goes to the smelter where the arsenic must be disposed of according to strict regulations (Long et al., 2012).

The smelting of copper, lead, zinc and nickel ores which contain arsenic is the largest anthropogenic contributor of arsenic, with copper smelting accounting for 80% of the emissions (Bissen & Frimmel, 2003b). Arsenic contamination of groundwater and soils due to mining processes occur globally in places such as Thailand, Ghana, Zimbabwe, South Africa, England, Greece, Mexico, Canada and the United States of America (Bissen & Frimmel, 2003b). Other pyrometallurgical activities such as roasting and converting generate As_2O_3 or As_2S_3 and create a need for arsenic removal and storage (Riveros et al., 2001). The long-term stability of As_2O_3 has been cause for concern because that form of arsenic is extremely water soluble and toxic (Filippou & Demopoulos, 1997). 260 000 tonnes of 76%As arsenic trioxide dust from 50 years of operations at the Giant Gold Mine in Canada is stored underground near the old mine (Riveros et al., 2001). Other anthropogenic sources include waste from other industries, arsenic from agriculture (pesticide production and usage), glass manufacturing, wood treatment and coal and oil production and processing (Cheng, Hu, Luo, Xu, & Zhao, 2009).

Natural sources of arsenic include weathering from naturally occurring minerals (Cheng et al., 2009), forest fires and volcanic eruptions (Bissen & Frimmel, 2003b). Naturally occurring arsenic in water aquifers poses a large problem for people living in India (West-Bengal), Vietnam, Mexico, Argentina, Chile, Hungary, Romania and parts of the United States (Bissen & Frimmel, 2003b). Arsenic-contaminated water sources are estimated to affect 144 million people globally (Clancy, Hayes, & Raskin, 2013). The World Health Organization guideline for total arsenic in drinking water is 10 µg/L; this was

lowered from 50 µg/L in 1993 (Basha et al., 2008; Bora et al., 2016; Leist et al., 2000; Smedley & Kinniburgh, 2002). The concentration of arsenic in mineral processing effluent streams is many orders of magnitude larger than that in naturally contaminated water sources. For example, copper electrorefineries may implement a bleed stream to maintain an arsenic concentration of less than 20 g/L (Riveros et al., 2001). Techniques to remove arsenic from wastewater at low concentrations may not be as effective at higher concentrations (Leist et al., 2000).

2.1.2 Arsenic Speciation

Arsenic can exist in different oxidative states and each state has its own characteristics such as toxicity, mobility and ability to precipitate. Arsenic is redox-sensitive (Cheng et al., 2009) and its oxidation state is affected by the acidity of the environment (pH) and oxidation-reduction potential (Eh) of the system (Gallegos-Garcia, Ramírez-Muñiz, & Song, 2012). The main oxidation states of arsenic are -3, 0, +3 and +5 (Cheng et al., 2009). Arsenic is typically found as inorganic oxyanions of arsenite (As^{3+}) or arsenate (As^{5+}) (Gallegos-Garcia et al., 2012). Arsenic species can be either organic or inorganic, and typically the inorganic soluble arsenic species are more toxic than soluble organic arsenic compounds (Mandal & Suzuki, 2002).

Figure 2-1 shows the dominant species within the water line boundaries for As-H_2O at 25 ºC and 1 bar total pressure. As shown in Figure 2-1, in oxidative conditions and low pH, arsenate is the dominant species. Generally, in oxidizing environments arsenate is the prevalent form of arsenic, and in reducing environments arsenite the dominant arsenic species.

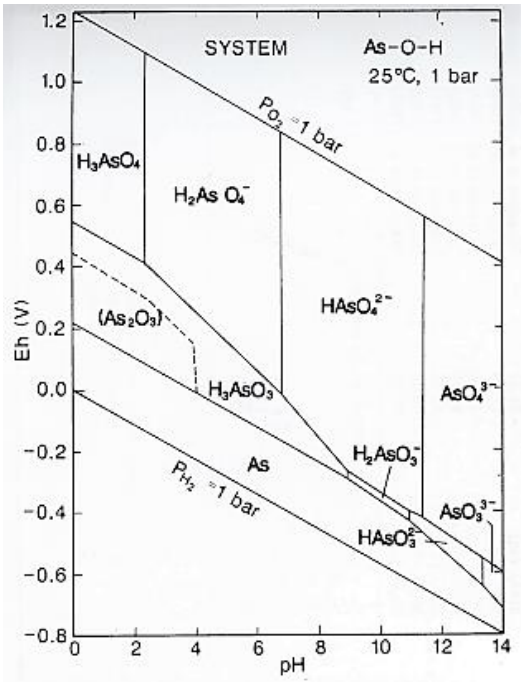

Figure 2-1: Eh-pH diagram for the system As–H_2O at 25 ºC and 1 bar (Brookins, 1988).

Arsenical waste from the smelting and other mineral processing is typically highly acidic (Cui, Du, Xiao, Yi, & Du, 2014). As mentioned previously, the arsenic concentration in effluent streams can be quite high. In a paper by J. Cui et al. (2014) the arsenic-bearing sulphuric wastewater from a non-ferrous metal plant in Hubei, China had a pH of less than 1 and between 7.4-14.7 g/L of arsenic.

2.1.2.1 Toxicity

The toxicity of arsenic varies between the arsenic oxidation states: arsine is more toxic than arsenite, which is more toxic than arsenate (Vaughan, 2006). Arsenite and arsenate, though both toxic, have different biological effects. Ingestion is the main route of exposure but inhalation can also cause toxic effects (Gallegos-Garcia et al., 2012). Arsenic in an inorganic form is a Group I carcinogen (Ng, Wang, & Shraim, 2003). Ingesting arsenic can cause bladder cancer, renal cancer, liver cancer and skin cancer, whereas inhaling arsenic can cause lung cancer (Bissen & Frimmel, 2003b). Chronic illnesses apart from cancer include: cardiovascular, pulmonary, immunological, neurological and endocrine disorders (Gallegos-Garcia et al., 2012). Both arsenite and arsenate inhibit functions relating to energy in the

mitochondria (Bissen & Frimmel, 2003b). Arsenic is harmful because it inhibits the ability for DNA to repair itself should damage occur. Arsenate can act as phosphorus in oxidative phosphorylation, thereby hindering the production of ATP (adenosine triphosphate), and arsenite deactivates enzymes by attaching to sulphhydryl groups (Bissen & Frimmel, 2003b). However, when soluble arsenate enters a human it is reduced to arsenite and is converted to an organic methylated arsenic species so that it can be excreted (Lengke, Sanpawanitchakit, & Tempel, 2009).

2.1.2.2 Mobility

The mobility of arsenic is dependent on the concentration of arsenic, other species present (eg.- metal cations, clay, etc.) the pH and Eh of the environment (Bissen & Frimmel, 2003b). Arsenic contamination is of great concern due to its high mobility under a large range of pH and Eh (Smedley & Kinniburgh, 2002). Arsenite in groundwater is shown to move 5-6 times faster than arsenate in an oxidizing environment at pH 5.7 (Smedley & Kinniburgh, 2002). In neutral conditions (pH 6.9) arsenite still moved faster than arsenate, but arsenate moved faster than it did in oxidizing conditions (Smedley & Kinniburgh, 2002). At a pH of 8.3 in reducing conditions both arsenite and arsenate moved quickly through the column which represented a groundwater system (Smedley & Kinniburgh, 2002).

2.1.2.3 Solubility

Both arsenite and arsenate are soluble in water, however arsenite is thought to be more toxic and soluble than arsenate in nature (Yang, Zhang, Deng, & Ma, 2013). The difference in arsenite and arsenate solubility is that arsenate will precipitate out of solution with the addition of metal cations (Ritcey, 2005). The metal-arsenate precipitates generally follow the form $Mn(AsO_4)_mdH_2O$ (Ritcey, 2005). The stability of the precipitate is dependent on the cation used to form the precipitate and the conditions at which the precipitate is maintained (Riveros et al., 2001). For arsenic fixation, arsenic is typically in the pentavalent state as pentavalent arsenic-containing precipitates exhibit more stability compared to those with trivalent arsenic.

2.1.3 Activated-Carbon Assisted Oxidation of Arsenic: Patent by Barrick Gold Corporation

2.1.3.1 Patent Summary

A patent was filed by Barrick Gold Corporation which describes a novel and robust process for oxidizing arsenic (and/or antimony)[1] as well as their removal from process and waste streams primarily from metallurgical processes (Choi et al., 2014a). In the United States the patent is filed under US 20140356261 A1. This patent has been published in various countries and consequently it is also published under the following codes: CA2912132A1, EP3004406A1, WO2014191833A1.

There are many claims stated in the patent claim (Choi et al., 2014a). A brief summary of the claims and processes patented which are most pertinent to the research presented in this thesis are as follows: an acidic stream containing arsenite and/or antimony will be almost completely oxidized from the trivalent to pentavalent state when contacted with both oxygen and a carbon source. The pH of the stream cannot exceed 2.5 in this specific process, and the oxidation-reduction potential must be higher than 350 mV vs. Ag/AgCl electrode. The liquid solution containing arsenic is then separated from the carbon. The separated solution predominantly containing arsenate is then mixed with a solution containing ferric ions in order to precipitate synthetically produced scorodite. Scorodite is a ferric arsenate with the chemical composition of $FeAsO_4 \cdot 2H_2O$. The precipitated scorodite is then separated from the liquid stream (Choi et al., 2014a).

2.1.3.2 Previous Work Completed on Activated Carbon-Catalyzed Arsenic Oxidation

Previous work under the Barrick patent has been published at the 2014 Conference of Metallurgists in Vancouver, Canada (Choi, Ghahremaninezhad, & Ahern, 2014b).

[1] This thesis is only concerned with the arsenic oxidation associated with this process and excludes antimony in experiments.

The first finding presented showed that in batch experiments an oxidation of over 93.5% was accomplished in systems when other metal ions, such as copper and both oxidation states of iron, are present. In these systems the oxygen sparge rate was 0.5 L/L of slurry/min. In the cases where ferric ions are in solution the arsenic was able to be directly precipitated as scorodite (Choi et al., 2014b).

Next, tests using a teflon column filled with 259 g of activated carbon was used to investigate the oxidation of arsenic in order to minimize the attrition of carbon that was occurring in batch reactors due to the rotation of the slurry. The arsenic concentration in the feed stream was 10 g/L arsenite, the arsenic acid feed rate was 0.5 mL/min and the oxygen rate was 0.5 L/min. During the first few days of the test the arsenite concentration in the column outlet stream was about 0.1 g/L which signifies a 99% oxidation efficiency (Choi et al., 2014a).

2.2 Activated Carbon

Activated carbon has a long history in metallurgical practices. In 1880, prior to the patent describing cyanidation as an approach to gold extraction, Davis patented a process which recovered gold from chlorination leach liquors via wood charcoal (McDougall & Hancock, 1981). Since then, activated carbon/charcoal use has been heavily researched and used in numerous industries due to its physical and chemical properties. Apart from metallurgical industries, activated carbon can be used to provide safe drinking water when used as part of a filtration system due to its adsorption capabilities.

2.2.1 Physical Properties

Activated carbon is an encompassing term for porous carbon materials that are not uniquely characterized by a specific structural formula or by chemical analysis, but are instead characterized by their adsorptive capabilities (McDougall & Hancock, 1981).

Activated carbon and graphite share common characteristics but differ in their structures. X-ray diffraction (XRD) shows that, structurally speaking, activated carbon is similar to graphite but differs

with respect to the highly ordered structure of graphite and disordered structure of activated carbon (Marsden & House, 2006; McDougall & Hancock, 1981). Figure 2-2 illustrates the ideal structure of graphite, which consists of sheets of hexagonal carbon that stay together due to Van der Waals forces that maintain the carbon layers at a distance of 0.335 nm (McDougall & Hancock, 1981). The structure of graphite is described as turbostatic (McDougall & Hancock, 1981). Unlike graphite, activated carbon contains small regions of crystalline/graphite structures that exist randomly oriented within disordered and cross-linked regions of hexagonally bonded carbons (Marsden & House, 2006). The dimensions of crystallites (crystalline structures) are dependent on temperature; however, they are typically 9-12 Å high and 20-23 Å wide which is approximately three layers high and nine carbon hexagons wide (Marsden & House, 2006).

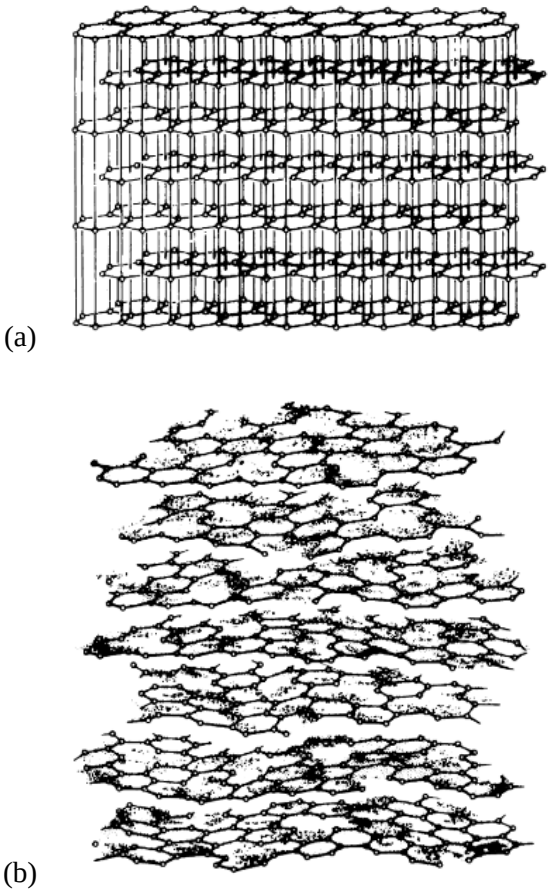

Figure 2-2: (a) Ideal crystalline structure of graphite (b) structure of activated carbon (Bokros, 1969).

The porous structure of activated carbon is produced by introducing the carbon to an oxidant at high temperatures (800-1100 °C) which reacts with the highly reactive carbon to produce carbon dioxide and carbon monoxide, consequently leaving an exceptionally porous material with a large surface area of 600-1500 m^2/g of carbon (McDougall & Hancock, 1981). The type of oxidizing reagent used will affect the size of the pores. For example, activation via carbon dioxide will create predominantly micropores (characteristic size less than 1.6 nm) with small pore volumes, whereas oxygen as an activation agent will not produce as porous a material due to pore blockage by surface oxides (Marsden & House, 2006).

Typical coconut shell activated carbon contains an ash content of 2-4% and a Brunauer–Emmett–Teller (BET) surface area of 900-1000 m^2/g (Marsden & House, 2006).

2.2.2 Chemical Properties

Oxygen preferentially sorbs onto the activated carbon surface compared to other elements and the functional groups formed on the surface affect the carbon's reactions with other compounds, the carbon's wettability and the electrical and catalytic capabilities (Marsden & House, 2006). It is estimated that 90% of the oxygen present on the carbon surface exists as a variant of a functional group and the remaining oxygen forms neutral bonds in ether bridges (Marsden & House, 2006). The disorderliness of the arrangement of carbon lattices in activated carbon, mainly graphene layers, allows for functional groups which mainly contain oxygen to be concentrated at the edges of broken graphite rings (Barkauskas & Dervinyte, 2004; McDougall & Hancock, 1981). Carboxyl, phenol, quinone, hydroxyl groups and ester groups (including cyclic peroxides) have been identified on the carbon surface (Marsden & House, 2006; McDougall & Hancock, 1981). The structures of these oxide complexes that exist on the carbon surface are shown in Figure 2-3.

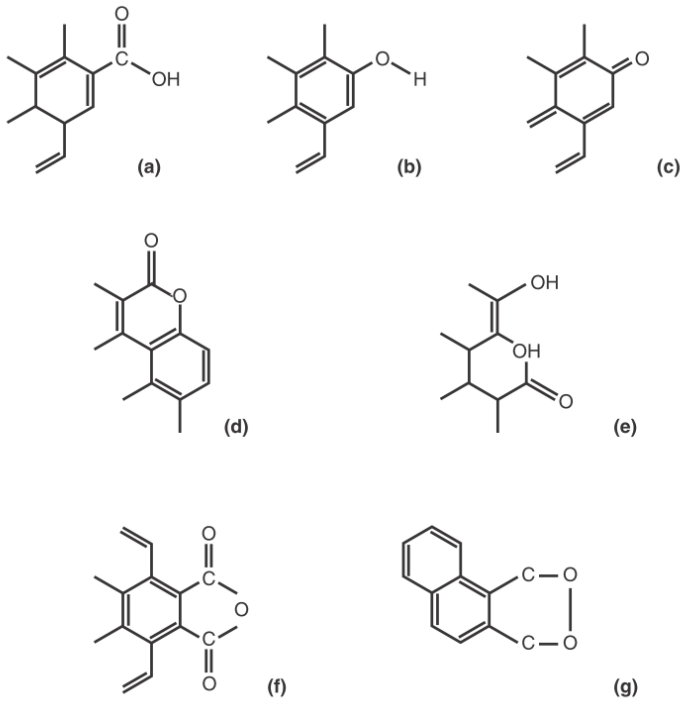

Figure 2-3: Surface oxide structures: (a) carboxylic acid, (b) phenolic hydroxyl, (c) quinone-type carbonyl groups, (d) normal lactones, (e) fluorescein-type lactones, (f) carboxylic acid anhydrides, and (g) cyclic peroxides (Marsden & House, 2006).

The surface charge on the carbon is dependent on the pH of the solution in which the carbon is suspended. Electro-kinetic effects heavily influence the interactions of particles suspended in solution, such as activated carbon, and the bulk solution (Carlson & Kawatra, 2013). Zeta potential, ζ, is a measure of electro-kinetic effects which is quantified as the energy difference between the surface of a particle suspended in solution and the bulk of the liquid (Carlson & Kawatra, 2013).

A model used to describe the phenomena of zeta potential is the electrical double layer model. A simplified schematic depiction of the model can be seen in Figure 2-4. The double layer contains two layers of ions separated by a shear plane: the Stern Layer and the Diffuse Layer (Carlson & Kawatra, 2013). The shear plane is the boundary that separates the ions that travel with the particle and the ions that exist in the bulk solution (Carlson & Kawatra, 2013).

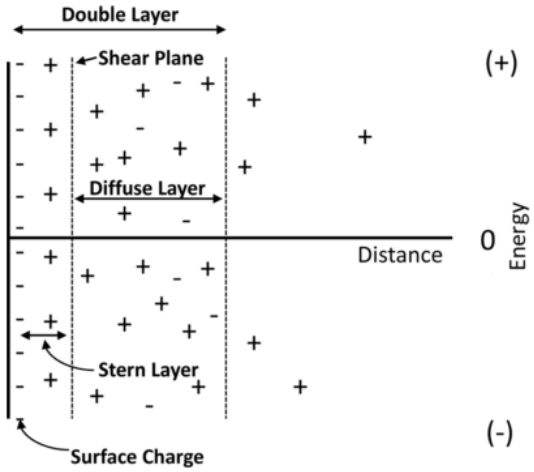

Figure 2-4: Schematic diagram of a particle suspended in a bulk solution which shows the surface charge, bulk solution charge and the respective layers (Carlson & Kawatra, 2013).

The zeta potential of activated carbon in solution is positive in acidic conditions up to a pH value of 6.2 and negative in subsequent higher pH values (Dai, 1994); however, different types of carbon will have a different point of zero charge (PZC). Figure 2-5 shows an activated carbon with a PZC of 6.2, but values as low as 2.5 have been reported for activated charcoal (Eguez & Cho, 1987). The reason for the discrepancy in PZC values is due to the oxidation of carbon (Kelebek, Salman, & Smith, 1982; Laskowski, 2001). The zeta potential will affect which functional groups can exist on the carbon surface and which ions will preferentially sorb onto the carbon. The zeta potential and PZC of activated carbon can be seen in Figure 2-5.

The zeta potential with respect to pH is dependent on the ionic strength of solution however the change in zeta potential with respect to ionic activity is more pronounced in basic solutions (Gustafsson, Mikkola, Jokinen, & Rosenholm, 2000). Figure 2-6 illustrates the effect of ionic activity on the zeta potential.

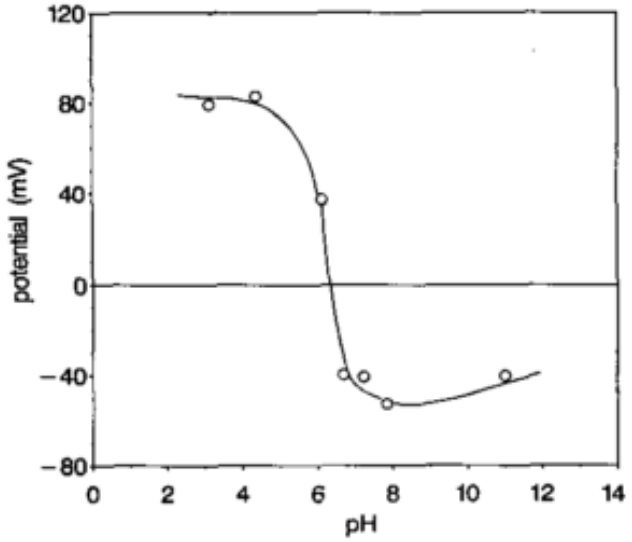

Figure 2-5: Effect of pH of the zeta potential of activated carbon in a solution (Dai, 1994).

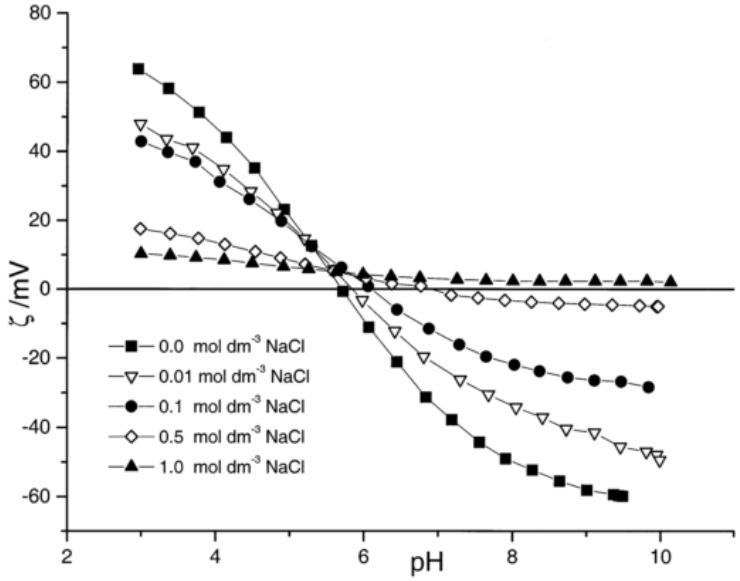

Figure 2-6: Zeta potential of anatase as a function of pH for various NaCl concentrations (Gustafsson et al., 2000).

2.2.3 Adsorptive Properties

Adsorption is defined as the tendency for molecules in a bulk fluid to attach to the surface of a solid due to attractive forces (Ruthven, 2001). Adsorption can be characterized into two categories: physical

adsorption where the forces are mainly weak van der Waals interactions or chemisorption where electrons are transferred between the absorbent and the solution (Ruthven, 2001). Table 2 summarizes the differences between physical adsorption and chemisorption for various parameters related to adsorption.

Table 2: Parameters of physical adsorption and chemisorption (Ruthven, 2001)

Parameter	Physical Adsorption	Chemisorption
Heat of adsorption (-ΔH)	Low, <1:5 or 2 times latent heat of evaporation	High, >2 or 3 times latent heat of evaporation
Specificity	Non specific	Highly specific
Nature of desorbed phase	Monolayer or multilayer, no dissociation of adsorbed species	Monolayer only may involve dissociation
Temperature range	Only significant at relatively low temperatures	Possible over a wide range of temperatures
Forces of adsorption	No electron transfer, although polarization of sorbate may occur	Electron transfer leading to bond formation between sorbate and surface
Reversibility	Rapid, nonactivated, reversible	Activated, may be slow and irreversible

Generally, selectivity in a physical adsorption system depends on differences in the equilibrium or kinetics, but most of the separation processes are dependent on the selectivity in regards to equilibrium (Ruthven, 2001). Molecular sieve adsorbents, such as carbon molecular sieves, zeolites or zeolite analogues are typically selective with respect to kinetics (Ruthven, 2001).

The pore size distribution of the adsorbent will affect the adsorptive properties. There are narrow or broad pore size distributions (of which activated carbon and activated alumina are broad) as well as polar or nonpolar surfaces (of which activated carbon is nonpolar and activated alumina is polar) (Ruthven, 2001). Both activated carbon and activated alumina are amorphous adsorbents (Ruthven, 2001).

Adsorption isotherms help characterize and explain the adsorptive characteristics of adsorbents. Two commonly used adsorption isotherms are the Langmuir and Freundlich isotherms. The constants from the two models indicate the sorption capacity of the material under investigation (Payne & Abdel-Fattah,

2005). The isotherm models may vary within a type material depending on how the material was produced and what its main components are. For example, one study compared the results of fitting the Freundlich isotherm to different activated material and it was determined that the activated carbon in a previous study was modelled differently than the activated carbon investigated in their study (Chuang et al., 2005), which can be seen in Figure 2-7.

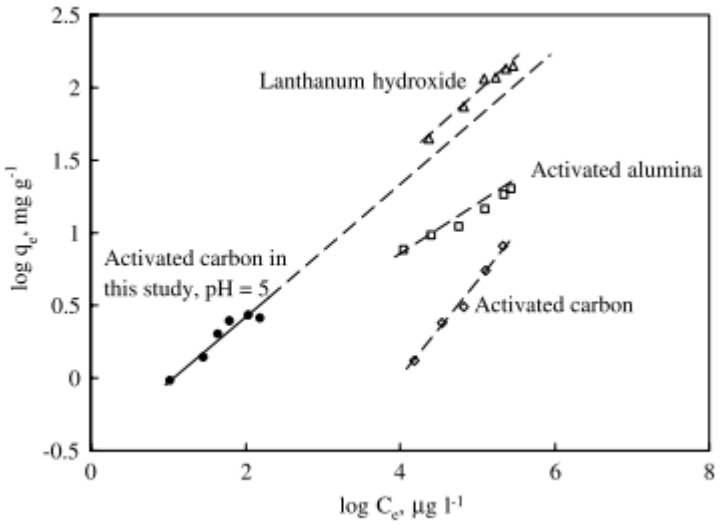

Figure 2-7: Adsorption isotherms of arsenate on various adsorbents (Chuang et al., 2005).

Granular activated carbon adsorption studies often have contradictory conclusions to other studies in regards to adsorptive capacity parameters (Vidic & Suidan, 1991). Activated carbon is a complex material. One study investigated the adsorbance of arsenite verses arsenate on activated carbon. In the study the magnitude of the heat of adsorption suggested that arsenite adsorption is due to weak van der Waals forces and that the adsorbance of arsenite is not changed between a pH of 0.16-3.5 while arsenate adsorption is decreased when the pH is lowered below a pH of 2.35 (Eguez & Cho, 1987).

2.3 Adsorption Isotherms

The Langmuir adsorption isotherm was developed to characterize the adsorption of gases onto activated carbon (Foo & Hameed, 2010). The Langmuir model has three assumptions: (1) the adsorption occurs

only at the surface of the solid and is comprised of a monolayer of adsorbate, (2) active sites may only have one adsorbed molecule and there are no interactions between adjacent adsorbed molecules and (3) the active sites are all equal (Foo & Hameed, 2010; Rennie, 2016). The Langmuir isotherm's main limitation is that in reality the interactions between adjacent adsorbed species are not negligible (Rennie, 2016). Past studies indicate that the Langmuir adsorption isotherm can be used to characterize activated carbon-related adsorption in certain situations (Barkauskas & Dervinyte, 2004; Payne & Abdel-Fattah, 2005). The Langmuir isotherm is described in Equation 1 (Payne & Abdel-Fattah, 2005). Table 3 summarizes the nomenclature for the Langmuir and Freundlich isotherm models.

$$\mathbf{q_e} = \frac{\mathbf{X_m K_L C_e}}{\mathbf{1 + K_L C_e}} \qquad \textbf{Equation 1}$$

The Langmuir isotherm can be linearized in four variations in order to plot different parameters (Foo & Hameed, 2010).

Table 3: Isotherm nomenclature, adapted from Payne and Abdel-Fattah (2005)

Isotherm	Parameter	Description
Langmuir	C_e	The concentration of the adsorbate in solution at equilibrium [mg/L]
	K_L	The Langmuir constant [L/mg]
	q_e	Mass of adsorbate per mass of adsorbant at equilibrium [mg/g]
	X_m	Mass of solute adsorbed per mass of adsorbant [mg/g]
Freundlich	q_e	Mass of adsorbate per mass of adsorbant at equilibrium [mg/g]
	C_e	The concentration of the adsorbate in solution at equilibrium [mg/L]
	K_f	Freundlich constant [mg/g]
	n	Freundlich constant [greater than 1]

The Freundlich adsorption isotherm is a more complex model compared to the Langmuir isotherm. The underlying theory of the Freundlich model is that adsorption occurs on non-uniform active sites. If the

constant ‘n’ is less than one then the model does not fit well to the system under investigation (Payne & Abdel-Fattah, 2005). Studies have indicated that anion adsorption typically follows the Langmuir model whereas adsorption involving cations often follows the Freundlich model (Payne & Abdel-Fattah, 2005). The Freundlich adsorption isotherm is used to describe multi-layer adsorption on a heterogeneous surface (Foo & Hameed, 2010). The governing equation for the Freundlich model is written as Equation 2 (Foo & Hameed, 2010; Payne & Abdel-Fattah, 2005) and the parameters are described in Table 3.

$$q_e = K_f C_e^{\frac{1}{n}} \qquad \textbf{Equation 2}$$

Many more isotherms exist but the two models described above are two common models investigated in the literature.

2.4 Arsenic Mobilization in the Mining, Mineral Processing and Metallurgical Operations

As mentioned earlier, there are many sources of arsenic from various industries – this section focuses on arsenic mobilization resulting from mining, mineral processing and metallurgical operations. It is estimated that anthropogenic sources of arsenic account for 70% of the global atmospheric arsenic (Smedley & Kinniburgh, 2002). There are five factors affecting the mobility of arsenic: (1) redox reactions, (2) adsorption and desorption, (3) ion exchange, (4) precipitation and dissolution, and (5) biological activity (Cheng et al., 2009).

2.4.1 Mining Operations and Mineral Processing

The mining of sulphidic ores can potentially lead to acid mine drainage (AMD) issues and elevated dissolved arsenic in water (Lengke et al., 2009). AMD is controlled by the hydrology, geology and geochemistry of the surrounding area (Cheng et al., 2009). AMD can occur as a result of old mine drainage tunnels and tailings and this poses issues to aquatic life, ground water and connected bodies of water (Cheng et al., 2009).

Mineral processing of arsenic-bearing ores can also mobilize the originally stable arsenic. As an example, during flotation tennantite and enargite (two copper bearing arsenosulphides) have similar floating characteristics as other copper sulphide ores so the arsenic-containing concentrate from the float goes to the smelter where arsenic is then volatilized (Long et al., 2012). Smelters are becoming increasingly stricter about the type of concentrate they process as they prefer to have a smaller concentration of arsenic so that disposal of the arsenic by-product is not as large an issue (Long et al., 2012).

2.4.2 Pyrometallurgical Activities

Pyrometallurgical activities such as roasting, converting and smelting create arsenic trioxide dust. Smelter and fossil-fuel activities create As_2O_3 which is an arsenite compound (Riveros et al., 2001). If the arsenic trioxide is in the form of a flue dust it can be stockpiled (Filippou & Demopoulos, 1997). 260 000 tonnes of As_2O_3 have been stored underground at the Giant Gold Mine in Canada and there is concern surrounding the solubility and mobilization of this dust (Riveros et al., 2001). Arsenic is volatilized as As_2O_3 or As_2S_3 (D. Zhang et al., 2015) and captured in an electrostatic precipitator or wet gas scrubbers so that the dust can then be treated (Riveros et al., 2001). The oxidation of arsenic-bearing sulphide minerals releases arsenic and sulphates, as can be seen by the Equation 3 (Yang et al., 2013):

$$\mathbf{4FeAsS + 13O_2 + 6H_2O \rightarrow Fe^{2+} + 4H_3AsO_4 + 4SO_4^{2-}} \qquad \textbf{Equation 3}$$

Coal processing can produce high concentrations of arsenic in process streams (Ng et al., 2003). Although the arsenic concentration in coal is typically low, levels of 35 000 mg/kg can be found (Ng et al., 2003; Vaughan, 2006). Locations that use arsenic-bearing coal for fuel, such as India and Czechoslovakia, face arsenic contamination in the environment (Ng et al., 2003).

As of 2010 the limit on arsenic in copper concentrates for smelting is 0.5 wt%, and it is hypothesized that this limit will be lowered in the future to 0.3 wt% (Safarzadeh, Moats, & Miller, 2012). Penalties are incurred by the company operating the smelter if the amount of arsenic entering the smelter is above 0.2 wt% arsenic with a penalty of 3 USD/kg arsenic (Peacey, Gupta, & Ford, 2010).

The copper industry faces issues regarding arsenic immobilization as arsenic is a main element in copper-bearing sulphide minerals such as enargite and tennantite, Cu_3AsS_4 and $Cu_{12}As_4S_{13}$, respectively (Filippou, St-Germain, & Grammatikopoulos, 2007). Arsenic-bearing copper sulphides can also be found in conjunction with lead sulphides which can change the processing chemistry (Johto & Taskinen, 2014). Typically arsenic-bearing sulphidic ore is roasted which consequently oxidizes arsenic species to arsenic oxides. Recently there have been studies on the As_2S_3-Cu_2S-PbS phase diagram to investigate if there are conditions that produce a molten state in order to improve metallurgical operations that have sulphide ore containing arsenic, copper and lead (Johto & Taskinen, 2014). Figure 2-8 shows a ternary phase diagram for arsenic, copper and lead sulphide ores.

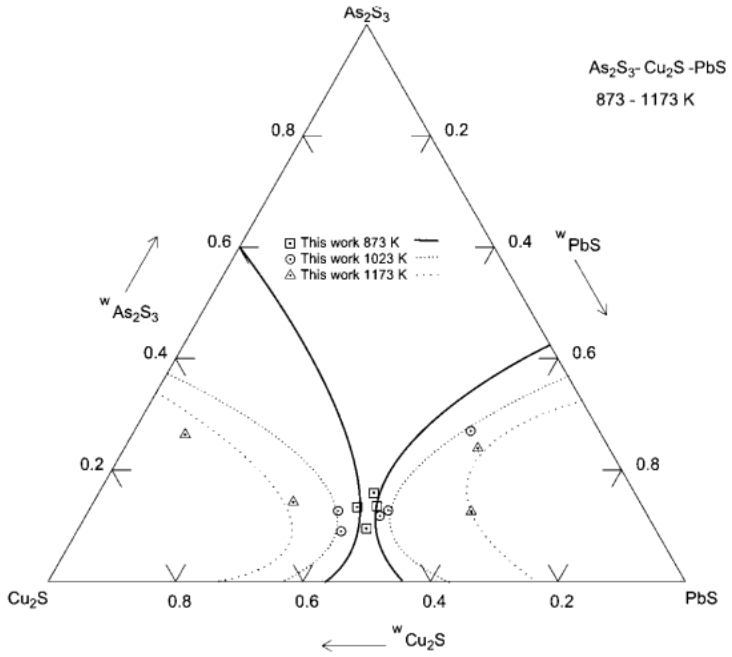

Figure 2-8: Ternary phase diagram of As_2S_3–Cu_2S–PbS at varying temperatures together with estimated and experimental findings (Johto & Taskinen, 2014).

Arsenic sits one row above antimony in period 15 on the periodic table, and because of their similar chemical characteristics they will often substitute for one another in orebodies. The most common copper-arsenic-antimony-sulphur minerals are listed in Table 4.

Table 4: Arsenic sulphides and respective properties (Johto & Taskinen, 2014)

Name	Ideal Composition	Crystal System	Colour	Density [g/cm^3]	Hardness [Mohs]
Enargite	Cu_3AsS_4	Orthorhombic	Steel grey/violet black	4.46	3
Luzonite	Cu_3AsS_4	Tetragonal	Grey/pink/brown/red	4.48	3.5
Tennantite	$Cu_{12}As_4S_{13}$	Cubic	Grey/brown/cherry red	4.64	3.5-4
Sinnerite	$Cu_6As_4S_9$	Triclinic	Steel grey	4.44	5
Lautite	CuAsS	Orthorhombic	Black/steel grey	4.82	3-3.5
Famatinite	Cu_3SbS_4	Tetragonal	Greyish black/steel black	4.69	3-4
Tetrahedrite	$Cu_{12}Sb_4S_{13}$	Cubic	Black/steel grey	4.95	3.5-4

Table 4 shows that many of the commonly occurring arsenic-bearing sulphide ores contain copper but each mineral is unique in its crystallinity and hardness which may affect processing operations. In order for the copper to be successfully extracted the arsenic must be dealt with according to environmental regulations so as to not harm the surrounding environment.

2.4.3 Hydrometallurgical Activities

Mineral processing from the non-ferrous industry can produce highly acidic waste streams which contain varying amounts of arsenic (Cui et al., 2014). Pyrometallurgical treatments for arsenic typically result in secondary arsenic pollution and require high amounts of energy (Guo, Shi, Yi, Tian, & Li, 2015). Hydrometallurgical treatments for arsenic are often more environmentally friendly options, and these include arsenic removal by dilute sulphuric acid, sodium sulphide or sodium hydroxide (Guo et al., 2015).

Hydrometallurgical operations can also mobilize arsenic into solution. Arsenic is liberated from arsenic-bearing ore and is dissolved into process streams and solutions via oxidation mechanisms in extraction

operations as well as being dissolved into solution via acidic dissolution (D. Zhang et al., 2015). Hydrometallurgical processes are still being developed for arsenic-bearing copper sulphides such as enargite (Safarzadeh et al., 2012). Enargite is a refractory arsenic mineral and its hydrometallurgical processing either dissolves both copper and arsenic into solution or selectively dissolves arsenic into solution (Safarzadeh et al., 2012). This arsenical solution must then be treated according to the regulations set out by the respective governing body.

2.4.4 Storage of Arsenic Waste

The use of ferric arsenates to store arsenic waste has been a popular method of immobilizing arsenic from the metallurgical industry due to its stable and insoluble characteristics (van Weert & Droppert, 1994). In the past iron hydroxide was used to store arsenic, however there was growing concern that the ferric-hydroxide would become α-goethite (α-FeOOH), thereby releasing arsenic into the environment (Filippou & Demopoulos, 1997). Various arsenic disposal options used in the past have proven to mobilize the previously stable arsenic. Calcium arsenates have been used to store arsenic waste; however, it was found that the compound would change to calcium carbonate and a soluble arsenic species (Smedley & Kinniburgh, 2002). As well, with arsenical ferrihydrite there is the potential for arsenate to reduce to arsenite, and ferric iron to reduce to ferrous iron due to biochemical activities (Smedley & Kinniburgh, 2002). Currently there is a large focus on scorodite as a means of arsenic immobilization/storage because it is found in nature and therefore the synthetic version of the natural mineral should have similar characteristics (Smedley & Kinniburgh, 2002).

2.5 Arsenic Immobilization Techniques

Regardless of the method used to remove arsenic from solution the arsenic must by oxidized to its pentavalent state. Though some arsenic immobilization techniques simultaneously oxidize arsenic and precipitate the solid arsenic species, and others require two or more steps, the dominant arsenic species

must be arsenate in order for the process to effectively remove arsenic. The process used to immobilize arsenic depends on the amount of arsenic in solution and arsenic species present (Demopoulos, 2014).

Most of the techniques used in the metallurgical industry are hydrometallurgical in nature but there are currently studies underway which use pyrometallurgical operations to oxidize arsenic for its immobilization.

2.5.1 Oxidation

The first step for arsenic removal in the mining and metallurgy industry is arsenic oxidation. The oxidation of trivalent arsenic to pentavalent arsenic can occur under ambient conditions with oxygen but without catalysts the kinetics of the oxidation reaction are slow (Molnár, Virčíkova, & Lech, 1994). As well, in the past air and oxygen are shown to act as oxidants to arsenic in basic solutions (Demopoulos, 2014).

2.5.1.1 Arsenite Oxidizing Reagents

A strong oxidant is required for the oxidation of arsenite to arsenate (Choi et al., 2014b). Reagents that are proven to oxidize arsenite to arsenate are hydrogen peroxide (Ritcey, 2005), sulphur dioxide/oxygen gas mixture (W. Zhang, Singh, & Muir, 2000), and ozone (Nishimura & Umetsu, 2001). Each of the reagents have their own respective advantages and disadvantages.

2.5.1.1.1 Hydrogen Peroxide as an Oxidant

Hydrogen peroxide is characterized by a peroxide group: two oxygen atoms with a single bond, with a hydrogen atom on each end as seen in Figure 2-9.

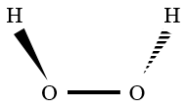

Figure 2-9: Hydrogen peroxide structure.

Hydrogen peroxide is a strong oxidant and has a variety of uses with many industries (Nogueira, Oliveira, & Paterlini, 2005). It can be synthesized by the electroreduction of oxygen in both acidic and basic solutions (Bonakdarpour et al., 2011). At a pH of 0 hydrogen peroxide has an oxidation-reduction potential (ORP) of 1.763 vs. SHE with the following reaction (Nogueira et al., 2005):

$$H_2O_2 + 2H^+ + 2e^- \rightarrow 2H_2O \qquad \textbf{Equation 4}$$

There have been many studies which investigate methods to quantify hydrogen peroxide in solution. Due to the reactive nature of hydrogen peroxide it can be difficult to measure before it decomposes into other species. In the past hydrogen peroxide quantification methods employed colourimetric methods such as titration and spectrophotometric techniques (Beers Jr. & Sizer, 1952); however, there are new methods proposed which use high-performance liquid chromatography (Gimeno et al., 2015).

Ultra-violet visible (UV-Vis) spectrophotometry is a colourimetric technique which measures the absorbance that a solution emits when a light beam at a specific wavelength is radiated through the solution. The absorbance spectrum for hydrogen peroxide is limited from 200-400 nm which means that within this range of wavelengths the hydrogen peroxide concentration can be quantified (Beers Jr. & Sizer, 1952). UV-Vis is not affected by electromagnetic interferences (Marcus et al., 2015).

Figure 2-10 shows the UV absorption of hydrogen peroxide in distilled water from a range of 200-400 nm. The wavelength, λ, selected might show interferences from other ions or noise, so to minimize the error associated with those issues a wavelength of 200-300 nm should be chosen or new calibration curves should be created in the case that there are other ions present (Beers Jr. & Sizer, 1952).

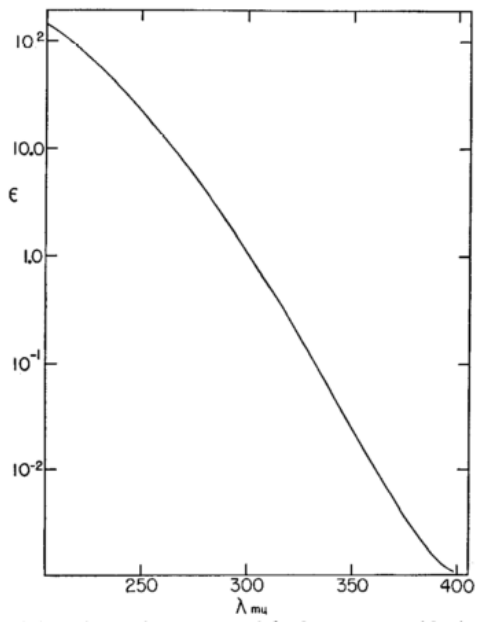

Figure 2-10: UV absorption of hydrogen peroxide in distilled water in regards to molar absorptivity versus wavelength (Beers Jr. & Sizer, 1952).

The Beer-Lambert Law, also known as Beer's Law, is described by Equation 5:

$$A = \varepsilon bc \qquad \textbf{Equation 5}$$

where A is the absorbance (negative logarithm of transmittance), ε is the molar absorptivity, b is the path length [cm] and c is the concentration [mol/L] (Cariolaro, 2015). An iodide solution is added to the hydrogen peroxide solution before being radiated with a wavelength of 352 nm (Alegria, Lion, Kondo, & Riesz, 1989). Iodide ions are oxidized by the hydrogen peroxide present and the resulting absorbance can then be correlated to a hydrogen peroxide concentration (Alegria et al., 1989). Wavelengths of 351, 352 and 353 nm have been used by various researchers (Alegria et al., 1989; Bonakdarpour et al., 2011; Kanthale, Ashokkumar, & Grieser, 2008). Using iodate and UV-Vis allows for detection limits of hydrogen peroxide on the scale of μM (Bonakdarpour et al., 2011).

Hydrogen peroxide can act as an arsenic oxidizing agent over a pH range of 2-11 (Ritcey, 2005). A study on the oxidation of arsenite by hydrogen peroxide shows that a time period of 5 minutes reduces the amount of arsenite in solution by 10-15 times (Molnár et al., 1994). Figure 2-11 illustrates the phenomena

in which, at a pH of 2 and 100% stoichiometric excess of hydrogen peroxide, the concentration at both high and low concentrations of As (III) is substantially reduced within the first 5 minutes of contact with the reagent. The oxidation efficiency for 15 g/L As (III) was between 91-93% (Molnár et al., 1994).

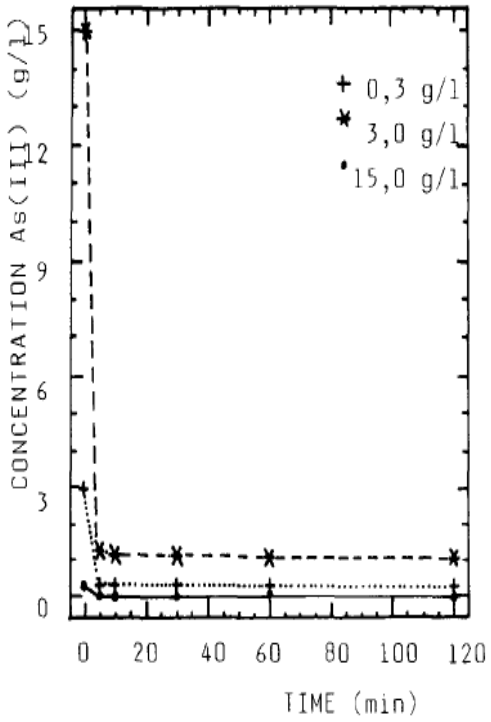

Figure 2-11: The concentration in g/L of As(III) at a pH of 2 with 100% excess hydrogen peroxide with respect to time (Molnár et al., 1994).

The study used a stoichiometric excess of 50% and 100% hydrogen peroxide according to Equation 6 which shows the stoichiometric ratio (Molnár et al., 1994):

$$\mathbf{As(III) + H_2O_2 \rightarrow As(V)} \qquad \textbf{Equation 6}$$

Equations 7 and 8 demonstrate the oxidation of arsenic trioxide under acidic conditions (pH of 1-7), where As_2O_3 is dissolved to form $HAsO_2$ (Molnár et al., 1994):

$$\mathbf{HAsO_2 + H_2O_2 \rightarrow H_3AsO_4} \qquad \textbf{Equation 7}$$

$$\mathbf{HAsO_2 + H_2O_2 \rightarrow H_2AsO_4 + H^+} \qquad \textbf{Equation 8}$$

Hydrogen peroxide is used as an oxidant in various industries. For example, the Ecometales scorodite plant in Chile uses hydrogen peroxide to oxidize arsenic before the scorodite process can commence

(Demopoulos, 2014). Hydrogen peroxide is expensive and decomposes when in contact with solids; however, the Ecometales plant in Chile experiences arsenite concentrations of less than 15% of the total arsenic (Demopoulos, 2014).

2.5.1.1.2 Sulphur Dioxide/Oxygen Mixture as an Oxidant

Oxygen mixed with sulphur dioxide is used as an oxidant for operations occurring in the acidic region (W. Zhang et al., 2000). It is a versatile oxidant as can be seen in Table 5.

Table 5: Usage of SO_2/O_2 in hydrometallurgical applications (W. Zhang et al., 2000)

Systems	Working pH range	Oxidation Products	Applications
Fe-SO_2/O_2	0-3	$Fe^{2+} \rightarrow Fe^{3+}$ $S(IV) \rightarrow SO_4^{2-}/S_2O_6^{2-}$	Leaching of metal sulphides and oxidation of As(III)
Mn-SO_2/O_2	3-6	$Mn^{2+} \rightarrow$ Mn(III)/Mn(IV) $S(IV) \rightarrow SO_4^{2-}/S_2O_6^{2-}$	Oxidative precipitation of Mn
Ni-SO_2/O_2	7-8.5	$Ni(II) \rightarrow Ni(III)$ $S(IV) \rightarrow SO_4^{2-}$	Production of $Ni(OH)_3$
Cu-SO_2/O_2	9-10	$Cu^{+} \rightarrow Cu^{2+}$ $S(IV) \rightarrow SO_4^{2-}$ $CN^{-} \rightarrow CNO^{-}$	Oxidation of CN^{-}

Due to the nature of sulphur dioxide, one can use sodium sulphite or metabisulphite instead of sulphur dioxide as they are easier to handle (Demopoulos, 2014). The SO_2/O_2 gas mixture can also oxidize ferrous to ferric and therefore it can be used to co-precipitate arsenic and iron from solution as a ferric arsenate (W. Zhang et al., 2000). SO_2/O_2 is relatively less costly than other oxidants used to oxidize arsenic (Demopoulos, 2014).

2.5.1.1.3 Ozone as an Oxidant

Ozone, O_3, is an oxidant which can effectively oxidize As (III) to As (V) (Bissen & Frimmel, 2003a). Ozone has a high oxidizing capability and it is therefore becoming a more commonly used oxidant for treating water and wastewater (Khuntia, Majumder, & Ghosh, 2014).

There are not many studies published which demonstrate the use of ozone for oxidizing arsenite to arsenate (Khuntia et al., 2014). The study reported by Khuntia et al. (2014) use an arsenic concentration of 995 ± 5 mg/L. This is lower than the arsenic concentrations typically found in mineral processing waste streams as mentioned previously. However, the study presented in Figure 2-12 shows that arsenite is oxidized quickly at low arsenic concentrations and a neutral pH of 7 (Khuntia et al., 2014). The pH of the solution is a factor which affects the rate of arsenite oxidation.

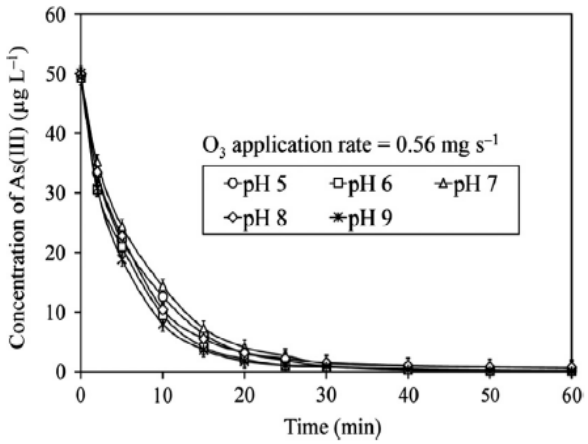

Figure 2-12: The effect of pH on the oxidation of arsenite to arsenate (Khuntia et al., 2014).

It has been shown that it can be advantageous to treat arsenic solutions at a pH of 1-2 with ozone in order to precipitate arsenic with manganese because ferric arsenate and ferric hydroxide do not precipitate under highly acidic conditions (Nishimura & Umetsu, 2001).

2.5.1.2 Biooxidation

Biological oxidation, "biooxidation," utilizes microbial mechanisms to oxidize chemical species. The oxidation mechanism is typically characterized as an indirect oxidation mechanism as the microorganisms oxidize ions, such as ferrous to ferric, which then oxidize other species. Heap leaching and dump leaching are two techniques that have been used in the copper industry to treat low-grade copper ores since the 1900s, and this works on the basis of bioleaching (Marsden & House, 2006). Biooxidation improves the kinetics of otherwise slower oxidation processes when bacteria such as *Thiobacillus thiooxidans* and *Thiobacillus ferroxidans* are present (Marsden & House, 2006).

Biooxidation of sulphidic gold ore was heavily researched in the 1970s-1980s. By 1986 a biooxidation process was implemented in a 10 tpd South African plant, and in 1990 a larger biooxidation process was underway at a 1500 tpd plant in Nevada, United States (Marsden & House, 2006). A biooxidation process was implemented at the Tasmanian Beaconsfield plant after the flotation circuit and before the cyanide circuit (Miller & Brown, 2005).

In the late 1970s Glencor Process Research in South Africa developed the BIOX™ Process which adds phosphorus, nitrogen and potassium to tanks containing flotation concentrate (van Aswegen, van Niekerk, & Olivier, 2007). The tanks are maintained at 40-45°C and are continuously sparged with oxygen (van Aswegen et al., 2007). This process also has the capability to oxidize arsenite to arsenate, and the arsenate can then be removed as a ferric arsenate in subsequent plant processes (van Aswegen et al., 2007).

2.5.1.3 Activated Carbon

Activated carbon catalyzes the oxidation reaction of arsenite and oxygen to arsenate (Bissen & Frimmel, 2003a). The addition of 5-10 g/L activated carbon to a system containing 40 µg/L As (III) will oxidize up to 90% As (III) in 20-30 minutes (Bissen & Frimmel, 2003a).

A novel and robust arsenic oxidation process was created which uses activated carbon to catalyze the arsenic oxidation reaction and only has one consumable reagent: oxygen (Choi et al., 2014b). This

process was patented in 2014 by Barrick Gold Corporation (Choi et al., 2014a, 2014b). The new process is carried out in acidic conditions, at ambient temperature and pressure, in less than 24 hours and has an oxidation efficiency of up to 99% (Choi et al., 2014a, 2014b). Though the process is proven to work effectively to oxidize arsenite, it is still unclear as to what oxidation mechanism is occurring (Choi et al., 2014b). One hypothesis proposed by the authors of a paper describing the novel process is that water and oxygen react on the activated carbon surface to produce a strong oxidant, such as hydrogen peroxide, which consequently reacts with arsenite to form arsenate (Choi et al., 2014b). Equation 9 shows the hypothesized reaction pathway for the production of hydrogen peroxide on the activated carbon surface (Choi et al., 2014b) and Equation 10 shows the oxidation of arsenite to arsenate with hydrogen peroxide as an oxidizing agent.

$$H_2O + \frac{1}{2}O_2 \xrightarrow{\text{carbon surface}} H_2O_2 \qquad \textbf{Equation 9}$$

$$H_3AsO_3 + H_2O_2 \rightarrow H_3AsO_4 + H_2O \qquad \textbf{Equation 10}$$

Two pieces of evidence that the authors of the study state which show that Equation 9 and Equation 10 are plausible are: (1) using pure oxygen has faster oxidation kinetics than that of air, and (2) both continuous and batch experiments show negligible changes in the system's pH and this is expected from the above reactions (Choi et al., 2014b).

2.5.2 Industrial Precipitation

The hydrometallurgical method of arsenic removal in the mining industry is accepted to be precipitation. There are a variety of factors that affect the stability of the arsenic precipitates. The degree of stability is measured using the toxicity characteristic leaching procedure (TCLP) that was developed by the United States Environmental Protection Agency (US EPA) in 1992 (U.S. Environmental Protection Agency, 1992). TCLP values are given in mg/L and this gives an overall appreciation of the solubility of a compound under a given set of conditions. Table 6 summarizes arsenic removal practices used in the copper industry and includes the TCLP for each technique. The following sections provide a brief

overview of the more common precipitation techniques and the importance of using arsenate as the arsenic species to be precipitated for the majority of the techniques.

Table 6: Treatment practices for arsenic-containing process streams (Harris, 2003)

Process	Initial As Species	Precipitate	Disposal Product	Precipitate Stability (EPA TCLP)
Neutralization with lime	As (III)	Calcium arsenite and gypsum	Filter cake in lined ponds	Low
	As (V)	Calcium arsenate and gypsum	Calcined cake in rotary kiln and calcine deposited in hazardous waste landfill	Low
Precipitation with sodium hydrosulphide	As (III)	Arsenic sulphide (>30% S)	Precipitate autoclaved with sulphur additions to As-S polymer to block stored in concrete	Moderate
Precipitation with ferric iron at high temperature	As(V)	Ferric arsenate and/or scorodite Fe:As=1.5 T = 90-200˚C	Tailings pond	High
Neutralization with ferric iron and base metals	As (III)	Arsenical ferrihydrite [As(III)-Fh] (Fe+Zn:As>4) with base metal hydroxides	Tailings pond	High
Neutralization with ferric iron	As (V)	Arsenical ferrihydrite As(V)-Fh Fe:As> 10	Tailings pond	High (US EPA best demonstrated available technology)

2.5.2.1 Lime Precipitation

Lime precipitation is where arsenic is precipitated as a calcium arsenate or calcium arsenite in alkaline conditions and is typically performed between a pH of 11-12. Investigations into the factors affecting the stability of the calcium-arsenic precipitate formed show that the pH and calcium:arsenic ratio directly affect the type of precipitate formed (Zhu, Zhang, Xie, Wang, & Cheng, 2006). The oxidation state of arsenic and aging time also affect the stability of the precipitate formed (Moon, Dermatas, & Menounou,

2004). It was found that calcium arsenite and calcium arsenate are not suitable for long term disposal for two main reasons: (1) calcium arsenic compounds will decompose to calcium carbonate, thus re-releasing arsenic compounds (Riveros et al., 2001; Robins & Jayaweera, 1992) and (2) because of the high TCLP value of 900-4400 mg/L for calcium arsenic compounds (Riveros et al., 2001). Calcium arsenite is precipitated at the Chuquicamata smelter in Chile, but this is because the arid climate of the Atacama Desert provides a low probability of the arsenic leaching back into the environment.

2.5.2.2 Co-precipitation with Ferric Ions

Co-precipitation of arsenic with ferric ions is the best demonstrated technology according to the US EPA (Opio, 2013; Riveros et al., 2001). This is a relatively cost-effective method and in order for the immobilized arsenic to pass the TCLP test when fixed via iron-coprecipitation the TCLP must be less than 5 mg/L (Riveros et al., 2001).

This method works on the basis of quickly neutralizing a ferric ion solution which consequently leads to the production of ferrihydrite (FH), which is illustrated in Equation 11 (Riveros et al., 2001). FH is a ferric oxyhydroxide which has sorptive characteristics conducive to the uptake of arsenic oxyanions which can be seen in Equations 11 and 12 (Riveros et al., 2001). This process is often used to remove and dispose of arsenic compounds in copper smelter weak acid streams and dust treatment bleed effluents, although arsenic must be in its pentavalent oxidation state. Arsenite is typically oxidized via oxidants discussed in section that describes arsenite oxidizing reagents.

$$\mathbf{Fe^{3+} + (3 + x)H_2O \rightarrow FeO(OH)(H_2O)_{1+x} + 3H^+} \qquad \textbf{Equation 11}$$

$$\mathbf{FeO(OH)(H_2O)_{1+x} + AsO_4^{3-} \rightarrow AsO_4^{3-}FeO(OH)(H_2O)_{1+x}} \qquad \textbf{Equation 12}$$

2.5.2.3 Scorodite Precipitation

Scorodite is a secondary arsenic-bearing mineral with a high amount of arsenic (25-30 wt%) and is extremely stable in nature (Filippou & Demopoulos, 1997). Scorodite is the most abundant secondary arsenic mineral (Lattanzi et al., 2008). Synthetic scorodite is recorded to have a TCLP of <5 mg/L

(Filippou & Demopoulos, 1997; Opio, 2013; Riveros et al., 2001). Filippou and Demopoulos (1997) state that scorodite precipitation is an effective method for arsenic disposal because it will typically leach less than 1 ppm of arsenic into solution at a pH of 5 (Filippou & Demopoulos, 1997).

Equations 13-16 show the process of High Temperature Pressure Oxidation (HTPOX) (Robins & Jayaweera, 1992). Equation 13 shows an arsenic bearing sulphide, in this case the sulphide is arsenopyrite that is roasted to produce an arsenate acid and ferrous sulphate. Sometimes elemental sulphur can be produced and this is shown in Equation 14. The ferrous sulphate is oxidized to ferric sulphate (Equation 15) and lastly ferric sulphate and arsenate react to form scorodite crystals.

$$4FeAsS_{(s)} + 13O_{2(aq)} + 6H_2O_{(l)} \leftrightarrow 4H_3AsO_{4(aq)} + 4FeSO_{4(aq)} \quad \textbf{Equation 13}$$

$$4FeAsS_{(s)} + 7O_{2(aq)} + 4H_2SO_{4(aq)} + 2H_2O_{(l)} \leftrightarrow 4H_3AsO_{4(aq)} + 4FeSO_{4(aq)} + 4S°_{(s)} \quad \textbf{Equation 14}$$

$$4FeSO_{4(s)} + O_{2(aq)} + H_2SO_{4(aq)} \rightarrow 2Fe_2(SO_4)_{3(aq)} + 2H_2O_{(l)} \quad \textbf{Equation 15}$$

$$Fe_2(SO_4)_{3(aq)} + 2H_3AsO_{4(aq)} + 2H_2O_{(l)} \rightarrow 2FeAsO_4.2H_2O_{(s)} + 3H_2SO_{4(aq)} \quad \textbf{Equation 16}$$

Atmospheric scorodite processes have also been developed which utilize stepwise supersaturation control to produce amorphous scorodite (Filippou & Demopoulos, 1997). The precipitation of scorodite at ambient pressure and a temperature of 90 °C is controlled by stepwise neutralization (Filippou & Demopoulos, 1997; González-Contreras et al., 2012). It is important to note that arsenic species present must be arsenate and that the arsenic stream is oxidized prior to entering the system.

Chapter 3

Materials and Experimental Methods

3.1 Raw Materials and Reagent Preparation

3.1.1 Activated Carbon

Granular activated carbon that was supplied by Barrick Gold Corporation was used for all tests that required activated carbon. The type of activated carbon used is called “Gold Plus” and was produced by Calgon Carbon Corporation. The activated carbon was derived from coconut shells and the maximum ash content of the activated carbon is 5% by weight (Calgon Carbon Corporation, 2013). The activated carbon was used as a catalyst to oxidize arsenic and other ion species present in tests. The activated carbon preparation and pretreatment varied for the kinetic tests, XPS analysis and zeta potential analysis because of the different particle size requirements for each of the tests.

3.1.1.1 Activated Carbon in Kinetic Tests

For the kinetic tests, which includes both batch and continuous column tests, activated carbon was stirred at 350 rpm for 25 hours in deionized (DI) water in order for the carbon to be wetted prior to the experiment and for attrition to occur. If the activated carbon was not wetted before the kinetic tests then the carbon would adsorb arsenic acid and the solution volume would drastically decrease over the duration of the test. After 25 hours the carbon-water slurry was decanted through a 16 mesh screen and wet screened in order for the carbon to be larger than 1.18 mm. The carbon was then stored in an 18-L bucket with DI water until it was required for the experiments.

The activated carbon requirement for the batch tests was 20% by weight of the total solution on a dry basis. In order to determine the wet/dry ratio of carbon three samples of 100 g of wet carbon were weighed and dried in an oven overnight. The dry mass of the samples was recorded and the average wet/dry ratio was calculated to be 1.79 ± 0.01.

3.1.1.2 Activated Carbon in X-ray Photoelectron Spectroscopy Tests

For X-ray Photoelectron Spectroscopy (XPS) experiments approximately 50 g of fresh activated carbon was pulverized for 5 s in a ring pulverizer. The pulverized carbon was then dry-screened for 15 minutes at a shaking amplitude of 1 mm to collect carbon that was -120 +400 (37-125 µm).

3.1.1.3 Activated Carbon in Zeta Potential Tests

Two zeta potential experiments were conducted: one used electrophoretic zeta potential analysis and one used an electroacoustic method of measurement.

For the electrophoretic method, the solid size requirements for the equipment used for the zeta potential experiments was for the particles to be less than 100 µm in diameter. Approximately 50 g of activated carbon was pulverized in a ring pulveriser from Bico for 5 seconds. The pulverized carbon was then dry-screened for 15 minutes at a shaking amplitude of 1 mm to collect carbon that was sized at -140 +400 (37-105 µm).

The activated carbon was saturated with water by soaking it in DI water for 24 hours prior to zeta potential experimentation so that the carbon would not adsorb the protons and hydroxide ions added to the solution when changing the pH of the sample solutions. 10.4 mg of the -400 mesh and 50 mL of DI water was added to a 50 mL Class A Digitube and the heavier particles sank to the bottom of the container. The suspended particles in solution were then diluted by four times into nine other tubes and the pH was adjusted using sulphuric acid (H_2SO_4) and sodium hydroxide (NaOH), both from Fisher Scientific.

The electroacoustic zeta potential measurements required a smaller particle size compared to the electrophoretic zeta potential machine. Approximately 50 g of fresh activated carbon was pulverized for 15 s in a ring pulverizer. The pulverized carbon was then dry-screened for 15 minutes at a shaking amplitude of 1 mm with a US standard 500 mesh screen (which only allows particles less than 25 µm to pass). This was repeated until 125 g of -500 mesh activated carbon was produced.

3.1.2 Activated Alumina

The activated alumina used was produced by BASF and is called “F-200 Activated Alumina for Liquid and Gas Drying.” The activated alumina is spherical in nature with a 1/8 inch diameter. The activated alumina was soaked in DI water for two days and rinsed with DI water to remove remaining activated alumina fines until the water ran clear prior to its use in a batch test. The surface area of the activated alumina is 530 m^2/g, the total pore volume is 0.5 cc/g, and the abrasion loss is 0.1 wt% (BASF, 2009).

3.1.3 Solution Preparation

To measure the pH and ORP of solutions during solution preparation as well as during testing an H-series H260g meter from Hach was employed. The pH probe used was calibrated prior to each use using pH 1.68, 4.01 and 7.00 standards. The calibration was often checked with a known pH 1.00 solution to ensure that the calibration curve was accurate to a pH of 1.

3.1.3.1 Column Tests Solution Preparation

Two main types of solutions were prepared for column tests: diluted sulphuric acid solution and arsenic acid solution. The reagents used were: arsenic trioxide (99.5% on a metals basis from Alfa Aesar), arsenic pentoxide (99.9% on a metals basis from Alfa Aesar), ferrous sulphate heptahydrate from Fisher Scientific and cupric sulphate pentahydrate from Fisher Scientific.

The diluted sulphuric acid solution was made by mixing DI water in a 2 L Erlenmeyer flask, via a magnetic stirrer, and adding approximately 10 mL of concentrated sulphuric acid. The pH of the solution was measured constantly using a pH probe and pH meter. Concentrated sulphuric acid was slowly added to the solution with a transfer pipette until the pH was constant at a pH of 1.

The second type of solution required a combination of arsenic, iron and cupric ions. A 2 L Erlenmeyer flask was placed on top of a magnetic stir plate. A magnetic stir bar, DI water and 20 mL of concentrated sulphuric acid was added to the flask. Arsenic trioxide powder, As_2O_3, was added to the mixture in a high dosage so that the solution could be diluted in a 5 gallon bucket and have a concentration of 2 g/L As

(III). The Erlenmeyer flask was heated to 75 °C until the arsenic had completely dissolved. The solution was then diluted with water to make approximately 14 L of solution to feed the column. Ferrous sulphate was added to the bucket and stirred via an overhead mixer. Concentrated sulphuric acid was then used to bring the pH down to a pH of 1. For tests requiring copper, two 2 L volumetric flasks were used to prepare 4 L of solution. Cupric sulphate was dissolved in each of the 2 L volumetric flasks with the diluted arsenic and iron solution that was previously prepared.

3.1.3.2 Batch Tests Solution Preparation

The volume of solution required for each batch test was 1 L and the pH was 1 ± 0.1. A stock solution of a high concentration of arsenite was created by heating 1.8 L of DI water, 20 mL of sulphuric acid and the respective amount of arsenic trioxide to 75 °C in a 2 L Erlenmeyer flask. Two concentrations of stock solutions were made during the testwork: 14 g/L (to be also used in column tests) and 10 g/L (used for the majority of the batch tests). The stock solution was heated and stirred for 2 days (or until the arsenic had completely dissolved). The solution was then cooled and filtered through a number 2 filter paper into a 2 L volumetric flask to filter out the impurities associated with the arsenic trioxide powder. Boiling water was used to clean the 2 L Erlenmeyer flask and rinse the remaining arsenite out of the Erlenmeyer flask. The 2 L volumetric flask was filled to exactly 2 L with DI water.

To make the 1 L of solution for each batch test a 1 L volumetric flask was filled with DI water and the volume of arsenic stock solution for the arsenite concentration required in the test. The contents of the volumetric flask were then transferred to a 2 L Erlenmeyer flask along with a magnetic stir bar. The flask was placed on a magnetic stir plate and a pH probe was fixed to the side of the flask to continuously measure the pH. The pH of the solution was decreased to a pH of 1 ± 0.1 via concentrated sulphuric acid additions. The pH and ORP of the solution was measured and recorded prior to introducing activated carbon, thereby starting the test.

3.2 Metals and Metalloid Quantification

3.2.1 Inductively Coupled Plasma Optical Emission Spectrometry

Inductively Coupled Plasma Optical Emission Spectrometry (ICP-OES) was employed to determine the total arsenic, total iron, total copper and aluminum in solution. This analytical technique to measure ion concentration was used in order to determine the initial concentration of ions in solution, to determine the degree of ion adsorption onto the activated carbon surface, and to calculate the extent of arsenic and iron oxidation when combined with the colourimetric titration technique used for arsenic and iron speciation. The ICP-OES was used, as opposed to ICP-MS (mass spectrometry) due to the relatively high arsenic concentrations. The ICP-OES analysis was conducted at the Queen's University Analytical Services Unit and the equipment used was a Vista Pro-axial CCD spectrometer from Agilent.

3.2.2 Colourimetric Titration for Arsenic Speciation

Colourimetric titration was used to determine the amount of ferrous and arsenite species present in the solution.

3.3 Kinetic Tests

3.3.1 Column Tests

Column tests were conducted to produce sample solutions to be analyzed without attrition of activated carbon occurring. A schematic diagram of the column set-up can be seen in Figure 3-1.

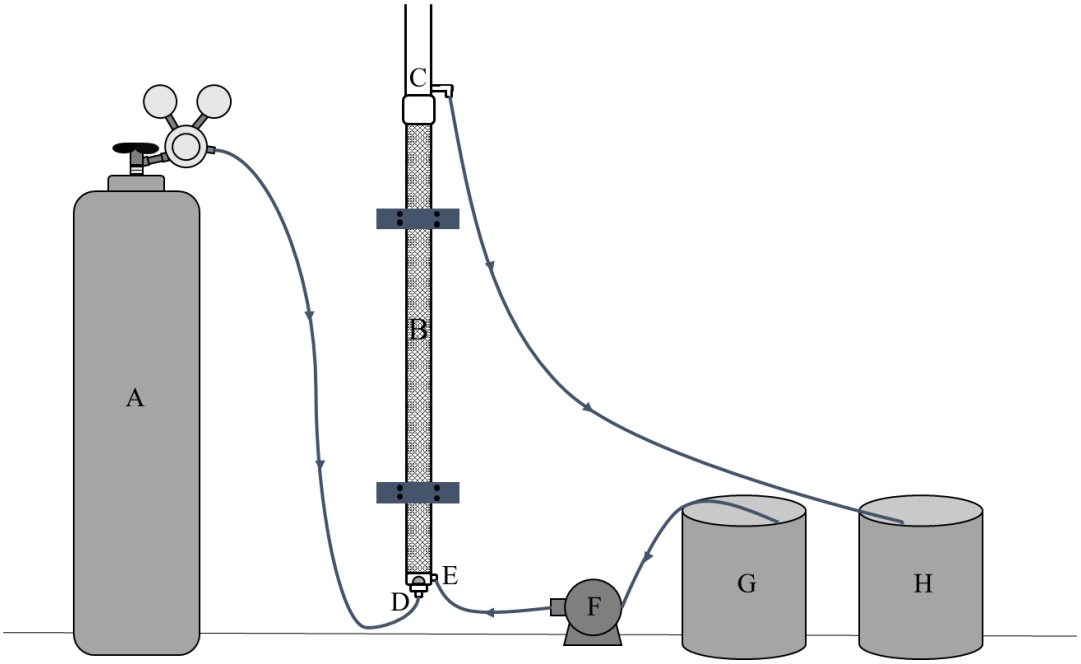

Figure 3-1: Schematic diagram of the column used for arsenic oxidation (not to scale) where: (A) is the gas tank for the test, (B) is the carbon filled section of the column measuring 1 m in height, (C) is the top of the column, (D) is the gas inlet port, (E) is the solution inlet, (F) is the peristaltic pump, (G) is the reservoir for solutions entering the column and (H) is the effluent waste.

Column tests proved useful for preliminary results but did not allow for samples to be taken at the beginning of the process which is when most of the oxidation and adsorption of ions occur. The gases used in experiments to add oxygen into the system were industrial grade oxygen (minimum 99.5% O_2) and compressed air that were supplied by Praxair. The flowrate of the gas ranged between 0.1-0.4 L/min depending on the experiment.

The solution entered the column at 0.5 mL/min through a port at the bottom and went through a fine filter. The filter served two purposes: (1) to ensure the carbon fines did not plug the gas and solution ports and (2) to sparge the gas and reduce the size of the gas bubbles for better mass transfer capabilities.

The pH and ORP of the column were taken from the exposed top of the column where the oxygen leaves in order to simulate the environment inside the column. Solution samples were also taken from the top of

the column, via a transfer pipette, in order to take kinetic samples that had not been collecting outside of the column due to the small solution flowrate of 0.5 mL/min from the effluent stream.

3.3.2 Batch Tests

Batch tests were experiments in which an arsenic-containing solution was brought down to a pH of 1±0.1 and added to a pre-weighed amount of carbon or alumina. The experiments with activated carbon had a stir rate of 200 rpm using an overhead mixer and a 2-sided impeller of 8.5 cm in length, and the test with activated alumina had a stir rate of 450 rpm to allow for better mass transfer. The gas used in the experiment was sparged at flowrates ranging from 0.04-1 L/min depending on the test, and the gases used were either industrial grade oxygen (minimum 99.5% pure) or compressed air. Both of the gases were provided by Praxair. A glass sparger with glass frit at the bottom was inserted into the 2 L batch reactor and it was situated just above the impeller. 10 mL samples were taken at 0, 0.5, 1, 2, 4, 8 and 24 hours and the pH and ORP of the solution were also measured during this time. A schematic diagram of the apparatus can be seen in Figure 3-2.

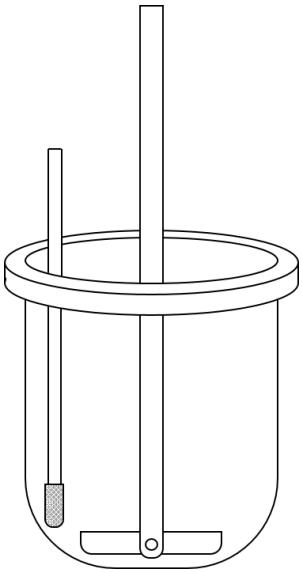

Figure 3-2: Schematic diagram of batch tests: a 2 L glass reactor was used as a vessel. An impeller which was attached to an overhead mixer was used to stir the solution and a glass sparger was fixed just above the impeller via clamps and a clamp stand. Parafilm was used to over the top of the reactor during tests to minimize splashing and evaporation.

3.4 Surface Chemistry Experimental Work

3.4.1 Cyclic Voltammetry Methods

Cyclic voltammetry (CV) solutions were created by adding 99.5% arsenic trioxide and 99.9% arsenic pentoxide from Alfa Aesar to distilled water and mixing for 24 hours. Sodium sulphate from Sigma Aldrich was then added to the solution to increase the ionic activity for the CV tests. The final solution, which was used as electrolyte, was 1 mM arsenite, 1 mM arsenate and 0.2 M sodium sulphate. The mixture was heated to 50 °C until all of the solids were dissolved. Aliquots of 100 mL were taken and the pH was reduced to 1 by addition of sulphric acid before the test began.

The cyclic voltammetry experiments were conducted on a Metrohm PGStat 101 potentiostat. For tests that required stirring the stirring was done via a magnetic stirrer at 350 rpm. The system was a standard three electrode system where the reference electrode was an Ag/AgCl electrode, the counter electrode was a graphite electrode, and the working electrode was either a graphite or platinum electrode. The graphite was cleaned by submerging the electrode in a hydrochloric acid solution and sonicating it for two minutes. All tests had a scan rate of 100 mV/s. All mention of ORP in subsequent chapters is in reference to Ag/AgCl unless otherwise noted.

3.4.2 X-ray Photoelectron Spectroscopy

Three vials each containing 1.00 ± 0.001 g of -140 +400 mesh activated carbon were prepared. 10 mL of 5 g/L arsenite solution was added to one vial, 10 mL of 5 g/L arsenate solution was added to another vial, and 10 mL of 5 g/L arsenite and 5 g/L arsenate solution was added to the third vial. The arsenic mixtures were left to adsorb onto the activated carbon for 1 hour. Each vial containing the arsenic and carbon mixture was heated in a warm water bath to 40 °C and dried under nitrogen gas. The set up for the initial drying apparatus can be seen in Figure 3-3. After the samples were dried they were then washed with DI water and centrifuged four times until the pH was the same as the pH of the DI water. The pH of the

liquid layer was analyzed with pH test strips. The samples were dried in a low temperature oven over night. The samples were stored in a dessicator under vacuum until they were brought for XPS analysis.

Figure 3-3: Initial drying apparatus for XPS.

A spectra scan was performed in order to identify species on the carbon surfaces using a Microlab 310-F spectrometer which used an XR-4 twin anode (Al/Mg) from VG Scientific. The carbon samples were fixed on a stub-type stainless steel holder via double-sided copper tape. The samples were placed in a high vacuum preparation chamber overnight (10^{-8} mbar) and then transferred into the analysis chamber of the XPS spectrometer which is held at 10^{-9} bar. MgK_{α} radiation was used at 1253.6 eV (280 W, 14 kV) as well as a spherical sector analyzer operating in constant analyzer energy mode. Binding energies are calibrated to the S 2p peak at 161.8 eV. Full spectra were recoded from -5 to 1000 eV at a pass energy of 40 eV using an energy scan rate of 2 eV. High resolution spectra were measured and recorded for C1s, O 1s, As 3d, S 2p, and S 2s in their respective regions at a pass energy of 20 V and a scan rate of 0.05 eV. The area analyzed for each sample was approximately 5 x 2 mm^2.

Initial analysis was processed using the Avantage software from Thermo Fisher Scientific; the Shirley algorithm was used to correct the spectra for background noise and the data was corrected for energy

shifts due to the influence of the X-rays charging the samples. XPSPeak 4.1 was used to determine the peaks and calculate the area under each of the curves.

3.4.3 Electrophoretic Zeta Potential

The pH of DI water with activated carbon suspended in solution was adjusted with H_2SO_4 and NaOH. Samples were sonicated for 5 minutes prior to the zeta potential measurement to minimize air bubbles in solution and to help in keeping the carbon suspended in solution. The refractive index selected was 2.470 and the absorption constant was 1.000, however these parameters won't affect the zeta potential and are only used for the nanosizer (which was not used in the experiment).

3.4.4 Electroacoustic Zeta Potential

Electroacoustic zeta potential measurements were conducted at a 10% pulp density of carbon particles less than 25 µm in diameter. Each zeta potential test used 5.55 g of activated carbon in 50 mL of 0.001 M KCl solution. The solution was sonicated for 30 s to suspend the particles in a UP400S ultrasonic processor from Hielscher. The solution was left to reach equilibrium with respect to pH and zeta potential prior to titrating the solution in regards to pH using an automatic titration unit which was used in conjunction with a FiledESA electroacoustic zeta potential analyzer from PartikelAnalytik. The solution was titrated to a pH of 10 from the equilibrium point and then down to a pH of 3 in 0.25 unit increments. The solution was given a 300 s delay before recording the measurements.

3.5 Safety Procedures

Safety was kept in mind throughout the duration of the experimental work. Arsenic is an extremely toxic element so many precautions were taken. Arsenic oxide was always measured in a fumehood and a P100 respirator mask was worn during measurements. Monogoggles were worn as eyewear to prevent fumes and acid from reaching the researcher's eyes in case of an incident. Batch tests and titrations were conducted in a fumehood. All arsenic-contaminated solid waste was disposed of separately in designated waste bins and arsenic-containing liquid waste was disposed of in a designated waste container.

Glassware that had been in contact with arsenic was rinsed thrice into an arsenic liquid waste container before being cleaned in a sink. An acid bath containing 2% hydrochloric acid was then used to remove any remaining residues.

The inhalation of carbon fines is dangerous so during carbon pulverization a P95 half face mask was worn. Steel-toed boots were worn during heavy lifting.

Personal protective equipment (PPE) was worn for the duration of the tests. The PPE worn included nitrile gloves, a labcoat, monogoggles, and closed-toed shoes.

Chapter 4

Fundamental Studies and Preliminary Findings

This chapter presents the fundamental studies conducted and preliminary findings relating to the scope of this thesis. This chapter is divided into five sections in which the following topics are discussed: (1) electrochemical tests with arsenic solution, (2) continuous column tests without arsenic to confirm the formation of an oxidant within the system, (3) the effect of hydrogen peroxide produced in the system, (4) experiments to determine the speciation of arsenic on the activated carbon surface and (5) adsorption isotherm models. Electrochemical tests were conducted to compare the catalytic ability of carbon to oxidize arsenic with platinum. The hypothesis that a strong oxidant is formed on the activated carbon surface was tested by investigating the steady-state system of activated carbon in an acidic environment which was modeled with a vertical packed-bed column. Next, adsorption models were explored to investigate the bonding characteristics of arsenic to carbon. The findings of these studies influenced the experiments outlined in Chapter 5, which further investigated the surface chemistry of activated carbon.

4.1 Cyclic Voltammetry Experiments

Cyclic voltammetry (CV) tests were conducted on a carbon or a platinum electrode to compare the potential required for oxidation on both of the surfaces. Figure 4-1 shows the results of the CV tests without mixing the solution for two cases: (1) platinum is the working electrode and (2) carbon is the working electrode. The dotted line signifies the trial with platinum as the working electrode and this test shows four anodic peaks. The two leftmost peaks can be attributed to hydrogen gas evolution on the working electrode (Doña Rodríguez, Herrera Melián, & Pérez Peña, 2000).

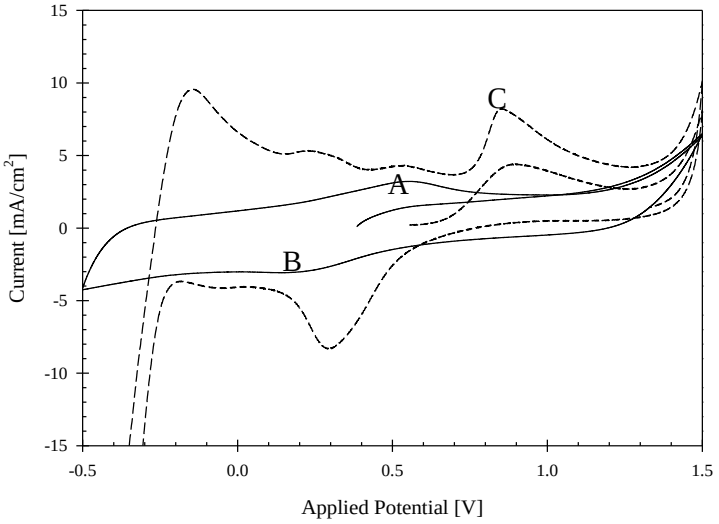

Figure 4-1: CV tests containing 1 mM As(III) and 1 mM As(V) at pH 1; scanning rate was 100 mV/s, and 100 mL of electrolyte was used. Peak A is the oxidation of arsenite with a carbon working electrode, peak B is the reduction of arsenate with a carbon working electrode, and peak C is the oxidation of arsenite with a platinum working electrode.

Figure 4-2 shows the tests in Figure 4-1 that were repeated with a stirring rate of 350 rpm in order to decrease the effects of hydrogen production and to diffuse the various ions throughout the electrolyte.

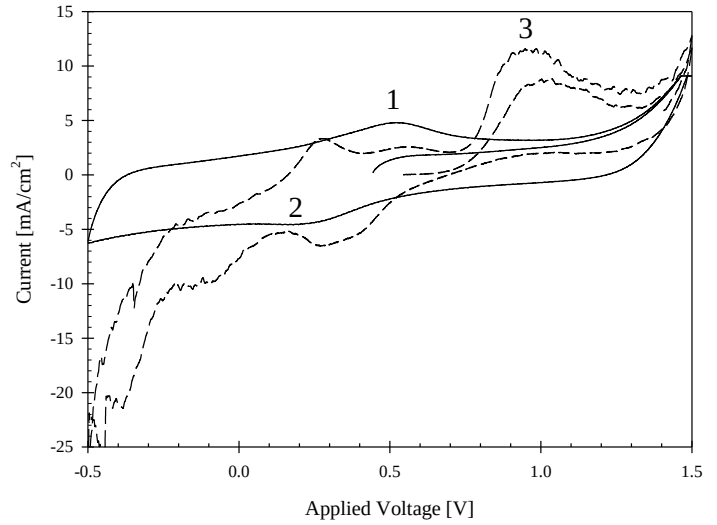

Figure 4-2: CV tests containing 1 mM As(III) and 1 mM As(V) at pH 1; scanning rate was 100 mV/s, 100 mL of electrolyte was used and the stirring rate was 350 rpm. Peak 1 is the oxidation of arsenite with a carbon working electrode, peak 2 is the reduction of arsenate with a carbon working electrode, and peak 3 is the oxidation of arsenite with a platinum working electrode.

Stirring the solution decreased the hydrogen adsorption on the platinum electrode and increased the current density peak on the carbon electrode (peak A vs peak 1). The hydrogen adsorption peaks are smaller in value in Figure 4-2 compared to Figure 4-1 because of the diffusion of the hydrogen produced during the cathodic cycle away from the electrode surface when mixing is introduced to the system.

A higher current density for arsenite oxidation with mixing is a result of more arsenite diffusion to the electrode surface which forms a thinner diffusion layer in comparison to the stationary CV test. This results in a more rapid oxidation rate and can consequently be seen by the difference in current density values of peak A and peak 1. The same reasoning also explains the larger arsenate reduction peak in Figure 4-2 compared to that in Figure 4-1 (peaks B and 2).

The anodic peak in Figure 4-2 for the carbon working electrode trial (peak 1) is either the oxidation of elemental arsenic to arsenite or the oxidation of arsenite to arsenate. The cathodic peak for the same test (peak 2) is respectively either the reduction of arsenite to elemental arsenic or the reduction of arsenate to arsenite (Wei & Somasundaran, 2004). However, the solution prepared contained arsenite and arsenate oxides so it can be concluded that these peaks represent the oxidation and reduction of arsenite and arsenate.

The cyclic voltammogram using the platinum working electrode and with stirring is similar to CV tests using a platinum rotating disk electrode (RDE) (Brusciotti & Duby, 2007) so their results can be used for comparative purposes. It is most likely that the anodic peak at an applied potential of 0.95 V in Figure 4-2 (peak 3) is the oxidation of arsenite to arsenate, and the leftmost anodic peak (applied potential of 0.29 V) and cathodic peak (applied potential of 0.3 V) are the oxidation and reduction of arsenite and elemental arsenic (Brusciotti & Duby, 2007).

In both figures, the anodic peak with carbon as a working electrode occurs at a lower applied voltage compared to the tests with platinum as a working electrode, these peaks being peaks A and C in Figure 4-1 and peaks 1 and 3 in Figure 4-2. This illustrates the catalytic ability of carbon to accelerate the arsenic

oxidation reaction. The results from the initial tests led to column testing to further explore the surface chemistry of activated carbon in acidic media.

4.2 Column Tests with Arsenic-Free Solution

4.2.1 Experimental Methods

4.2.1.1 Column Test Procedure

A teflon column that was 1 m in length was used for the experiments. Activated carbon which was supplied by Barrick Gold Corp. was pretreated as outlined in Chapter 3. The +16 mesh carbon was dried and 270 g was added to the column.

The water used for the water tests was distilled or DI water at room temperature (depending on the test). The solution flowed into the column at a flow rate of 0.5 mL/min and industrial oxygen was sparged co-currently with the solution at 0.2-0.3 L/min.

Diluted sulphuric acid solution for the tests using an acidic solution was made by slowly adding approximately 10 mL of concentrated sulphuric acid from Fischer Scientific to DI water in a 2 L Erlenmeyer flask. The solution was stirred at a low rpm via a magnetic stirrer to homogenize the solution. The pH of the solution was measured and the pH probe and meter were calibrated prior to each use using pH 7.00, 4.01 and 1.68 standards. Concentrated sulphuric acid was slowly added to the solution with a transfer pipette until the pH was constant at a pH of 1±0.1.

4.2.1.2 Hydrogen Peroxide Determination Procedure

A calibration curve was created by mixing 1 mL of an iodide solution containing a 0.4 M potassium iodide, 0.05 M sodium hydroxide and 0.00016 M of a molybdenum catalyst in the form of ammonium molybdate tetrahydrate and 1 mL of a solution containing 0.1 M potassium hydrogen phthalate (KHP) in a UV-Vis cuvette prior to measuring the absorbance of a sample containing hydrogen peroxide (Alegria et al., 1989; Kanthale et al., 2008). The potassium iodide was from BDH, the sodium hydroxide from BDH,

the ammonium molybdate tetrahydrate from BDH and KHP from Sigma Aldrich. Next, 1 mL of a standard solution containing a known amount of hydrogen peroxide was added and the solution was radiated with a wavelength of 353 nm (Kanthale et al., 2008). The hydrogen peroxide was purchased from Fisher Scientific. Iodide ions are oxidized by the hydrogen peroxide present and the resulting absorbance can then be correlated to a hydrogen peroxide concentration (Alegria et al., 1989; Kanthale et al., 2008).

A calibration curve, which plots the absorbance of sulphuric acid with varying concentrations of hydrogen peroxide, was produced for a wavelength of 353 nm. The calibration curve can be seen in Figure 4-3.

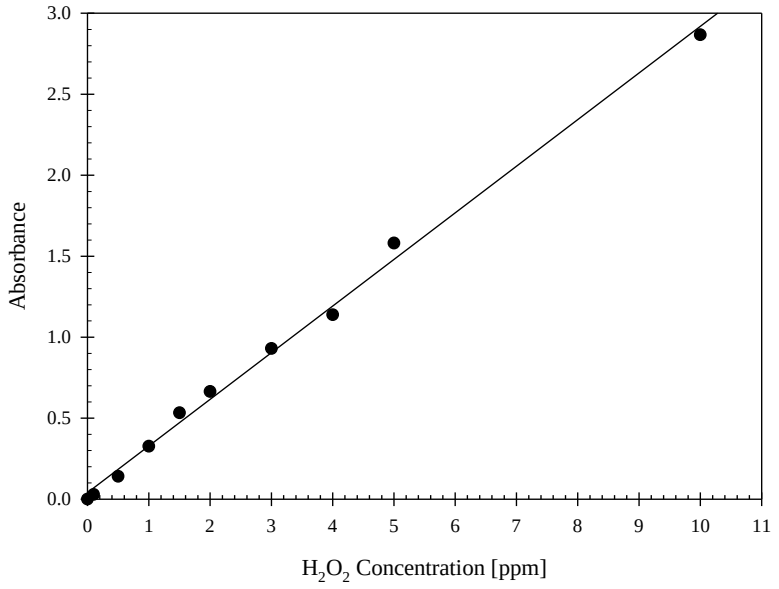

Figure 4-3: UV-Vis calibration curve for hydrogen peroxide determination in a pH 1 sulphuric acid at a wavelength of 353 nm.

1 mL of sample was mixed with 1 mL of the iodide solution and 1 mL of KHP to quantify the amount of hydrogen peroxide produced during experiments. The hydrogen peroxide concentration was then determined by plotting the respective absorbance value on the calibration curve shown in Figure 4-3 and finding its corresponding hydrogen peroxide concentration.

4.2.2 Column Tests with Water: pH, ORP and Zeta Potential Experiments

DI water was pumped through the column until steady state was reached with respect to pH and ORP. This also ensured that there were no leaks in the column and that residual carbon fines remaining from the attrition process were removed from the system as they flowed out with the effluent water. The flowrate of industrial oxygen was 0.3 L/min.

The effluent steady-state conditions indicate that there is a phenomena occurring within the column which changes the pH and ORP of the solution in the column. Table 7 illustrates that the pH increases from slightly acidic conditions to slightly basic conditions and the ORP is increased by 26 mV.

Table 7: Final pH and ORP at the top of the column for the water test

Location	pH	ORP [mV]
Solution Reservoir	5.8	235
Top of the Column	8.4	261

The initial pH of the water is below 7 and this is likely due to dissolved carbon dioxide in the water which acts as a buffer. The effluent is more alkaline because water molecules in the column have partially dissociated into a proton and a hydroxide ion due to existing functional groups on the carbon surface or monoatomic oxygen that can be produced on the surface of activated carbon. The zeta potential, although it can vary between different activated carbon samples, is negative above a pH of 2.5-6.2 according to various sources (Dai, 1994; Eguez & Cho, 1987). If the zeta potential of the carbon is negative because it is past the PZC then the protons may adsorb onto the carbon surface, thereby increasing the pH of the resulting solution. Arsenic forms an oxyanion when dissolved in solution, so if the solution is highly acidic (pH 1-2) then the zeta potential of the carbon should be positive which would attract the arsenic species to the surface of the carbon for the oxidation reaction to occur.

Electrophoretic zeta potential analysis was conducted on solutions containing DI water, powdered activated carbon and varying amounts of sulphuric acid and sodium hydroxide (for pH adjustment). The

PZC of the activated carbon under investigation ranged between a pH of 2.1-3.5. Electroacoustic zeta potential analysis was also completed at a pulp density of 10%. This analysis showed that the PZC occurred at a pH of 4.0. Figure 4-4 shows the zeta potential points for five runs of electroacoustic zeta potential measurements. The starting pH of the column test is above the PZC pH value for activated carbon which means that when water partially dissociates the cation (proton) will more preferentially adsorb onto the activated carbon compared to the anion (hydroxide) because the zeta potential of the activated carbon is negative.

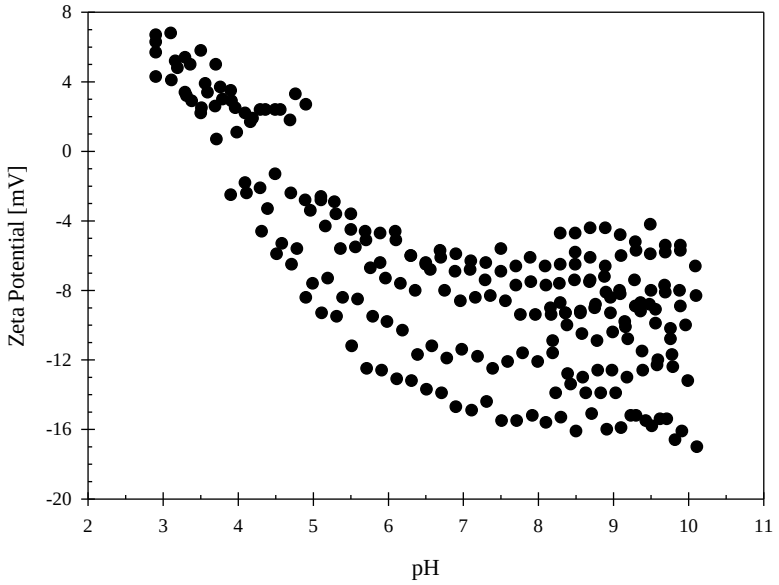

Figure 4-4: Combined data for five runs of electroacoustic zeta potential measurements.

The increase in the ORP is small which implies that if an oxidant is being produced then it is formed in small quantities that may not be substantial enough for the complete oxidation of arsenic, alone. The amount of oxidant formed must be quantified before drawing conclusions.

4.2.3 Column Tests with Sulphuric Acid

The solution reservoir for the column was switched to pH 1 sulphuric acid once steady-state operation was achieved in the column with DI water. The oxygen flow rate remained at 0.3 L/min. The pH of the

top of the column was measured and recorded. The data, as seen in Figure 4-5, shows that once the column reaches steady-state under the new set of conditions, the pH at the top of the column does not differ from the acid reservoir. Steady-state was achieved after approximately 75 hours. The sharp decrease in Figure 4-5 corresponds to the time it took for the solution inside the column to be completely changed from water to the diluted sulphuric acid solution.

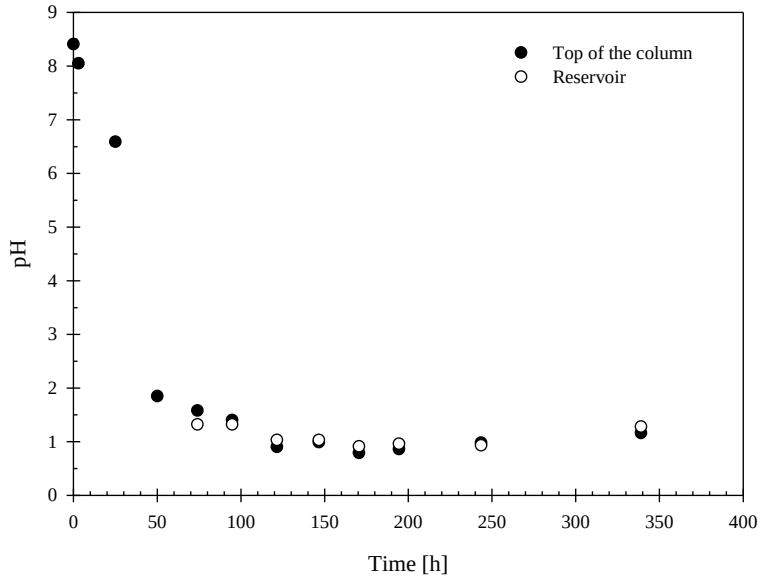

Figure 4-5: pH with respect to time of the top of the column and the reservoir at 25 °C.

The ORP of the reservoir solution and the top of the column was monitored. The ORP at the top of the column was slightly higher than that of the reservoir, as depicted by Figure 4-6. Although the increase in ORP only averages 10-15 mV, it indicates that if an oxidant is formed then the amount produced is very small so there are likely other phenomena occurring on the carbon surface which is helping to oxidize the arsenic. The increase of ORP during the first 50 hours is due to sulphuric acid being introduced into the system.

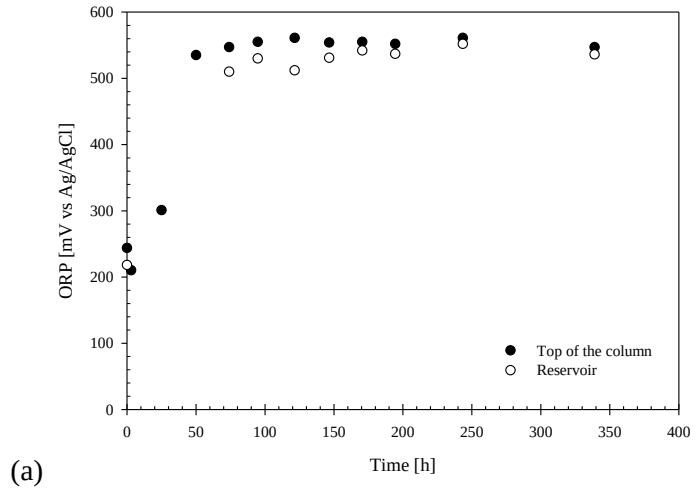

(a)

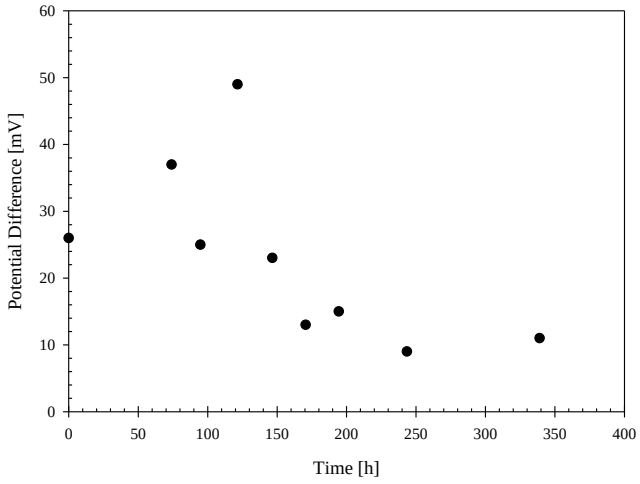

(b)

Figure 4-6: (a) ORP of the top of the column with respect to time at 25 °C (b) potential difference between the sulphuric acid reservoir and the top of the column.

Results indicate that an oxidant may be being produced within the column and it was hypothesized that the oxidant formed is hydrogen peroxide. To test this theory a sample from the column was analyzed for peroxide using UV-Visible spectroscopy. It was calculated that just under 1 ppm of peroxide was being produced and was still in existence by the end of the column reactor. There may be a higher concentration of peroxide in the column if it is lowered by the end due to the decomposition of hydrogen peroxide when in contact with solids, which in this case is the activated carbon present.

The column test with sulphuric acid was repeated but with 0.2 L/min oxygen. The pH and ORP of the top of the column and the acid reservoir were measured with respect to time. Results were similar to the results with 0.3 L/min oxygen. The pH remained relatively constant and had a negligible difference between the top and bottom of the column, and the ORP was on average 75 mV higher at the top of the column compared to the solution reservoir. Figure 4-7 shows the pH of the top and bottom of the column over time and Figure 4-8 shows the ORP of the top of the column and the solution reservoir over the five-day test.

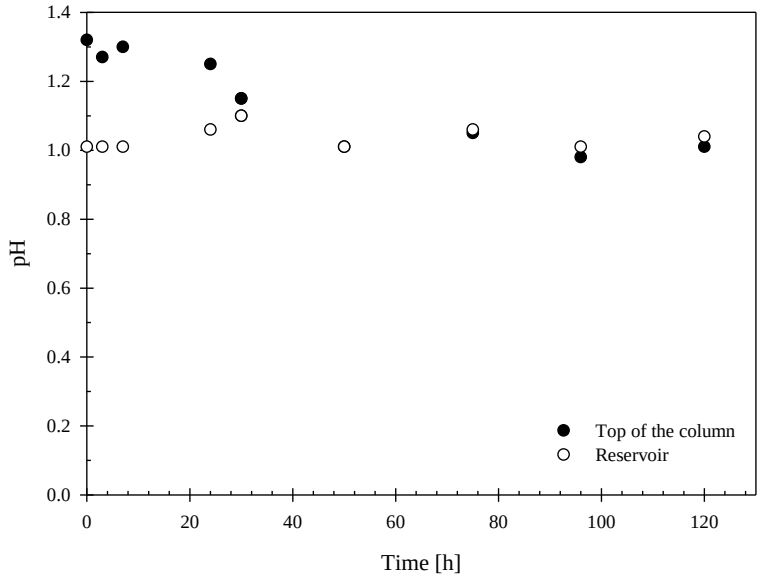

Figure 4-7: pH of the top of the column and pH of the reservoir solution with respect to time at 25 °C.

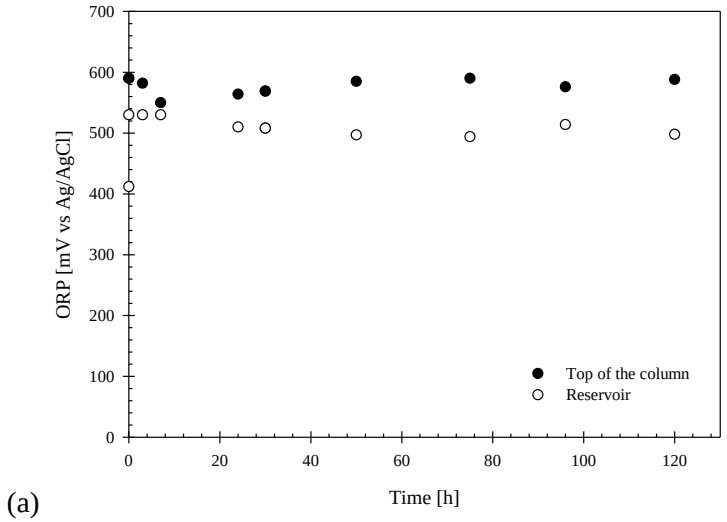

(a)

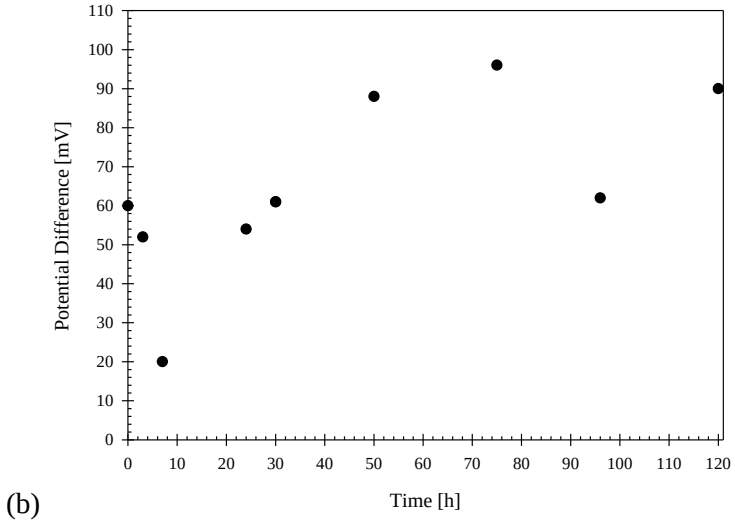

(b)

Figure 4-8: (a) ORP of the top of the column and the reservoir with respect to time and (b) potential difference between the sulphuric acid reservoir and the top of the column.

The amount of hydrogen peroxide produced in this system with respect to time was assayed via UV-Vis analysis. At each sampling time 1 mL of solution from the top of the column and 1 mL of solution from the acid reservoir were placed in cuvettes and mixed with the potassium iodide and KHP solutions, respectively. The hydrogen peroxide concentration in the solution reservoir was measured in order to validate that the peroxide measured at the top of the column was being produced in the column and not

present in the reservoir. The reservoir and column solutions were always measured against a blank and this verified that the peroxide was produced inside the column as there was no measureable amount present in the reservoir before being pumped into the column. The amount of hydrogen peroxide produced increased over time until it plateaued at approximately 40 hours, as can be seen in Figure 4-9.

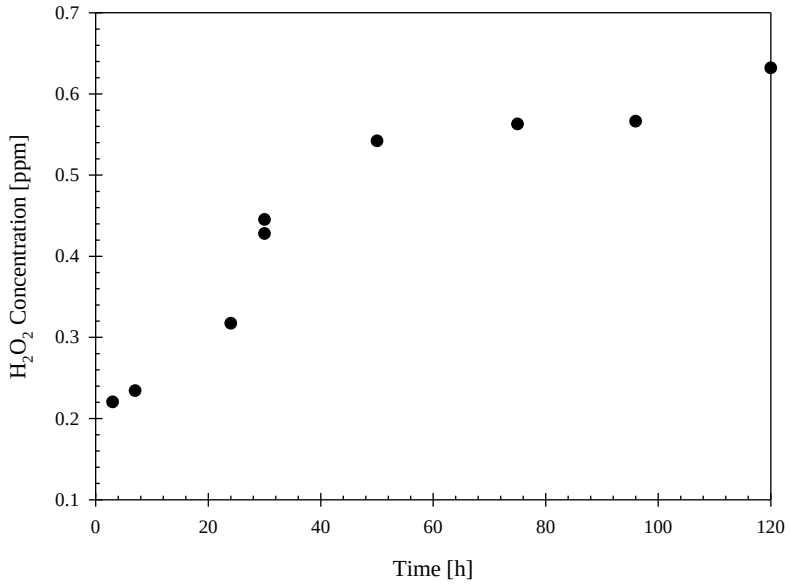

Figure 4-9: The concentration in ppm of the hydrogen peroxide produced in the column as a function of time.

The amount of hydrogen peroxide formed at steady state is 0.55 ppm, however an increase can be seen between 100-120 hours and this is due to a spike in oxygen overnight in which the oxygen flowrate was increased to 0.4 L/min. This increased the hydrogen peroxide formation to 0.63 ppm at sampling time. It is thought that, given time, the peroxide formation would increase past 1 ppm because the previous column test produced 1 ppm hydrogen peroxide with a 0.3 L/min oxygen flowrate.

4.3 Effect of Hydrogen Peroxide Produced from Activated Carbon on Arsenic Oxidation

4.3.1 Experimental Methods

4.3.1.1 Hydrogen Peroxide Desorption Tests

The amount of hydrogen peroxide produced on the activated carbon surface with and without the introduction of oxygen was studied.

This set of experiments was based on a procedure outlined in a paper by Lamb and Elder (1931). Peroxide in charcoal was studied by mixing 2 g of charcoal in 100 mL of distilled water for five minutes in a stream of air, separating the charcoal from solution and then placing the charcoal in water and sulphuric acid of varying acidity. The charcoal was removed and the filtrates were mixed with an acidified starch-iodide solution (Lamb & Elder, 1931). No colour change was evident with water as the filtrate, but a deep colour was produced with 0.5, 1.0, 1.5 and 2.0 M sulphuric acid solutions. However, it was stated that the optimum sulphuric acid concentration (based on colour intensity) was 1.0 M and so conclusions were drawn that a peroxide is present in charcoal which is most soluble or active in 1.0 M sulphuric acid solutions (Lamb & Elder, 1931).

In this experiment, two flasks were prepared with 40.0 g of pre-wetted and pre-attrited activated carbon. Each flask had 100 mL of pH 1.0 sulphuric acid solution added to the carbon and the solution was stirred at 250 rpm for one hour. A sample of the initial solution was titrated with potassium permanganate for peroxide to verify that the starting solution did not contain any of the species under investigation. The liquid and carbon were separated. The filtrate was assayed for hydrogen peroxide and the carbon was immersed in 100 mL of 1.0 M sulphuric acid and shaken for 5 minutes. The solution and the carbon were separated and the stripped solution was then titrated for hydrogen peroxide. Flask A was stirred at 250 rpm with no aeration and flask B was stirred at 250 rpm with 0.2 L/min of industrial oxygen gas.

Potassium permanganate titration is a common method for hydrogen peroxide quantification as the detection limit is as low as 3 µM of hydrogen peroxide (Klassen, Marchington, & Mcgowan, 1994).

A potassium permanganate solution of 0.020 M was prepared using potassium permanganate crystals from BDH and DI water.

The stoichiometric equation used to characterize the reaction is shown in Equation 17:

$$2MnO_4^- + 5H_2O_2 + 6H^+ \rightarrow 2Mn^{2+} + 8H_2O + 5O_2 \quad \textbf{Equation 17}$$

The colour of the titrant is a deep purple. When added to a beaker containing hydrogen peroxide, the deep purple colour of potassium permanganate vanishes and the mixture remains clear until the end point is reached, which is signified by the solution turning a pale pink/brown colour.

4.3.1.2 Batch Test with no Activated Carbon

A 1 L solution containing 2 g/L As (III) was brought to a pH of 1.0 and added to a 2 L batch reactor. An overhead mixer was used to stir the solution at 200 rpm while industrial oxygen was sparged at 0.2 L/min. The top of the reactor was covered in parafilm to minimize spray and losses due to evaporation. Samples were taken at 0, 0.5, 1, 2, 4, 8 and 24 hours for arsenic concentration and speciation. The pH was also recorded at the sampling times.

4.3.1.3 Arsenic Adsorption Shake Tests

The arsenic adsorption test measured the amount of total arsenic adsorbed on the carbon surface and the arsenite and arsenate still in solution without the introduction of oxygen. Three flasks were prepared: flask 1 had 2 g/L As (III), flask 2 had 2 g/L As (V) and flask 3 had 2 g/L As (III) and As (V). All solutions were initially at a pH of 1.0 ± 0.1.

90.0 g of wet carbon was weighed into 250 mL Erlenmeyer flasks and the respective solution was added to the flask. The flasks were shaken on a table shaker at a stir rate of 200 rpm for the first 15 minutes and then 250 rpm for the remainder of the test. Samples were taken at 0, 15, 30, 45, 60, 90, 120, 180 and 240 minutes. The pH and dissolved oxygen (DO) were also recorded for specific times. The DO meter used was a Fisher Scientific portable dissolved oxygen meter.

4.3.1.4 Arsenic Speciation on the Carbon Surface

Arsenic desorption tests were done to see which arsenic oxidation preferentially desorbed from activated carbon. Three solutions of 100 mL were prepared in 100 mL volumetric flasks: flask 1 was 2 g/L As (III), flask 2 was 2 g/L As (III) and 2 g/L As (V), and flask 3 was 1 g/L As (III) and 1 g/L As (V). Each solution was adjusted to a pH of 1 via sulphuric acid additions. Next, 45.0 g of wet carbon was added to an Erlenmeyer flask. The respective solution was poured into the flask and shaken at 250 rpm for 60 minutes. The solution was removed via a vacuum pump and 1.0 M sulphuric acid was added to the carbon. The mixture was shaken for 5 minutes and the solution was once again separated from the carbon. ICP analysis and arsenic titration were done on the initial solution, the filtrate and the stripped solution.

4.3.2 Results and Discussion

4.3.2.1 Hydrogen Peroxide Desorption

The results from the hydrogen peroxide stirring tests are presented in Figure 4-10. The results are interesting because they indicate that the activated carbon in flask A, which does not have extra oxygen added into the system, has a limited ability to produce hydrogen peroxide even without the introduction of oxygen into the system. This ability to produce a small amount of peroxide can be attributed to either the dissolved oxygen in solution or the functional groups present on the activated carbon surface.

The error associated with the titrations is approximately 0.9 mg/L and this was determined by averaging the peroxide measured in the initial solution. From UV-Vis experiments it is known that there is no peroxide present in pH 1 sulphuric acid solutions, so the values of peroxide calculated for the initial solution via potassium permanganate titration are due to adding a single drop of titrant to the acidic solution.

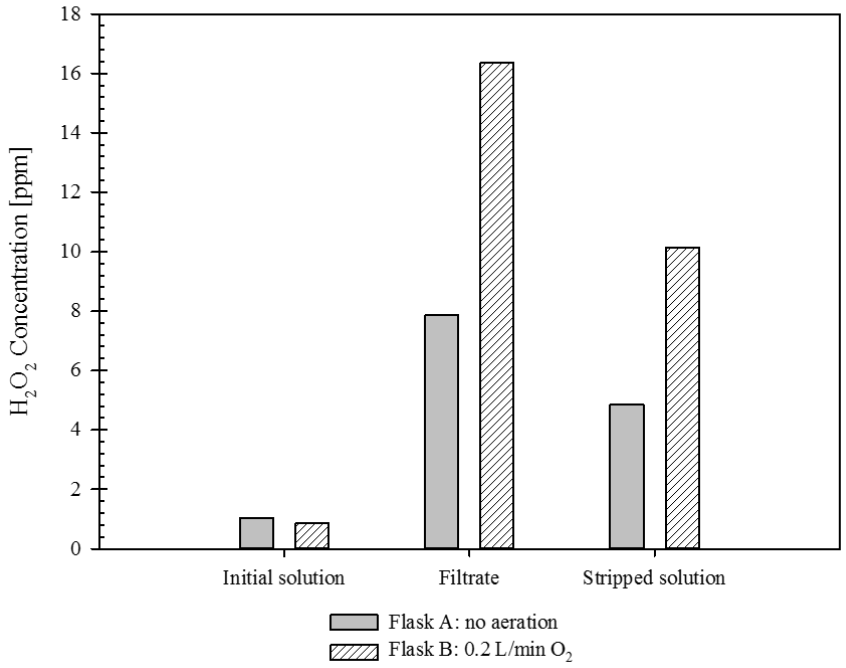

Figure 4-10: Hydrogen peroxide produced on activated carbon and desorbed into the solution with and without oxygen; flask A was not aerated and flask B was initially aerated with 0.2 L/min oxygen.

Flask B produced over 16 mg/L of hydrogen peroxide which is substantially more than what was measured in the column tests. Interestingly, the test with no oxygen added also produced hydrogen peroxide, though to a much smaller degree. The surface of activated carbon is extremely porous and it has a high surface area relative to its mass. The high porosity may allow for oxygen to become trapped in the macro- and micro- pores. The oxygen can exist as free gas in the pores or as a part of the carbon structure due to various carbon-oxygen bonds.

For both flasks the stripped solution contained approximately 62% of the hydrogen peroxide concentration that was in the filtrate. This indicates that the peroxide in the stripped solution is contributed by the oxygenated carbon surface rather than the trapped oxygen in the carbon surface pores. If it was solely the trapped oxygen that subsequently dissolved in solution then the amount of peroxide formed in both flasks should have been equal because there was no oxygen added during the second

phase of these experiments. Dissolved oxygen in solution may also be a contributing factor to the peroxide formation, but it alone likely does not supply enough oxidative force to oxidize arsenite to arsenate without the use of a catalyst so there must be another phenomena occurring. The standard Gibbs free energy of the oxidation reaction with oxygen, as seen in Equation 18, gives insight into the spontaneity of the reaction:

$$\mathbf{H_3AsO_3 + \frac{1}{2}O_2 \rightarrow H_3AsO_4} \qquad \textbf{Equation 18}$$

The standard Gibbs free energy values of the arsenic species in the reaction described by Equation 18 are shown in Table 8; the standard Gibbs free energy of oxygen (O_2) is 0 kJ/mol.

Table 8: Standard Gibbs free energy values for the oxidation of arsenic at 298.15 K and 1 bar (Henke, 2009)

Species	Standard Gibbs Free Energy [kJ/mol]
H_3AsO_3	-639.8
H_3AsO_4	-766.3

The standard Gibbs free energy of the reaction in Equation 18 is determined by subtracting the standard Gibbs free energy of the reactants from the products which yields a standard Gibbs free energy value of -126.5 kJ/mol. The standard Gibbs free energy of the arsenic oxidation reaction with oxygen as the oxidant is negative which means that the reaction can proceed as written without the addition of a catalyst or a change of conditions (temperature or pressure). However, the standard Gibbs free energy does not take into account the kinetics of the reaction because it assumes the system is at equilibrium, so although the reaction could theoretically proceed as written the kinetics of arsenic oxidation in these conditions is extremely slow and therefore do not predominantly contribute to the oxidation of arsenic.

In a solution that contains carbon and that is simultaneously being sparged with oxygen there will be at least two types of oxygen present: dissolved oxygen in the liquid medium as well as adsorbed oxygen on the carbon surface. A study on pyrite oxidation proposed that adsorbed oxygen could react with protons and electrons in solution which yields hydrogen peroxide which is adsorbed on the surface (Schoonen,

Harrington, Laffers, & Strongin, 2010). In the study by Schoonen et al (2010), the results indicate that hydrogen peroxide is an intermediate compound produced during the oxidation of pyrite when dissolved molecular oxygen is present. The hydrogen peroxide may further react with a proton and an electron to form water and a hydroxyl radical which is adsorbed onto the surface. The hydroxyl radical may then react with another proton and electron to form water. Equations 19-22 show the full cycle of peroxide and hydroxyl formation (Schoonen et al., 2010).

$$\mathbf{O_{2_{ads}} + 2e^- + 2H^+ \rightarrow H_2O_{2(ads)}} \qquad \textbf{Equation 19}$$

$$\mathbf{H_2O_{2(ads)} + 2H^+ + 2e^- \rightarrow 2H_2O_{(l)}} \qquad \textbf{Equation 20}$$

$$\mathbf{H_2O_{2(ads)} + H^+ + e^- \rightarrow H_2O_{(l)} + OH_{(ads)}} \qquad \textbf{Equation 21}$$

$$\mathbf{OH_{(ads)} + H^+ + e^- \rightarrow H_2O_{(l)}} \qquad \textbf{Equation 22}$$

Studies employing XPS and IR show that molecular oxygen can adsorb onto the surface of carbon and form O_2^-. These ions can then subsequently react with the carbon surface to produce surface groups or further react with protons in solution to form water or hydrogen peroxide (Biniak, Szymański, Siedlewski, & Światkoski, 1997).

Hydrogen peroxide and hydroxyl radicals are known to be effective oxidants containing oxygen so the biomedical research field has named them, as well as the superoxide $O_2^{\bullet-}$, as reactive oxygen species (ROS) because of their affinity to react with biomolecules (Schoonen et al., 2010). In the case of arsenic oxidation, it has been shown in this chapter that peroxide does exist within the system. Further studies on the pH of the system will be investigated.

4.3.2.2 Batch Test with no Activated Carbon

A batch test was conducted with no activated carbon present in order to confirm that carbon is a catalyst for arsenic oxidation and that dissolved oxygen in an aerated solution is not sufficient as the sole oxidizing force for arsenic oxidation. This test was conducted in a 2 L batch reactor with a flow rate of 0.2 L/min O_2. The amount of arsenite in solution did not vary over the 24 hour test period which indicates

that no oxidation had occurred, as illustrated in Figure 4-11. The ORP of the system started at 459 mV vs Ag/AgCl and decreased to 417 mV at the end of the 24 hour test. The pH stayed constant between 1.0 and 1.1 for the first 8 hours, but at the 24 hour sample the pH measured was 1.3. It was not uncommon for the pH of the system to reach 1.4-1.8 at the end of a batch test as it is believed that this range of acidity is the buffering pH of the system.

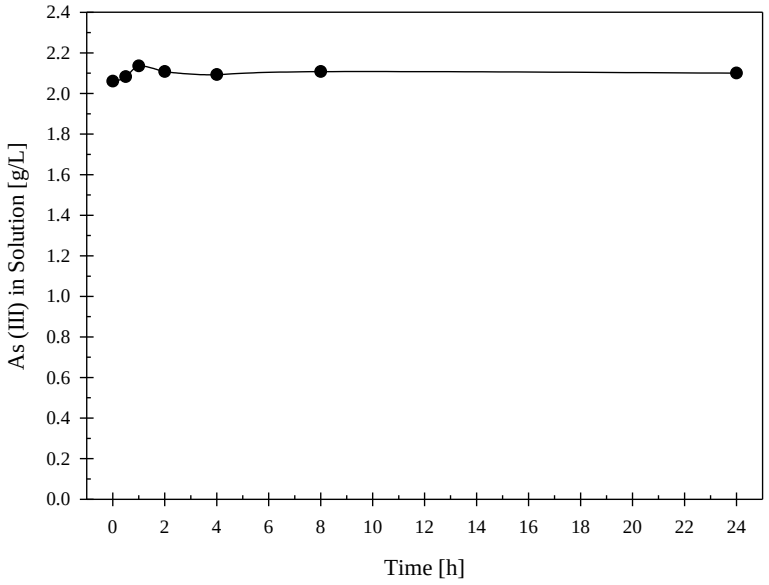

Figure 4-11: As (III) in solution with respect to time during a batch test without activated carbon added.

From Figure 4-11 it is clear that the dissolved oxygen which can be generated via oxygen aeration is not alone able to effectively oxidize arsenic. However, it may be possible that the dissolved oxygen reacts with the carbon surface to generate or replenish functional groups that are capable of effectively oxidizing arsenic. A study on pyrite oxidation proposed that adsorbed oxygen could react with protons and electrons in solution to yield hydrogen peroxide which is then adsorbed on the surface (Schoonen et al., 2010).

4.3.2.3 Arsenic Adsorption Shake Tests

A shake test to investigate the adsorption characteristics of arsenite and arsenate was performed. Three flasks were prepared with initial conditions as presented in Table 9.

Table 9: Initial conditions and final pH values for arsenic adsorption tests

Flask	Arsenic concentration	Initial pH	Final pH	Initial dissolved oxygen [mg/L]
1	2 g/L As (III)	1.0	2.03	8.2
2	2 g/L As (V)	1.0	2.04	8.5
3	2 g/L As (III) 2 g/L As (V)	1.0	1.76	8.4

The shake tests were conducted over four hours. The final pH of each of the flasks was higher than the beginning: flask 1 increased to a pH of 2.0, flask 2 to 2.0, and flask 3 to 1.8. As shown in Figure 4-12, there was no significant difference between the adsorption rates of the three flasks; however, flask 2 had slightly more arsenic adsorbed, on average, compared to flask 1 which indicates that arsenate has a higher affinity to adsorb onto activated carbon in these specific test conditions.

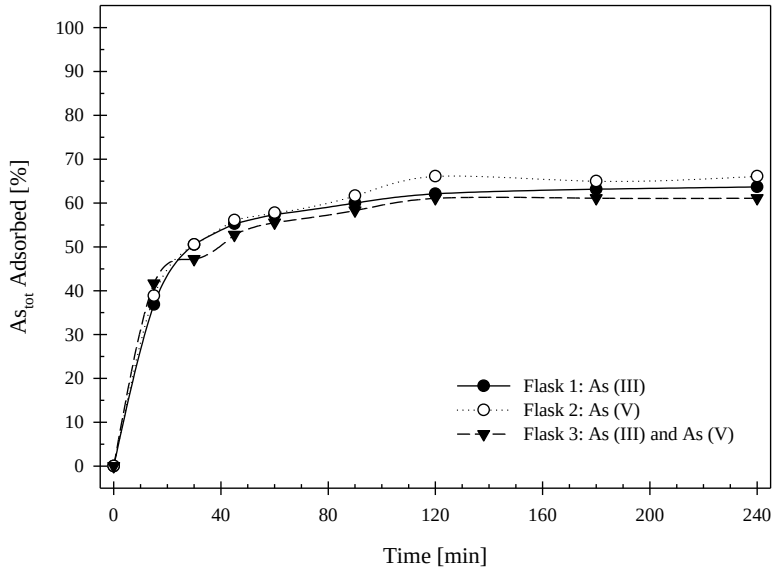

Figure 4-12: The percent of total arsenic adsorbed onto activated carbon as a function of time for solutions containing: As (III), As (V) and a mixture of As (III) and As (V), respectively.

Figure 4-12 only looks at the total arsenic that was originally in the solution rather than the speciation of arsenic in solution. A more thorough investigation shows the solution composition of each flask which is presented in Figure 4-13.

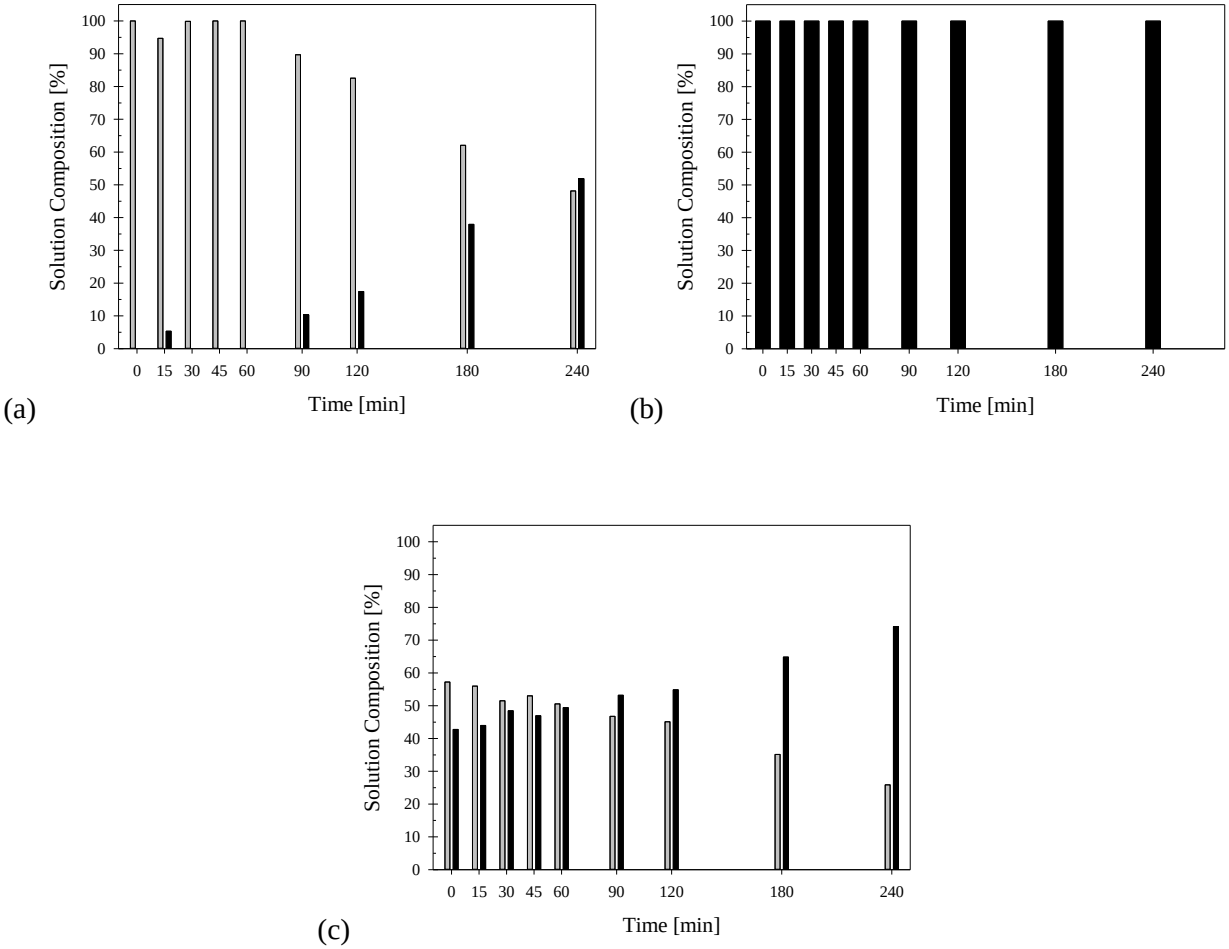

Figure 4-13: Arsenic speciation of the solution in (a) flask 1: As (III) (b) flask 2: As (V) and (c) flask 3: As (III) and As (V); the grey bars indicate the amount of arsenite in solution and the black bars indicate the arsenate in solution.

It appears that the arsenic in solution is slowly oxidized to form arsenate. In flask 1 arsenate does not appear in the solution until the 90 min sampling point with the exception of a small amount of arsenate detected at 15 minutes which is likely due to errors associated with titration and ICP analysis. The percentage of arsenate in flask 3 also increases starting at the 90 min sampling time. Figure 4-14 illustrates the efficiency of arsenic oxidation in the solution for flask 1 and flask 3. Although the oxidation

efficiency of the solution is continually increased for flasks 1 and 3, the total amount of arsenic in solution is drastically reduced during the first 45 minutes due to adsorption (Figure 4-12).

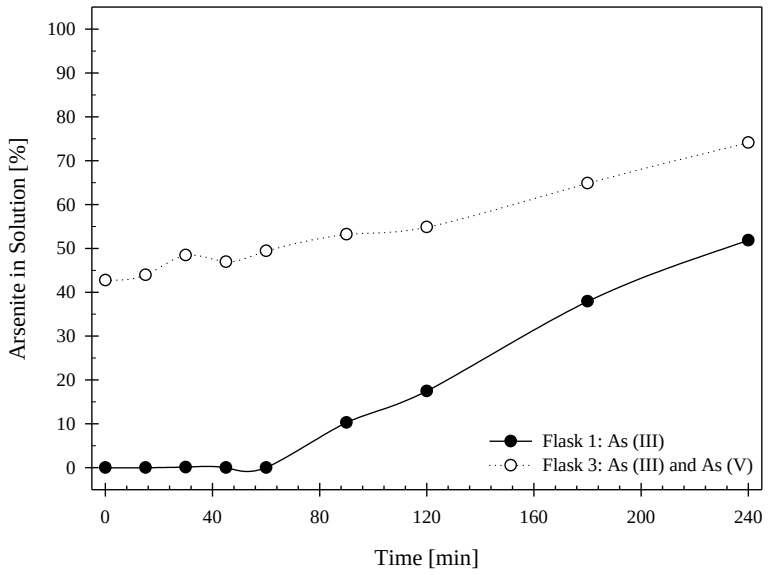

Figure 4-14: The speciation of arsenic in solution as a function of time.

Figure 4-15 compares the amount of total arsenic adsorbed on the carbon surface and the amount of arsenic oxidized in solution on a percentage basis for flask 1 which initially contained arsenite and flask 3 which initially contained arsenite and arsenate (Figure 4-15(a) and Figure 4-15(b), respectively). It is evident from these graphs that arsenic in solution is not oxidized until the adsorption curve has essentially plateaued for both flask 1 and flask 3. This is perhaps due to the higher affinity for arsenite to adsorb onto the activated carbon surface, so for the first sampling times all of the arsenic that had oxidized to arsenate had already instantly adsorbed on the surface of carbon.

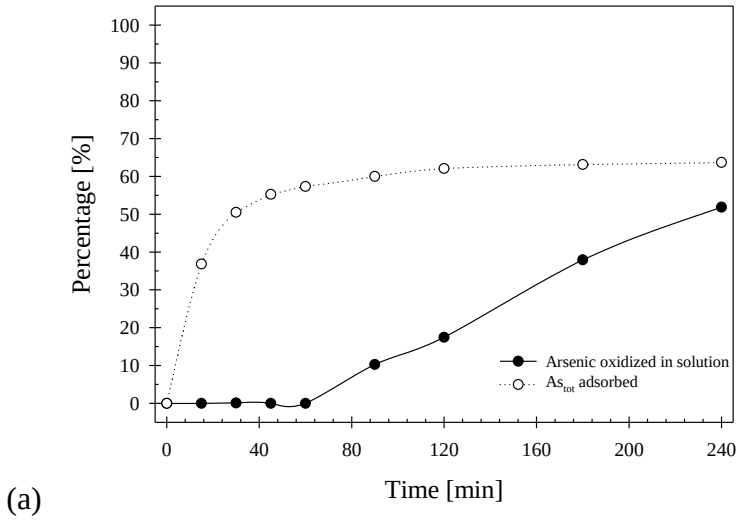

(a)

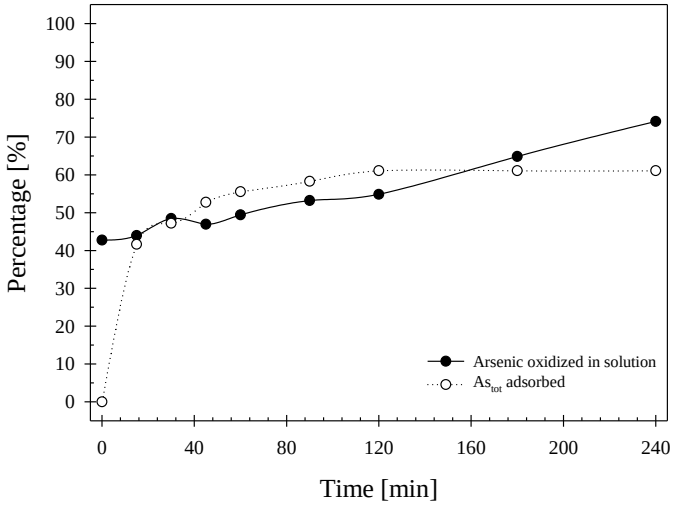

(b)

Figure 4-15: Comparison of the % of total arsenic adsorbed and % of arsenic oxidized in solution for (a) flask 1 which contains 2 g/L As (III) and (b) flask 3 which contains 2 g/L of As (III) and 2 g/L As (V).

The dissolved oxygen of the three flasks was monitored during the test. Each flask started with a dissolved oxygen content between 8.2-8.5 mg/L which is expected at ambient conditions. The dissolved oxygen decreased over the first hour of tests and then fluctuated between 7.1-7.9 mg/L depending on the flask. Figure 4-16 shows the dissolved oxygen of each flask throughout the duration of the test.

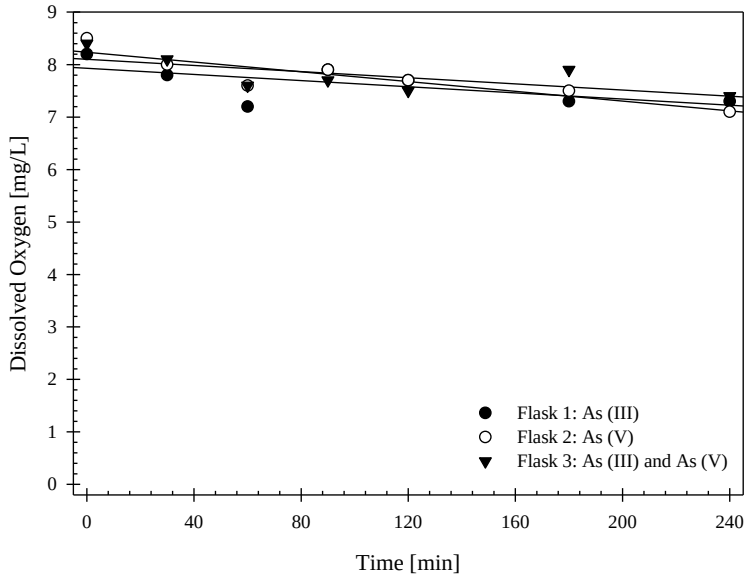

Figure 4-16: DO of flasks 1-3 in which flask 1 contained As (III), flask 2 contained As (V) and flask 3 contained equal amounts of As (III) and As (V); linear trend lines are included.

There is no oxygen being introduced into any of the flasks so it is possible that the dissolved oxygen in solution is being used to create hydrogen peroxide which subsequently oxidizes the arsenite. Ahumada et al (2002) studied the oxidation of ferrous to ferric in the presence of activated carbon. Experiments showed that the iron was oxidized by either the hydrogen peroxide produced or by the catalytic ability of carbon (Ahumada et al., 2002). Activated carbon chemistry is very complex and therefore it is difficult to confidently state the exact mechanism of oxidation; however, it can be confirmed that the arsenic oxidation is due to interactions with the functional groups and oxidants on the activated carbon surface.

4.4 Arsenic Speciation on the Carbon Surface

The oxidation of arsenic in solution seemingly follows a trend in which the arsenic in solution is not of the pentavalent oxidation state until the arsenic adsorption has reached equilibrium which is seen as a plateau in Figure 4-15(a) and (b). From the arsenic adsorption tests it is evident that arsenate does not exist in solution until after 90 minutes of stirring/mixing the system.

4.4.1 Shake Tests for Arsenic Desorption

A shake test was performed to determine the amount of arsenic adsorbed on activated carbon after 1 hour and to determine the speciation of arsenic on the carbon surface. If arsenate exists on the surface of the activated carbon then there are two possibilities going forward regarding the mechanism of arsenic oxidation. The first mechanism is that the arsenic contacts the peroxide and/or oxidative functional group on the carbon surface and is oxidized. The arsenate ion then adsorbs onto the activated carbon due to its proximity to the carbon surface. The second mechanism is that the arsenite ion first adsorbs onto the activated carbon surface and is subsequently oxidized to arsenate where it then remains on the carbon surface until it is desorbed. Regardless, it is clear that the arsenic must make contact with the activated carbon in order to oxidize or else it would also exist in solution as the affinity for arsenate to adsorb onto activated carbon is only slightly more than that of arsenite.

Three flasks were prepared for the arsenic desorption speciation test. Flask A had 2 g/L As (III), flask B had 2 g/L As (III) and 2 g/L As (V), and flask C had 1 g/L As (III) and 1 g/L As (V). Three solutions were analyzed for As (III) and total arsenic: the initial solution, the filtrate and the stripped solution. The filtrate solution is the solution that was separated via vacuum filtration after 1 hour of contact between the initial solution and the carbon. The stripped solution is the resulting solution of a 1.0 M sulphuric acid solution that was added to the impregnated carbon and mixed for 5 minutes to desorb the arsenic from the carbon surface. The total arsenic in each flask for the three solutions can be seen in Figure 4-17.

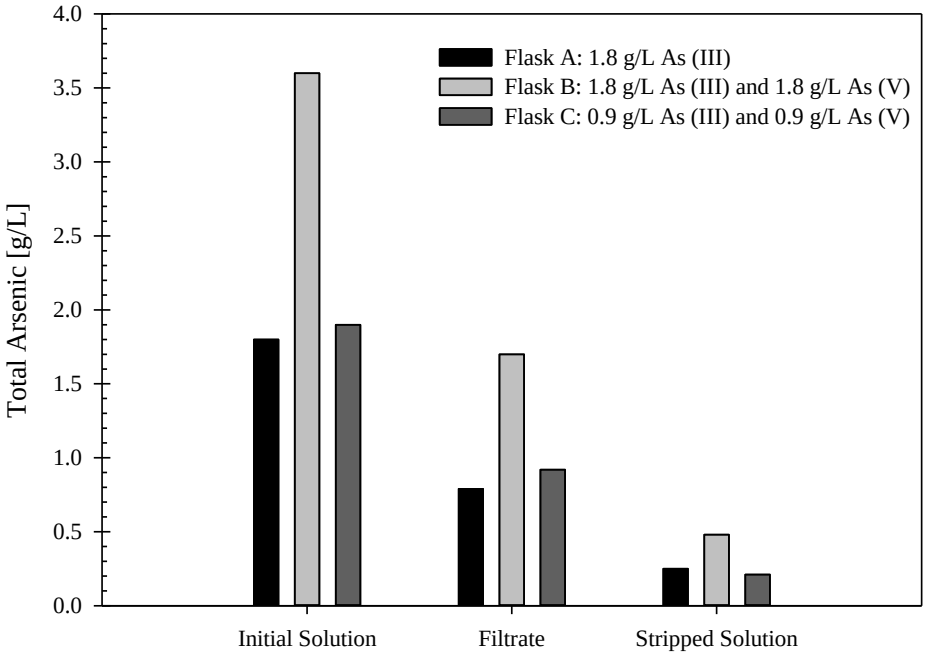

Figure 4-17: Total arsenic in the initial solution, filtrate and stripped solution.

The percent of arsenic adsorbed onto the activated carbon and the respective recoveries of the stripped solution compared to the filtrate can be seen in Table 10. There is no trend evident with respect to the total arsenic adsorbed to the carbon or recovered in the stripped solution. The recovered arsenic is not a complete recovery and therefore a mass balance on arsenic cannot be achieved. However, the speciation of arsenic desorbed can give insight into the type of arsenic that is preferentially desorbed from the activated carbon surface.

Table 10: Adsorption and recoveries of arsenic in the desorption flask tests

Flask	Initial Arsenic Concentration	Initial pH	% Adsorbed	% Recovered
A	2 g/L As (III)	1.0	56.1	24.8
B	2 g/L As (III) 2 g/L As (V)	1.1	52.8	25.3
C	1 g/L As (III) 1 g/L As (V)	1.1	51.6	21.4

The changes in solution composition are interesting. Table 11 summarizes the composition of arsenic species in each of the flasks. In flask A the arsenic in the filtrate is 98% As (III) and 2% As (V) but the As (V) percentage of the stripped solution is 13.7 % which reveals that there is oxidized arsenic on the carbon surface before there is oxidized arsenic in solution. This finding is significant because it supports the hypothesis that arsenate is produced early in the oxidation process but is adsorbed to the activated carbon surface and, therefore, does not appear in the solution until later. This could be due to two scenarios: (1) arsenic is oxidized while in solution and is then instantly adsorbed onto the activated carbon surface or (2) As (III) adsorbs onto the carbon surface and is then oxidized by oxygenated surface functional groups. The As (V) would then remain on the carbon surface until the surface is saturated with 50% As (III) and 50% As (V) at which point the As (V) desorbs into the solution.

The composition of arsenic in the stripped solutions is presented in Figure 4-18. As discussed, the arsenate desorbed from the carbon increased in flask A. Flask B and flask C, although both having slightly different initial solutions and filtrate solutions, have the same stripped solution composition. The results prove that the interactions holding the arsenite to carbon are weaker than those holding the arsenate to the carbon as the arsenate in the stripped solution is 7-7.5% less than that of arsenite.

Table 11: Solution composition of flasks A, B and C

		% As (III)	% As (V)
Flask A	Initial Solution	100.0	0.0
	Filtrate	98.0	2.0
	Stripped Solution	86.3	13.7
Flask B	Initial Solution	57.9	42.1
	Filtrate	47.3	52.7
	Stripped Solution	53.7	46.3
Flask C	Initial Solution	48.5	51.5
	Filtrate	55.1	44.9
	Stripped Solution	53.5	46.5

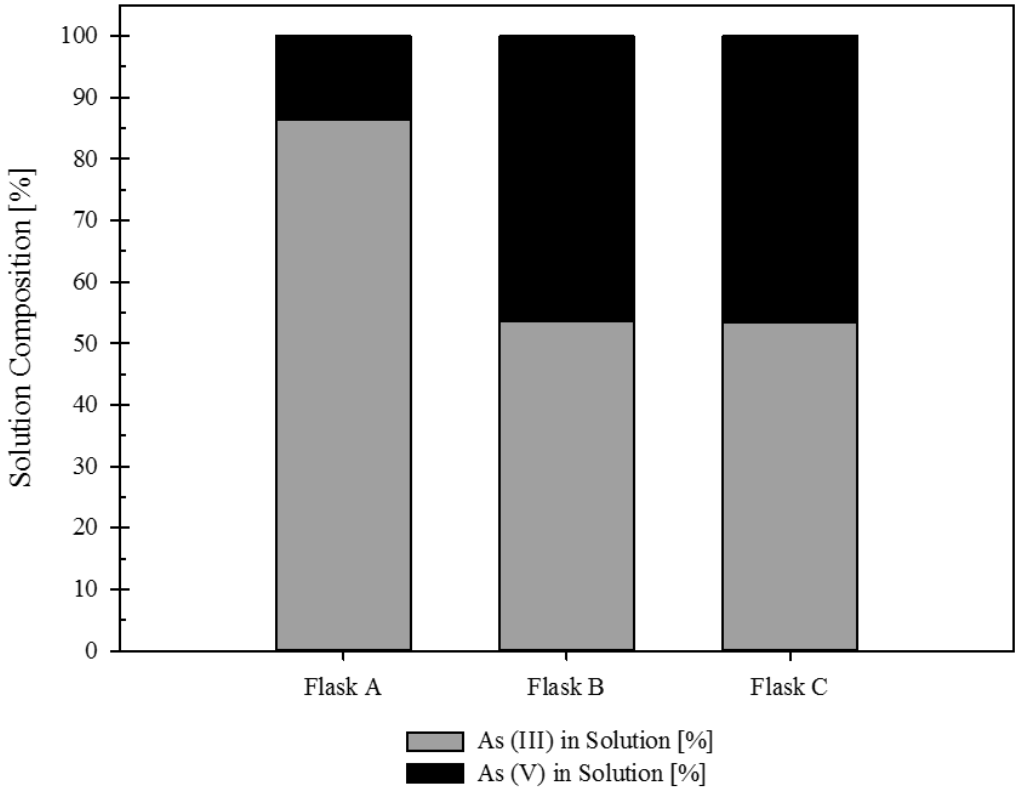

Figure 4-18: Solution composition in the stripped solution for flasks A, B and C.

The solution used to strip the arsenic from activated carbon was a 1.0 M sulphuric acid solution with a pH of less than 1. The dominant arsenate species at pH 1 is H_3AsO_4 (Molnár et al., 1994; Smedley & Kinniburgh, 2002). Using this information, the following equations predict the reaction pathway of arsenic oxidation for the two proposed oxidation scenarios. Both cases assume that there is an oxidant, such as hydrogen peroxide, present. Equations 23 and 24 propose the reaction pathway for the case where arsenite is oxidized to arsenate in solution and then adsorbs as arsenate.

$$\mathbf{H_3AsO_3 + H_2O_2 \rightarrow H_3AsO_4 + H_2O} \qquad \textbf{Equation 23}$$

$$\mathbf{H_3AsO_4 \xrightarrow{carbon\ surface} H_3AsO_{4(ads)}} \qquad \textbf{Equation 24}$$

Equations 25 and 26 predict the reaction pathway for the case in which arsenite is adsorbed on the carbon surface and is then oxidized to arsenate.

$$H_3AsO_3 \xrightarrow{\text{carbon surface}} H_3AsO_{3(ads)} \qquad \textbf{Equation 25}$$

$$H_3AsO_{3(ads)} + H_2O_2 \rightarrow H_3AsO_{4(ads)} + H_2O \qquad \textbf{Equation 26}$$

4.4.2 XPS for Arsenic Speciation

XPS was conducted on one pellet sample and three powdered samples. The carbon pellet was subjected to an arsenic solution, whereas the powder samples were subjected to 5 g/L arsenite (sample 1), 5 g/L arsenate (sample 2) and 5 g/L arsenite and 5 g/L arsenate (sample 3).

A full spectrum scan, Figure 4-19, clearly shows the carbon and oxygen peaks in each of the samples. However, the wide scan does not depict the peaks for sulphur, nitrogen or arsenic.

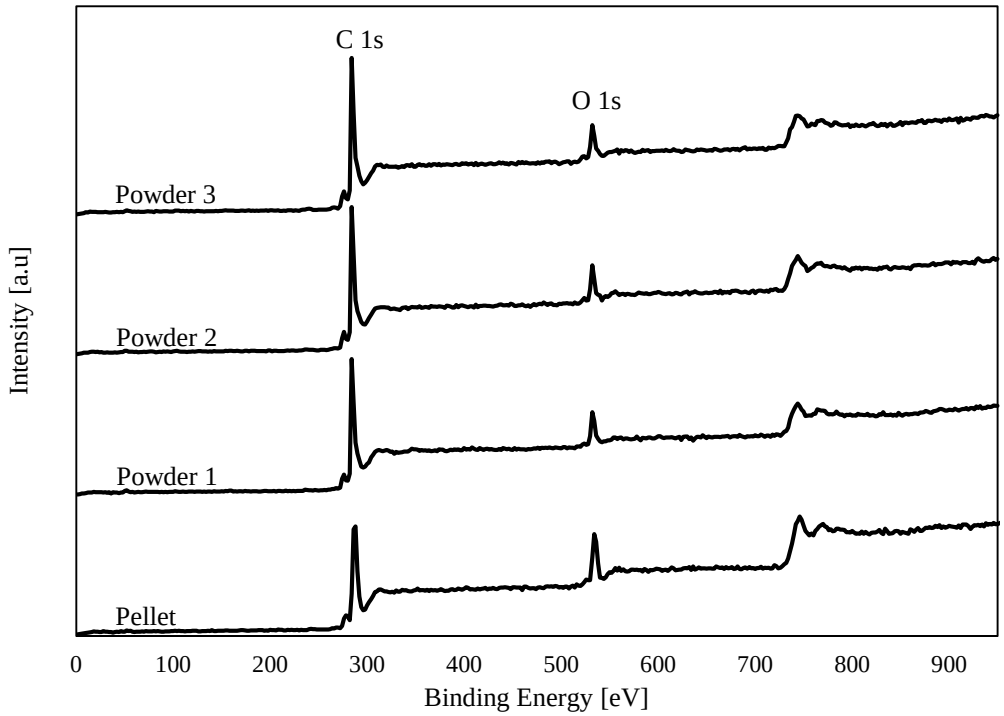

Figure 4-19: XPS spectra for four samples which have come into contact with varying concentrations and speciation of arsenic; the carbon and oxygen peaks are labeled.

Figure 4-20 to Figure 4-24 show the individual elemental peaks for each of the samples. Figure 4-20 shows the N 1s peaks for each of the powdered samples and there is no appreciable difference between the peaks. Figure 4-21 depicts the As 3d peaks for all four samples. The pellet sample has a smaller scan range and shows a lot of background range due to the nature of the pellet. The pellet snapped under vacuum which is why the rest of the XPS analysis was conducted on powdered samples. There is clearly no arsenic peak seen from the pellet sample in Figure 4-21 and this is likely due to the nature of the sample. There is no sulphur detected in Figure 4-22 because the samples were washed with DI water prior to analysis to remove acidic species and this also removed the sulphur species that would have otherwise been present, such as SO_4^{2-}. Figure 4-23 illustrates the O 1s peak for each of the samples and Figure 4-24 shows the C 1s peak for each sample. There does not seem to be a noticeable difference between the samples but further analysis will be done by fitting Gaussian-Lorentzian curves to the peaks.

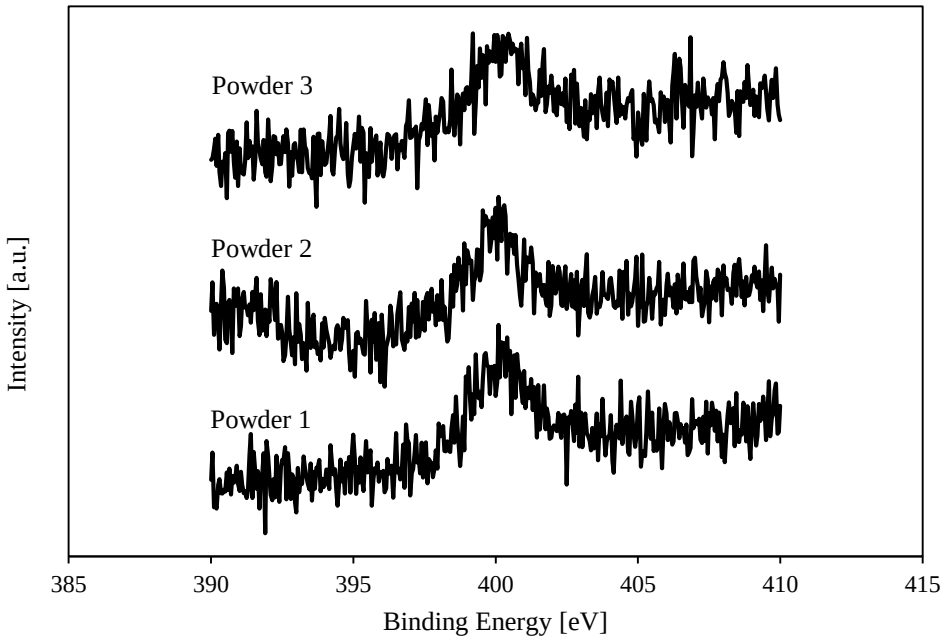

Figure 4-20: Comparison of N 1s peaks on the powdered activated carbon samples.

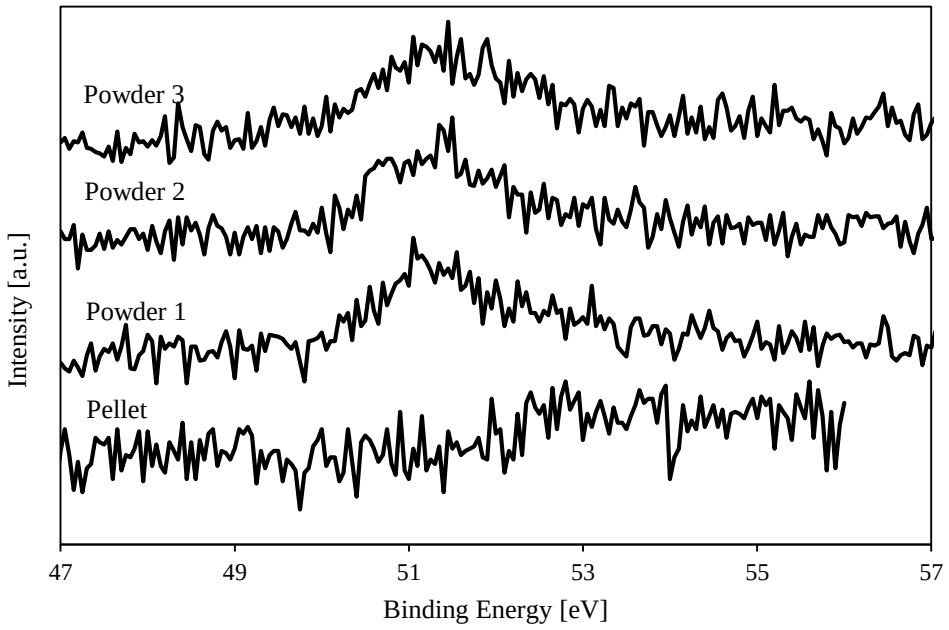

Figure 4-21: Comparison of As 3d peaks on the activated carbon samples.

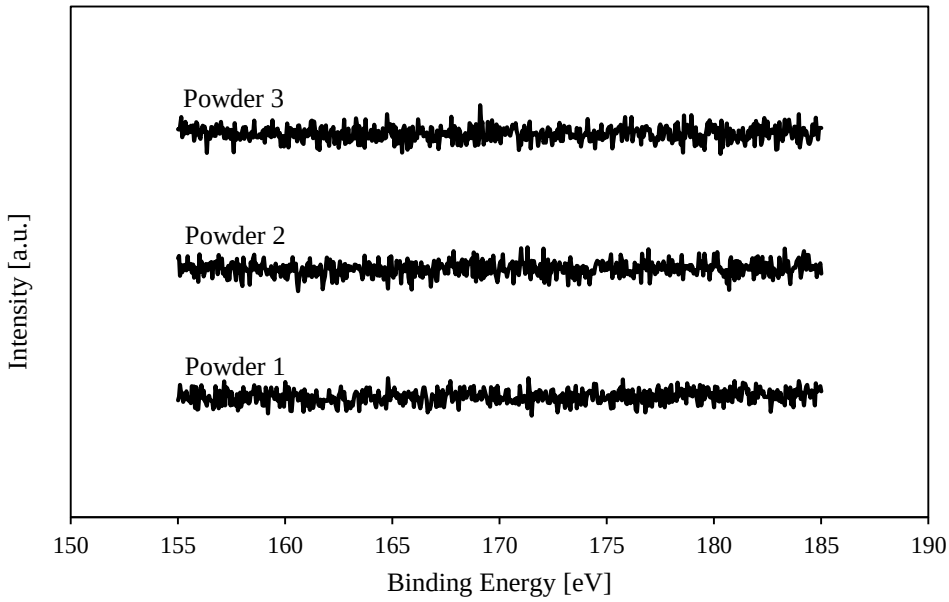

Figure 4-22: Comparison of S 2p peaks on the powdered activated carbon samples; there is no sulphur present.

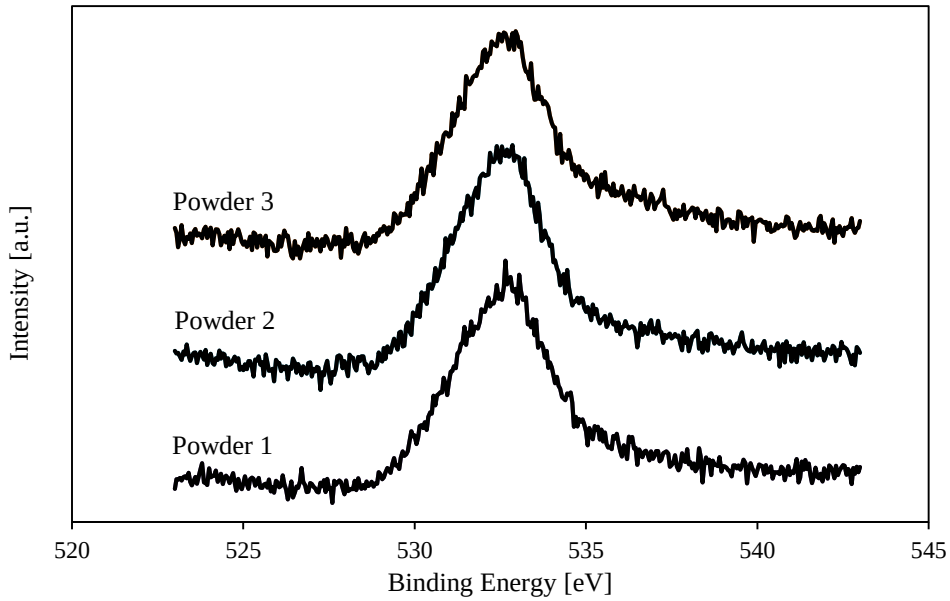

Figure 4-23: Comparison of O 1s peaks on the powdered activated carbon samples.

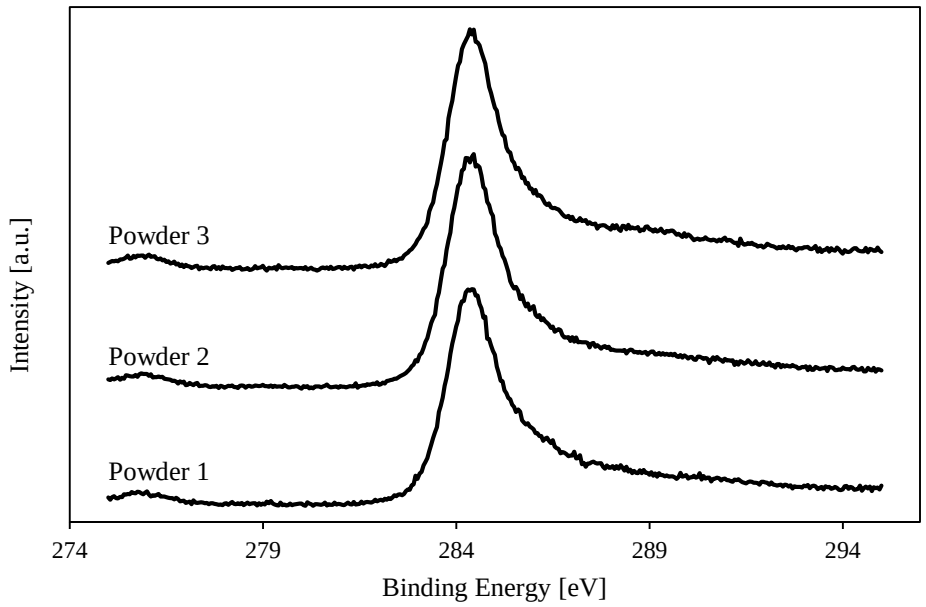

Figure 4-24: Comparison of C 1s peaks on the powdered activated carbon surface.

The peaks of the elements of interest for the powdered sample 1 are presented in Figure 4-25.

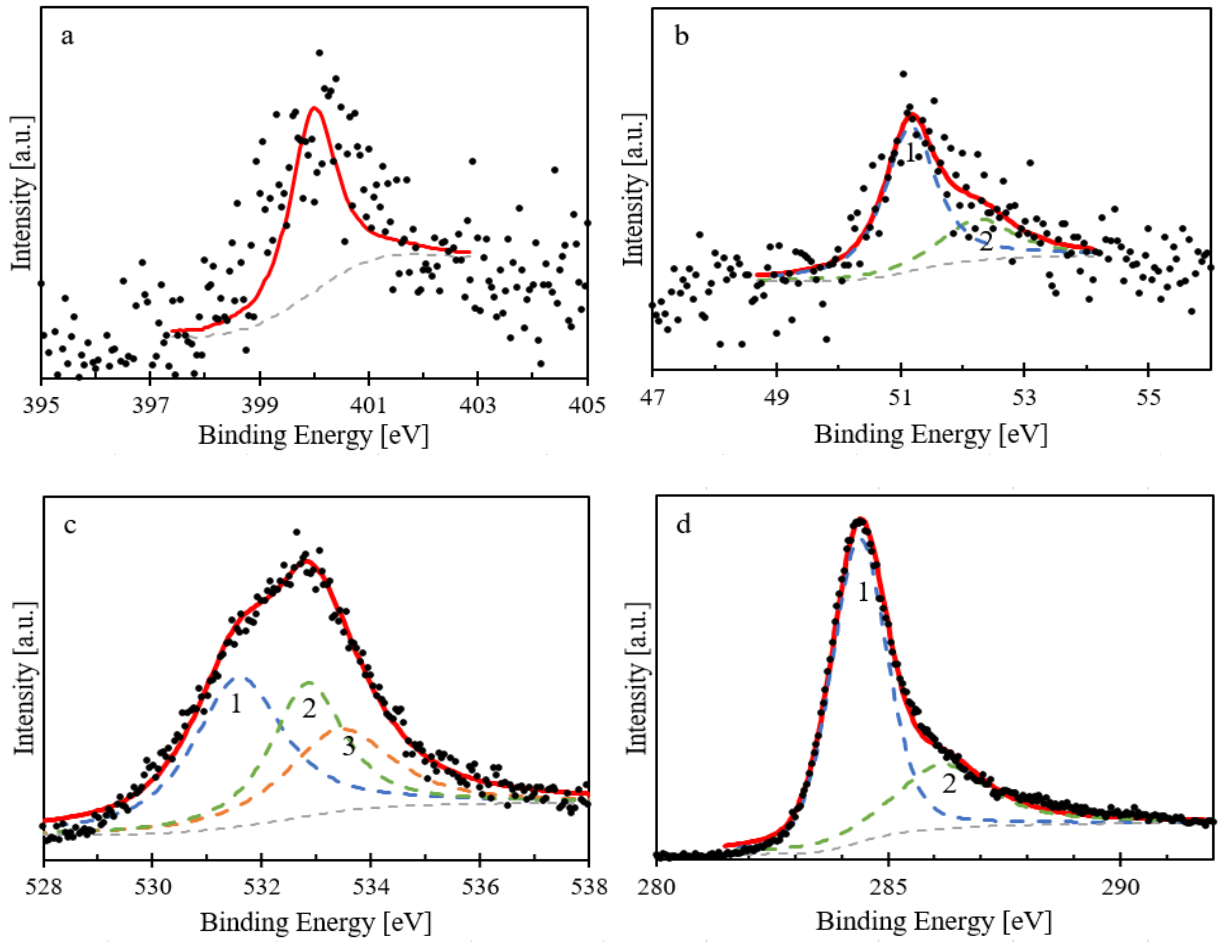

Figure 4-25: Sample 1 spectrum scans for (a) N 1s, (b) As 3d, (c) O 1s, and (d) C 1s. Samples were treated with 5 g/L arsenite solution.

The tail of each curve is denoted by a dashed grey line and the summed peak is represented by a solid red line. The N 1s peak is 400.0 eV, the As 3d peak is 51.2 eV, the O 1s peak is 532.8 eV and the C 1s peak is 284.4 eV. The summed peaks presented in Figure 4-25(b)-(d) are further broken down into more peaks to better describe the system. Table 12 presents the individual and summed peak binding energy values, and Table 13 lists the area under each of the curves according to analysis conducted on XPSPeak 4.1 as well as the percentage of each peak in relation to the summed peak. Figure 4-26 and Figure 4-27 show the sample 2 and sample 3 spectrum scans, respectively, for (a) N 1s, (b) As 3d, (c) O 1s, and (d) C 1s. Sample 2 was treated with a 5 g/L arsenate and sample 3 was treated with a 5 g/L arsenite and 5 g/L arsenate solution.

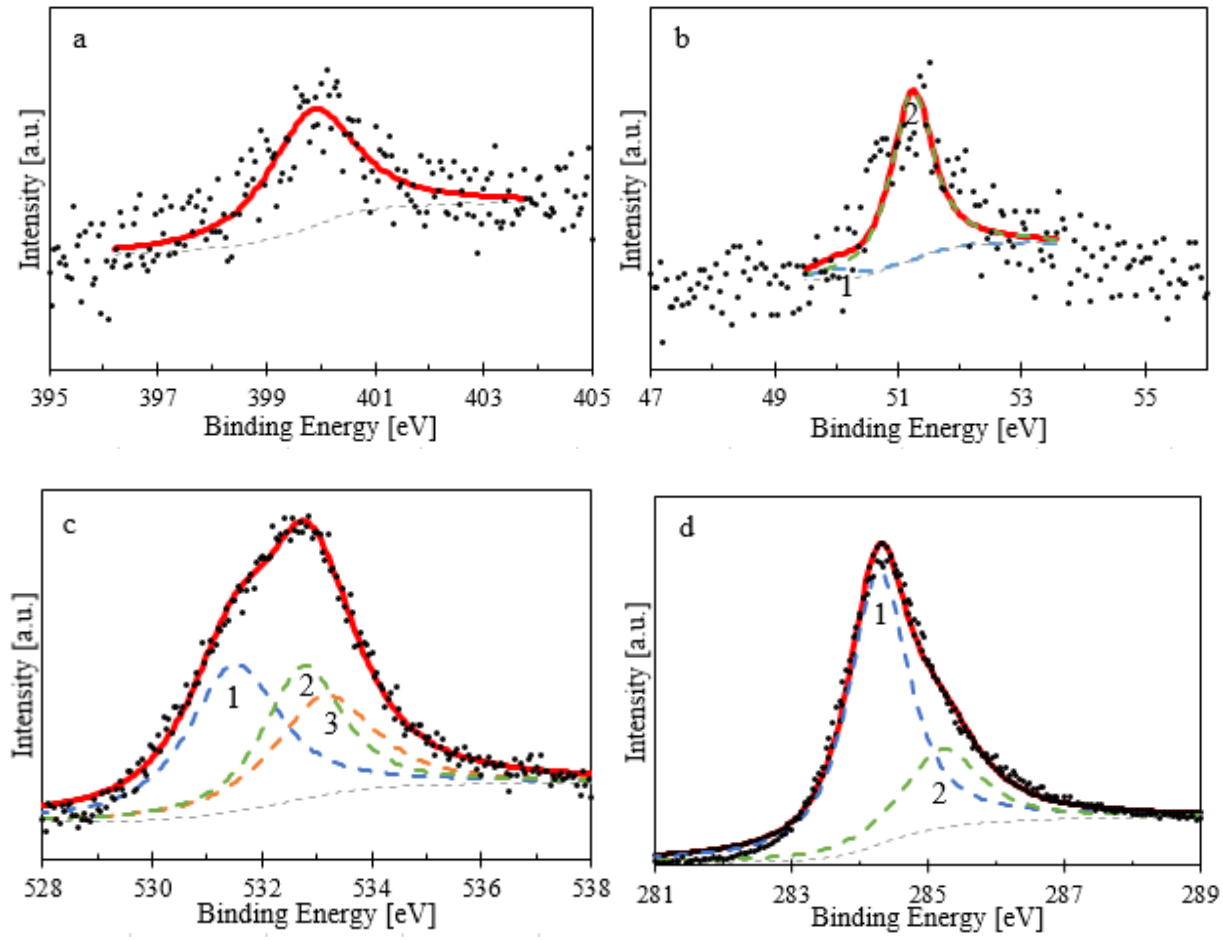

Figure 4-26: Sample 2 spectrum scans for (a) N 1s, (b) As 3d, (c) O 1s, and (d) C 1s. Samples were treated with 5 g/L arsenate solution.

The tail of each curve in Figure 4-26 is denoted by a dashed grey line and the summed peak is represented by a solid red line. The N 1s peak is 399.9 eV, the As 3d peak is 51.3 eV, the O 1s peak is 532.8 eV and the C 1s peak is 284.3 eV for sample 2. The difference in binding energies between sample 1 and sample 2 are minuscule as they only differ by a maximum of 0.1 eV. The difference between the binding energy peaks in sample 3 are also similar and this is seen by a maximum binding energy difference of 0.2 eV between the first and third samples. Figure 4-27 shows the spectrum scans for N 1s, As 3d, O 1s and C 1s for sample 3 which was activated carbon powder that was subjected to a 5 g/L arsenite and 5 g/L arsenite (10 g/L total arsenic) solution. The binding energy peaks for sample 3 are as follows: the N 1s peak is 400.1 eV, the As 3d peak is 51.2 eV, the O 1s peak is 532.6 eV and the C 1s peak is 284.3 eV.

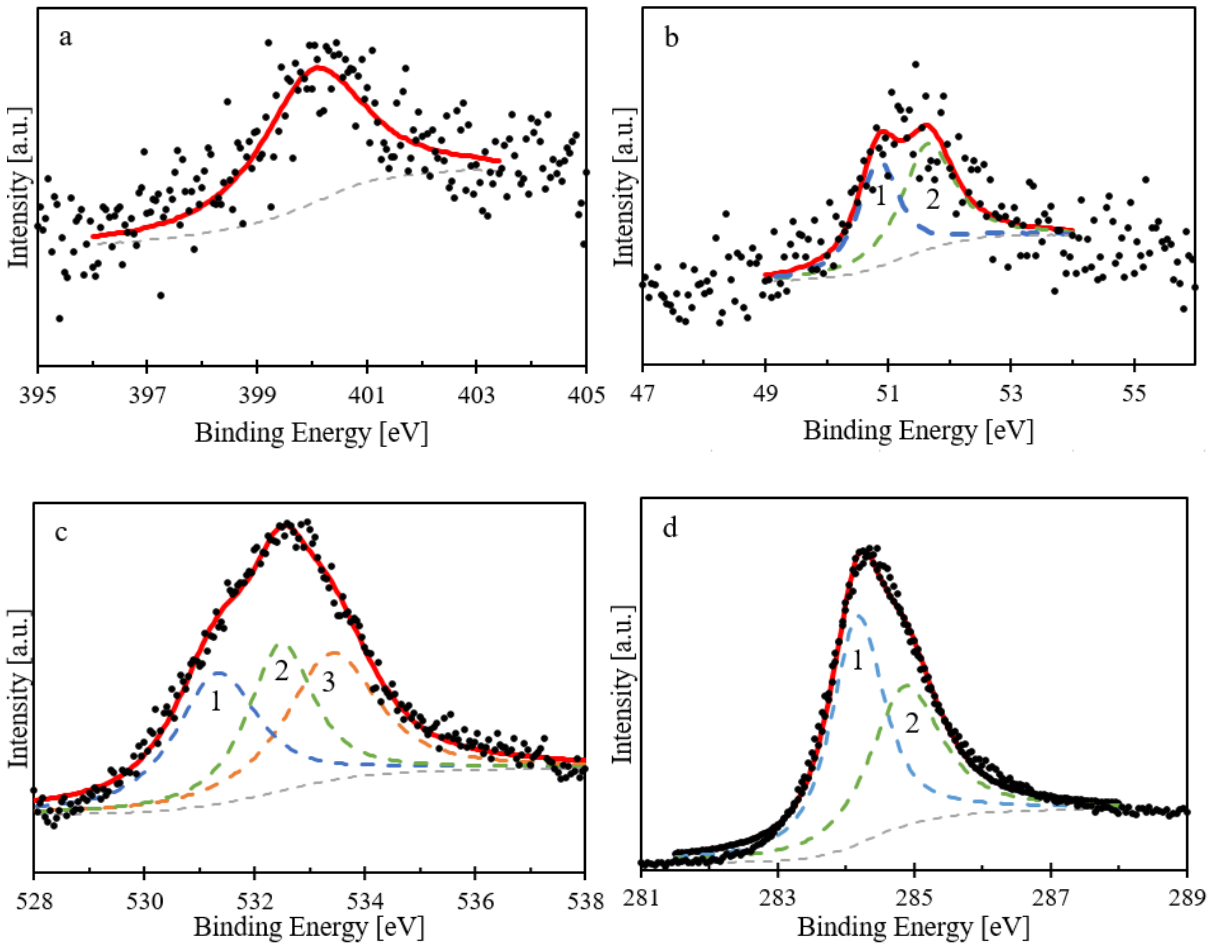

Figure 4-27: Sample 3 spectrum scans for (a) N 1s, (b) As 3d, (c) O 1s, and (d) C 1s. Samples were treated with 5 g/L arsenite solution and 5 g/L arsenate solution.

Interestingly, the arsenic binding energy peak is higher than the values found in literature. In Martinson and Reddy (2009) the binding energy for arsenic species on various compounds ranges from 45.0-45.28 eV. The As 3d binding energy for arsenite is typically approximately 1 eV lower than the binding energy of arsenate (Martinson & Reddy, 2009). Results from the N 1s, O 1s and C 1s spectrum scans indicate that the shift in binding energy for the arsenic peak is not due to errors in calibration as the respective nitrogen, oxygen and carbon peaks fall well within expected values.

Table 12: Binding energies for powdered samples 1-3: N1 s, As 3d, O 1s and C 1s

		Peak Sum [eV]	Peak 1 [eV]	Peak 2 [eV]	Peak 3 [eV]
Sample 1	N 1s	400.00	400.00		
	As 3d	51.20	51.15	52.24	
	O 1s	532.80	531.60	532.85	532.85
	C 1s	284.40	284.40	286.20	
Sample 2	N 1s	399.90	399.90		
	As 3d	51.30	50.85	51.40	
	O 1s	532.75	531.50	532.80	533.20
	C 1s	284.30	284.30	285.25	
Sample 3	N 1s	400.10	400.10		
	As 3d	51.15	51.05	51.90	
	O 1s	532.55	531.35	532.50	533.45
	C 1s	284.25	284.20	284.90	

The N 1s main peak occurred at a binding energy of 399.9-400.1 eV which fits values from literature (Biniak et al., 1997). The O 1s region, for each sample, was fitted with three internal peaks to denote C=O groups, C-O-C groups and chemisorbed oxygen and water species, as in Biniak et al (1997). The binding energy of the O 1s peak typically lies within the range of 531-534 eV (Jansen & van Bekkum, 1995). The O 1s peaks from samples 1, 2 and 3 are 532.8 eV, 532.8 eV and 532.6 eV, respectively, so the peaks fall within an appropriate range and are therefore validated. According to Biniak et al, binding energies of 530.4-530.8 eV relate to C=O bonds, binding energies of 532.4-533.1 refer to C-OH or C-O-C bonds, and binding energies of 534.8-535.6 correspond to chemisorbed oxygen and/or water. The peak analysis conducted does not convey similar results as the internal peaks vary from the literature values. However, if these oxygen species are assumed to be present then the relative amount of species can be determined by comparing the areas under each of the peaks (which is shown in Table 13). If the highest binding energy peak is assumed to be adsorbed oxygen or water then the relative amount of those species is quite high, comparatively. It has been determined from other studies that when the oxygen percentage is low, which is due to a dissolved oxygen content ranging between 7.1-8.5 mg/L in other tests discussed in this

thesis, the peak corresponding to adsorbed water is relatively high compared to other oxygen-containing functional groups (Jansen & van Bekkum, 1995).

Table 13: XPS peak areas for powdered samples 1-3: N1 s, As 3d, O 1s and C 1s

		Area			Peak Percentages [%]			
		Peak 1	Peak 2	Peak 3	Peak Sum	Peak 1	Peak 2	Peak 3
Sample 1	N 1s	116.6			116.6	100.0		
	As 3d	175.2	70.4		245.6	71.3	28.7	
	O 1s	3006.7	2139.0	1895.0	7040.7	42.7	30.4	26.9
	C 1s	14490.1	6235.3		20725.4	69.9	30.1	
Sample 2	N 1s	223.0			223.0	100.0		
	As 3d	10.1	165.3		175.4	5.7	94.3	
	O 1s	2968.4	2255.6	2142.9	7366.9	40.3	30.6	29.1
	C 1s	13959.8	5160.0		19119.8	73.0	27.0	
Sample 3	N 1s	240.8			240.8	100.0		
	As 3d	104.2	130.6		234.8	44.4	55.6	
	O 1s	2079.0	2458.1	2375.6	6912.8	30.1	35.6	34.4
	C 1s	10009.9	8192.6		18202.5	55.0	45.0	

The binding energies for the C 1s peaks in samples 1, 2 and 3 are 284.4 eV, 284.3 eV and 284.3 eV, respectively, and this is in accordance with the literature value of 284.50 eV (Jansen & van Bekkum, 1995) and falls within carbidic carbon (which has a peak at a binding energy of 282.6-282.9 eV) and graphitic carbon which has a peak at a binding energy of 284.6-285.1 eV (Biniak et al., 1997). Although the main peak occurs at 284.50 eV, a smaller peak can occur at 286 eV and this peak is attributed to carbon that is bonded to nitrogen and oxygen (Jansen & van Bekkum, 1995). In all three powdered samples a second peak is fit to the high resolution spectrum at a binding energy of 284.9-286.1. The second peak for sample 1 constitutes 30.1% of the total carbon, for sample 2 the second peak is 27% and for sample 3 the second peak is 45%. These values indicate a high degree of oxygen (and nitrogen) adsorbed onto the carbon surface although nitrogen on the carbon constitutes less than 1% of the system

so the most probable explanation for the large second peak on the C 1s high resolution scan is primarily due to oxygen. The breakdown of each of the samples is presented in Table 14.

Table 14: Elemental composition of the powdered XPS samples according to relative areas under peaks

		Sample Composition [%]
Sample 1	N 1s	0.41
	As 3d	0.87
	O 1s	25.03
	C 1s	73.68
Sample 2	N 1s	0.83
	As 3d	0.65
	O 1s	27.40
	C 1s	71.12
Sample 3	N 1s	0.94
	As 3d	0.92
	O 1s	27.01
	C 1s	71.13

The speciation of arsenic is difficult to ascertain due to two reasons. First, the arsenic present in the system ranges from 0.65-0.92% which is on the scale of mg so this may not be a good representation of the larger system. Secondly, the peaks for arsenic occur over 5 eV higher than what has been found in literature. This could be due to the chemisorption of arsenic species onto the activated carbon which would increase the binding energy of the peak as the peak for C 1s is at approximately 284.5 eV. The amount of carbon in each of the samples is 71.12-73.68% and therefore the interference with the C 1s orbital would have an effect on the arsenic peak, just as the chemisorbed water and oxygen had an effect on the second C 1s peak. However, the arsenic speciation can still be determined by comparing the surface area of peak 1 (arsenite) and peak 2 (arsenate) in Figure 4-25(c), Figure 4-26(c) and Figure 4-27(c). The resulting surface area ratios were converted into percentages and are listed in Table 15.

The results shown in Table 15 are consistent with what was expected. Sample 1 was subjected to a 5 g/L arsenite solution and therefore the speciation of arsenic on the surface should be predominantly arsenite. The speciation of arsenic on sample 1, according to XPS was roughly 70% As (III) and 30% As (V). The

As (V) present on the surface is due to the catalytic ability of carbon when it interacts with arsenic to oxidize it. The short contact time between the arsenite solution and the powdered activated carbon of only 1 hour was still a sufficient amount of time for oxidation to occur. Sample 2 was subjected to a 5 g/L arsenate solution and the results indicate that approximately 94% of the arsenic on the activated carbon was of the pentavalent state. The 5.7% of arsenic that is As (III) is likely due to error associated with the XPS equipment. Each scan on the powder will modify the surface from the X-rays used for measurement and this contributes to error. Sample 3 was subjected to 5 g/L arsenite and 5 g/L arsenate and therefore the results are in accordance with what was anticipated because some of the As (III) should be oxidized to As (V). The results from sample 3 are also in accordance with the results in Section 4.4.1 which discussed the arsenic speciation on the carbon surface by calculating the relative amounts of As (III) and As (V) from a stripped solution resulting from carbon that had been in contact with varying amounts of arsenic and different arsenic species.

Table 15: Arsenic speciation on the XPS powdered carbon samples

	As (III) [%]	As (V) [%]
Sample 1	71.3	28.7
Sample 2	5.7	94.3
Sample 3	44.4	55.6

4.5 Adsorption Isotherm Models

The adsorption model which best fits a set of data gives insight into the kinetics and chemistry of the adsorption bonds. Two adsorption isotherms were investigated for the arsenic-activated carbon system: the Langmuir isotherm model and the Freundlich isotherm model.

Batch tests were conducted with 0.5, 1 and 2 g/L As (III). The mass of carbon used ranged between 10-20% on a dry basis of the total weight of solution. These tests were conducted with 1 L of solution plus carbon in a 2 L batch reactor with a flow rate of 0.2 L/min O_2. The solution was stirred with an overhead mixer at 200 rpm. Samples that were taken were analyzed for As (III) via a colourimetric

titration and As_{total} by ICP analysis. The results in Table 16 summarize the data from the batch tests that are pertinent to the adsorption isotherm modelling.

Table 16: Data from batch tests for adsorption isotherm modelling

Initial As concentration [g/L]	Final As concentration [g/L]	Time [min]	Mass of dry carbon [g]	Carbon pulp density on a dry basis [%]
0.5	0.14	1440	249.4	20
0.92	0.25	1440	248.2	20
1.8	0.48	1440	250.2	20
1.9	0.64	1440	175.9	15
1.7	0.84	1440	110.8	10

The data in Table 16 were fitted to the Langmuir adsorption isotherm and graphed as a plot of $1/q_e$ as a function of $1/C_e$, as seen in Figure 4-28. There are five data points present in Figure 4-28 but the linearized model appears to fit well because the corresponding r^2 value was 0.9973. The linearized Langmuir equation is written as Equation 27 but can then be divided by C_e to yield Equation 28 (which was then graphed):

$$\frac{C_e}{q_e} = \frac{1}{X_m K_L} + \frac{C_e}{X_m} \qquad \textbf{Equation 27}$$

$$\frac{1}{q_e} = \frac{1}{C_e X_m K_L} + \frac{1}{X_m} \qquad \textbf{Equation 28}$$

The equation of the line of best fit for this model is $y = 0.0967x - 0.0048$, where y is $1/q_e$, the slope is equal to $(X_m \bullet K_L)^{-1}$ and X_m^{-1} is the y-intercept.

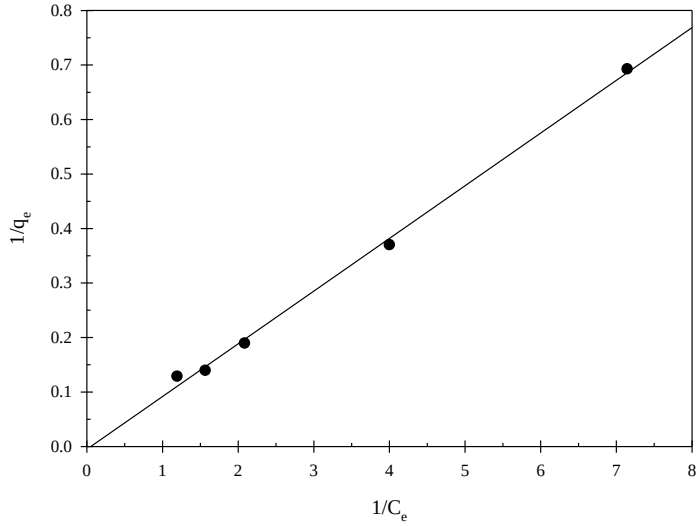

Figure 4-28: Linearized Langmuir adsorption isotherm of $1/q_e$ as a function of $1/C_e$.

The Freundlich model was linearized with $\log(q_e)$ with respect to $\log(C_e)$ as shown in Equation 29. Figure 4-29 presents the graphical representation of the linearized Freundlich model with $\log(q_e)$ as a function of $\log(C_e)$. The r^2 value is similar to that of the first linearized Langmuir model as it is extremely close to 1. The r^2 value is 0.9891 for the best fit line of $y = 0.9762x + 1.0107$. For this model, y is $\log(q_e)$, the slope is n^{-1} and the y intercept is $\log(K_f)$.

$$\mathbf{\log(q_e) = \log(K_f) + \frac{1}{n}\log(C_e)} \qquad \textbf{Equation 29}$$

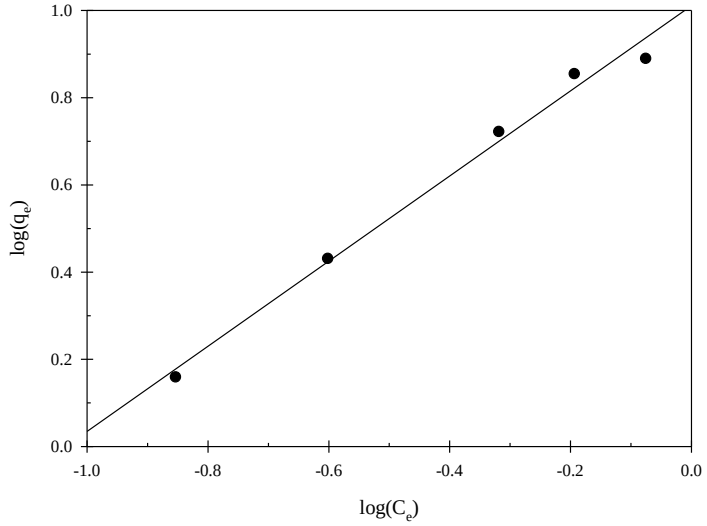

Figure 4-29: Linearized Freundlich adsorption isotherm with log(q_e) with respect to log(C_e).

The parameters and constants from the models presented in Figure 4-28 and Figure 4-29 are presented in Table 17.

Table 17: Langmuir and Freundlich model constants

Langmuir	q_{max}	K_L	r^2
	10.34	-20.14	0.9973
Freundlich	n	K_F	r^2
	1.02	10.25	0.9891

Both adsorption isotherms appear to be a decent fit for the arsenic-carbon system according to the r^2 values of the trendlines because they are very close to 1. However, when comparing the parameters of the two models to the system under study the Freundlich model better characterizes the system. The K_L value in the Langmuir model is negative which does not make sense empirically as the units for this constant are mg/L. K_L indicates the degree of sorption affinity for the specific adsorbate/adsorbent system (Payne & Abdel-Fattah, 2005). A negative value indicates that there is not a high affinity for the arsenic to adsorb onto the activated carbon but in actuality this is not the case. The value of the parameter 'n' in the

Freundlich isotherm is 1.02 which is only slightly larger than 1. As stated previously: if n is less than 1 then the Freundlich model is not an adequate model for the adsorption of the system being investigated.

The Langmuir and Freundlich isotherms describe different systems: one has a monolayer of active sites and the latter can have more complex intermolecular interactions between sites. The speciation of arsenic complicates the modelling of adsorption isotherms as there have been various studies which focus on just one oxidation state (Chuang et al., 2005; Lorenzen, van Deventer, & Landi, 1995; Payne & Abdel-Fattah, 2005). It is perhaps possible that one oxidation state can be better modeled by one model, while the other oxidation state is more effectively modeled by another. Although the Langmuir isotherm has been proven to be a suitable fit for activated carbon (Barkauskas & Dervinyte, 2004; Payne & Abdel-Fattah, 2005), the hypothesized system of equations which predict the adsorption and oxidation of arsenic in this study assume that molecules in adjacent active sites interact. One of the main differences between the Langmuir isotherm and Freundlich isotherm is that the Langmuir model does not allow for adjacent molecules in active sites to interact, while the Freundlich isotherm allows this phenomenon to occur. From the results in Table 17 it is evident that the Langmuir isotherm offers a higher r^2 value then the Freundlich isotherm but the parameters from modeling the Freundlich isotherm to the system make more sense empirically. For this reason the Freundlich model is selected as the model which best describes the interactions between activated carbon and the increasingly oxidized arsenic system. However, it is possible that another model that was not investigated is a better fit for this system.

4.6 Chapter Conclusions

These experiments have shown that the chemistry of both activated carbon and arsenic speciation are complex and that there are many mechanisms occurring which contribute to the oxidation, adsorption and oxidant formation in the studied systems.

It was determined that peroxide is formed on the carbon surface due to functional groups already existing on the activated carbon surface as well as from the dissolved oxygen of the system. XPS results show that

there is oxygen on the surface of activated carbon. It was also concluded that activated carbon has a limited ability to oxidize arsenic and produce hydrogen peroxide without the introduction of oxygen due to dissolved oxygen and activated carbon functional.

Arsenic speciation and oxidation is a complex area of study. Shake tests show that arsenate is typically not present in the bulk solution of a system until the arsenic adsorption has reached equilibrium; however, arsenate appears on the carbon surface as early as 1 hour of contact between pH 1 acidic arsenite solution and activated carbon. From desorption tests it was concluded that arsenite is more preferentially desorbed as 53.5-53.7% of the arsenic species in the stripped solution were arsenite species. The difference between arsenite and arsenate species was 7-7.5% in the stripped solution.

There are two arsenic oxidation mechanisms that are hypothesized to be occurring. The first mechanism is that arsenite is oxidized via previously produced hydrogen peroxide when it comes into contact with activated carbon and is subsequently adsorbed as an arsenate compound. The second hypothesized mechanism of oxidation is that arsenite adsorbs onto the surface of activated carbon and is then oxidized by previously produced hydrogen peroxide that is in the solution near the activated carbon surface. The newly formed arsenate species remains on the surface until it is desorbed due to movement in the solution. It is likely that both of these mechanisms are occurring simultaneously.

XPS results from the C 1s, O 1s and N 1s high resolution scans are in accordance with values in literature. The binding energy value for arsenic is over 5 eV higher than that found in literature. The suspected reason for this is due to the arsenic being chemisorbed onto the carbon surface which might increase the binding energy due to the higher peak value of carbon (284.5 eV). Similar cases are true for a second peak in the C 1s scan which is due to chemisorbed water and/or oxygen on the carbon surface.

Chapter 5

Batch Test Kinetics

A series of batch tests were conducted in order to investigate the factors affecting arsenic oxidation kinetics in a system at a low pH and a relatively high arsenic concentration. This chapter is divided into three sections. The first section discusses factors which alter the liquid and solid characteristics of the system these being mainly the initial arsenite concentration and the amount of solids present. The second section discusses the effect of oxygen flowrate and concentration. The arsenic speciation in solution and the arsenic adsorption is analyzed for experiments which have compressed air sparged 0.2 L/min compared to oxygen sparged at a rate of 0.2 L/min. Finally, a test comparing the oxidative capability and adsorptive properties of activated carbon and activated alumina is presented. This test shows that the oxidation of arsenic is not due to oxygen trapped in micro or macropores, but is due to functional groups of activated carbon interacting with the bulk solution.

5.1 Effect of Liquid and Solid Components in the Batch System

All batch tests used fresh +16 mesh activated carbon that was stored in room temperature DI water. Batch tests were carried out as described by the procedure in Chapter 3.3.2.

5.1.1 Effect of Initial Arsenite Concentration

The concentration of arsenic-containing mining waste solutions is typically much higher than one would find in contaminated drinking water. Copper electrorefineries will often implement bleed streams in order to keep the concentration of arsenic in the electrolyte under 20 g/L (Riveros et al., 2001), but by contrast the World Health Organization's drinking water guidelines limit the arsenic in the water to just 10 µg/L (Basha et al., 2008; Bora et al., 2016; Leist et al., 2000; Smedley & Kinniburgh, 2002).

Three batch tests were conducted with varying initial arsenite concentrations: 0.5 g/L, 1 g/L and 2 g/L of arsenite solutions created from dissolved arsenic trioxide in acidic solution. Prior to each test the pH was

brought to a pH of 1.0 ± 0.1 via sulphuric acid additions. A typical plot of the As (III), As (V) and As_{tot} concentrations throughout a batch test is presented in Figure 5-1. The test results shown in Figure 5-1 had an initial arsenite concentration of 2 g/L, 20% carbon on a dry basis, and an oxygen flow rate of 0.2 L/min. It is interesting to note that the arsenate concentration in solution is negligible for the first 2 hours of the test although, from previous experiments that are discussed in Chapter 4, it is likely that the arsenate actually starts to appear in solution after 1.5 hours of testing. It is likely that arsenate is actually being produced from the onset of the experiment but it is instantly adsorbed onto the activated carbon surface and remains there until the concentration is high enough to desorb into the solution.

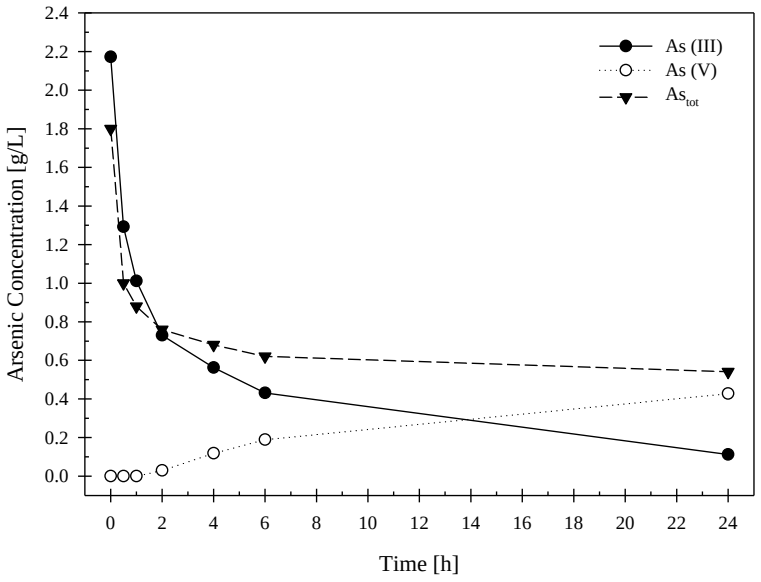

Figure 5-1: Typical trends for As (III), As (V) and As_{tot} in solution during batch tests.

The total arsenic in solution behaved as expected. the initial uptake of arsenic on the activated carbon was rapid and then plateaued starting at approximately 4 hours. Figure 5-2(a) shows the total arsenic in solution for this set of tests and Figure 5-2(b) shows similar data but takes into account the initial arsenite concentration.

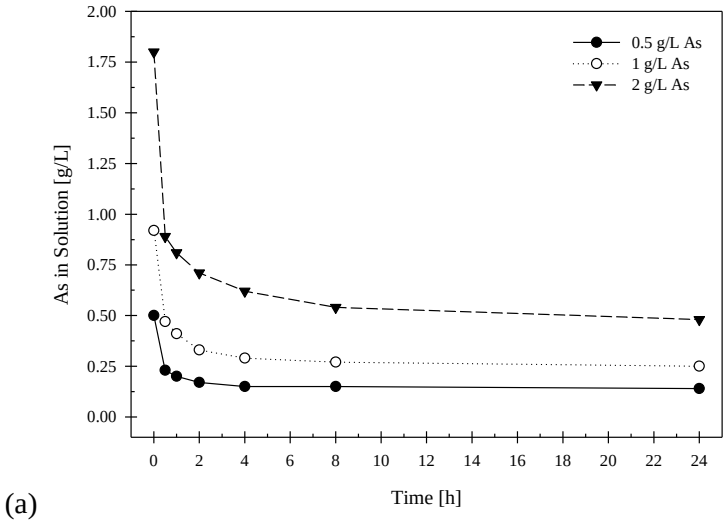

(a)

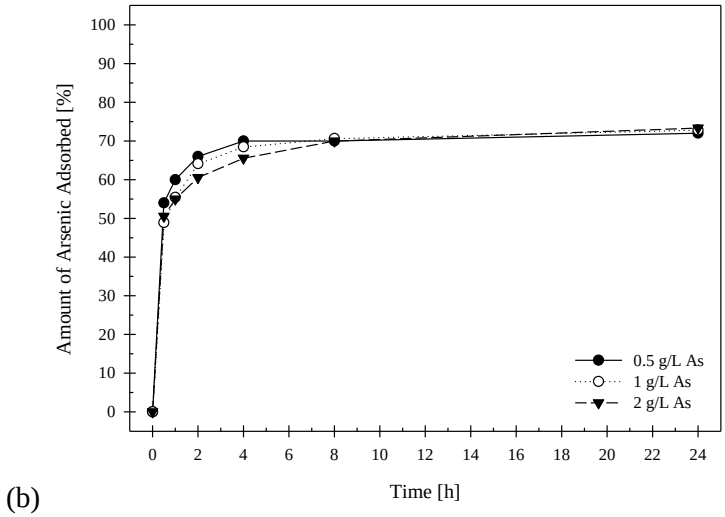

(b)

Figure 5-2: (a) The amount of total arsenic remaining in solution with respect to time (b) the percentage of arsenic adsorbed onto the activated carbon surface with respect to time.

A discussion on adsorption isotherm models for this system is previously discussed in Chapter 4. The placement of the curves between 1 and 8 hours in Figure 5-2(b) gives an indication on the adsorption rate but not necessarily the oxidation of arsenic. Figure 5-3 is a plot of the arsenic adsorbed onto the activated carbon graphed against time. Neglecting the initial data point at 0 hours, the three curves closely follow a logarithmic trend as r^2 values range from 0.8547 to 0.9758. The data displayed in Figure 5-3 was

linearized to produce an equation in the form of y = m x + b (Figure 5-4). The graph presented in Figure 5-4 includes the lines of best fit for the three initial arsenite concentrations and their respective r^2 values. The slopes in Figure 5-4give an appreciation of the rate of adsorbance of total arsenic in the system. The test with a higher concentration of arsenic, although being the lowest curve in Figure 5-2b, actually has the highest rate of adsorbance. The test with an initial concentration of 2 g/L As has a higher rate of adsorption compared to 1 g As (III)/L, which is higher than the test with an initial concentration of 0.5 g As (III) /L.

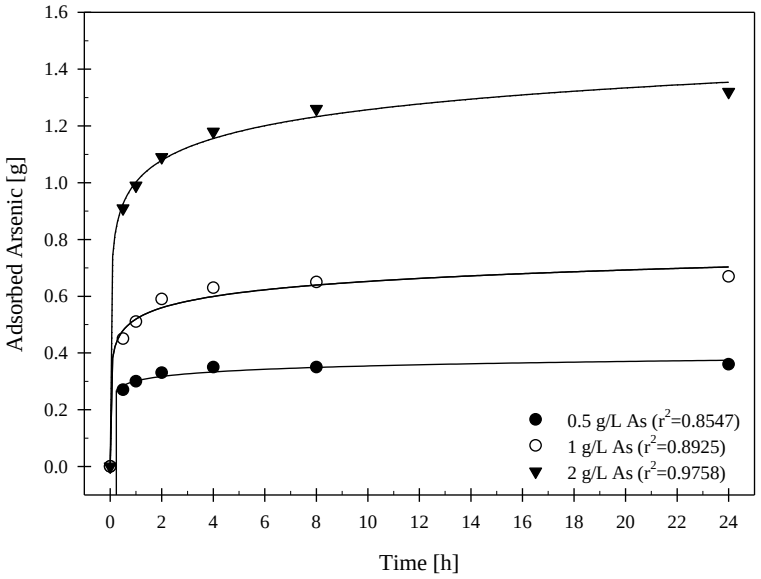

Figure 5-3: Adsorbed arsenic with respect to time; logarithmic lines of best fit and their respective r^2 values are included.

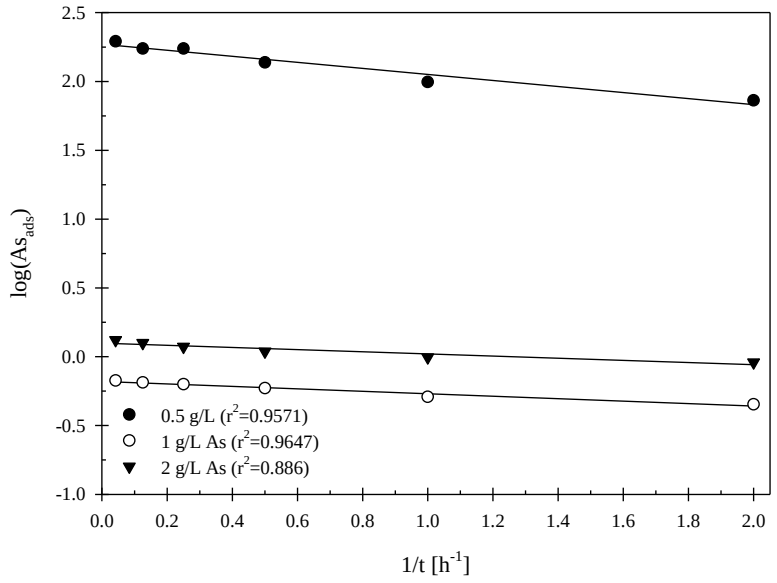

Figure 5-4: Linearization of adsorbed arsenic with respect to time with the logarithm of arsenic adsorbed versus the inverse of time.

Each of the solutions in the tests investigating the effect of initial arsenite concentration was oxidized between 73.2-80.5%. The corresponding increases in pH and ORP for each test is shown in Table 18. It is interesting that the test with the highest oxidation efficiency is the test with a higher concentration of arsenite. This could be due to only measuring the oxidation efficiency in the solution. The percent of oxidized arsenic in solution is likely higher in solutions with a larger initial arsenite concentration until a threshold concentration. In solutions with higher concentrations of arsenic there are more arsenic molecules which can bond with the activated carbon thereby filling active sites at a quicker rate than a solution with a smaller concentration. There is then a higher statistical probability that more arsenic that has been oxidized will be desorbed from the activated carbon due to the mixing and mass transfer occurring in the reactor.

Table 18: Final oxidation efficiency, pH and ORP for tests investigating the effect of initial arsenite concentration

Initial As (III) concentration	Oxidation [%]	Initial pH	Final pH	Initial ORP [mV]	Final ORP [mV]
0.5 g/L	73.2	1.0	1.6	467	535
1 g/L	77.5	1.1	1.8	442	552
2 g/L	80.5	1.1	1.8	478	522

The final pH of the liquid in the batch reactor is higher than the initial pH for all tests however this does not affect the adsorption of the arsenic onto the activated carbon because arsenite adsorption is not affected between a pH range of 0.16-3.5 and arsenate adsorption decreases below a pH of 2.35 but the pH does not reach that value (Eguez & Cho, 1987). There are a few reasons why there is an increase in pH. First, it could be due in part to the buffering capacity of the arsenite/arsenate system. Secondly, sulphuric acid is a strong acid that dissociates in water to two protons and a soluble sulphate ion. The protons can adsorb onto isolated negatively charged functional groups on the carbon surface thereby decreasing the acidity of the solution. The protons may also be getting used as a reagent to produce hydrogen peroxide with dissolved oxygen or adsorbed water molecules on the activated carbon surface. This supports the hypothesis discussed in Chapter 4.

The ORP of each solution is increased from 462 ± 20 mV to 536 ± 15 mV which is an average increase of 74 mV within 24 hours.

The Pourbaix diagram of the system under study is illustrated in Figure 5-5. This diagram was modeled for a solution containing 2 g/L arsenic. From the diagram is it clear that an increase in ORP changes the overall equilibrium of the system which consequently makes the dominant arsenic species an arsenate compound as opposed to an arsenite compound. The change in ORP is due to two changes in the system that occurred during the test: (1) peroxide, which is a strong oxidant, is produced which raises the ORP and (2) as the ORP increases arsenate is produced which, in turn, increases the ORP of the system due to its higher oxidative state. The second point is analogous to having more ferric than ferrous in a system.

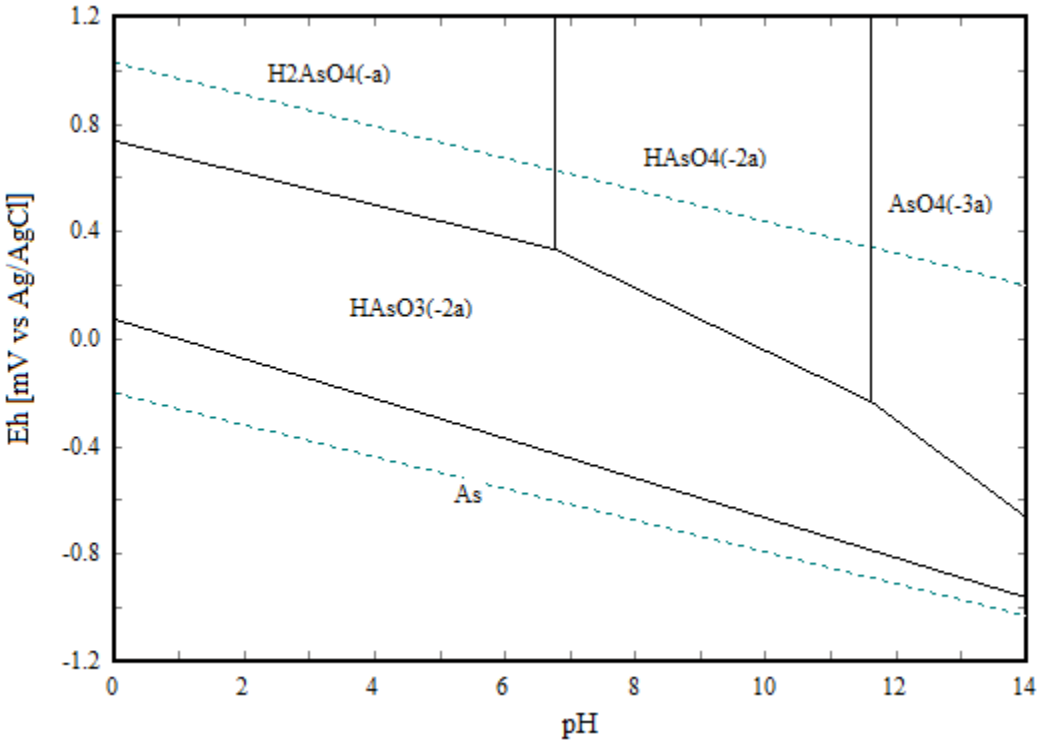

Figure 5-5: Pourbaix diagram for the system As–H_2O at 25 °C, 0.0267 M and 1 bar total pressure (produced on HSC 6.1).

5.1.2 Effect of Changing the Activated Carbon Pulp Density

Four mass ratios of carbon versus the total mixture were studied: 0%, 10%, 15% and 20%. Each of the tests used an oxygen flowrate of 0.2 L/min and an initial arsenite concentration of 2 g/L. The total arsenic in solution had a rapid decrease as soon as the arsenic solution and activated carbon were introduced and mixed. Figure 5-6 shows how the total arsenic in solution varies over time for tests with 0%, 10%, 15% and 20% carbon by mass on a dry basis. It is clear that there is a relationship between the amount of activated carbon in solution and the initial uptake of arsenic by the activated carbon: the more activated carbon there is to adsorb the arsenic the less arsenic there will be in solution. The initial bumps in the 0% carbon pulp density curve in Figure 5-6 are due to errors inherent in ICP analysis.

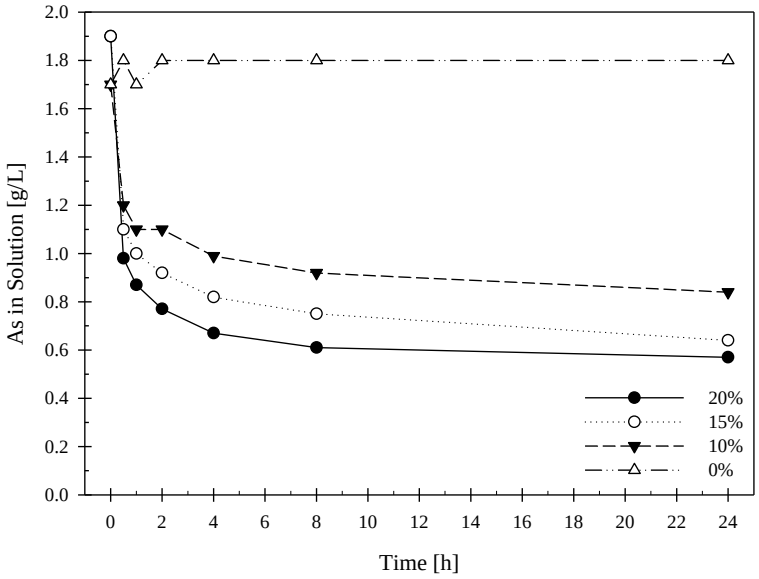

Figure 5-6: Total arsenic in solution with respect to time for experiments with varying amounts of carbon in the reactor.

However, when looking at the speciation of arsenic a different conclusion may be drawn. Excluding the test where there was no activated carbon added to the arsenic solution, Figure 5-7 shows that at 24 hours the arsenite in solution is essentially the same for each of the test conditions. However, the data presented in Figure 5-7 is due to both arsenic adsorption onto activated carbon and the oxidation of arsenic. Figure 5-8 shows the differences between the tests with respect to arsenic oxidation rather than in conjunction with adsorption. Taking adsorption out of the picture yields the same results as in Figure 5-7. The more activated carbon in the reactor the smaller the fraction of arsenite present except for the initial arsenic measurement.

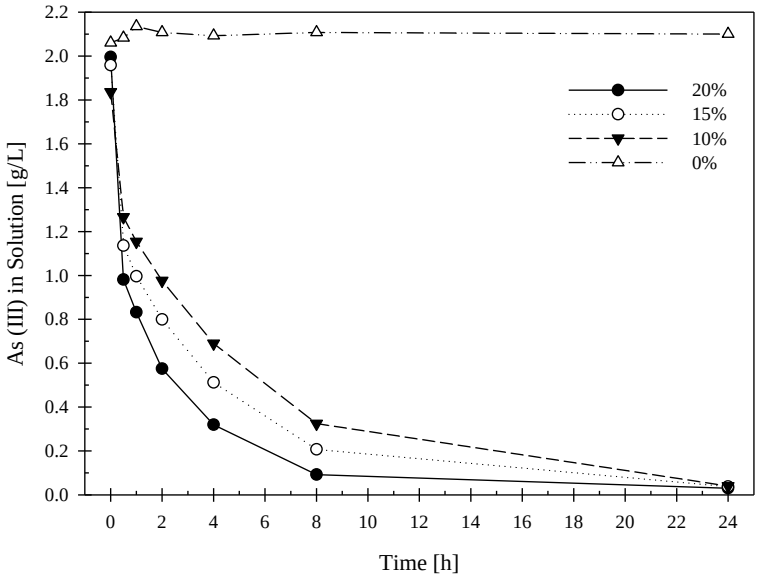

Figure 5-7: As (III) in solution with respect to time with carbon pulp densities ranging from 0-20%.

The same end trend holds true in Figure 5-8 as in Figure 5-7 because the oxidation efficiency in the solution at the end of the test is essentially the same across all three tests with activated carbon present. The first portion of Figure 5-8(a) appears linear in nature and the slope is indicative of how fast the arsenic is oxidized. The tests with more carbon have a steeper slope until a plateau is reached but the tests with less carbon do not appear to reach a plateau with the time points that samples were taken. It is hypothesized that the tests with less activated carbon have the same trend as the test with 20% carbon by weight on a dry basis but the trend is not clear due to the system taking a longer time to reach equilibrium.

The equilibrium previously mentioned will be the same for each test because oxygen is continuously being introduced into the system so the functional groups on the carbon surface which aid in arsenic oxidation will continually be replenished. The oxygen supply is not limited in a way that the system is being starved of oxygen so the oxidation efficiency of the system will be the same for all three cases with carbon present.

Figure 5-8(b) shows the oxidation efficiency of the system assuming that 50% of the adsorbed arsenic is of the pentavalent state. The same trends mentioned for Figure 5-8(a) hold true for Figure 5-8(b).

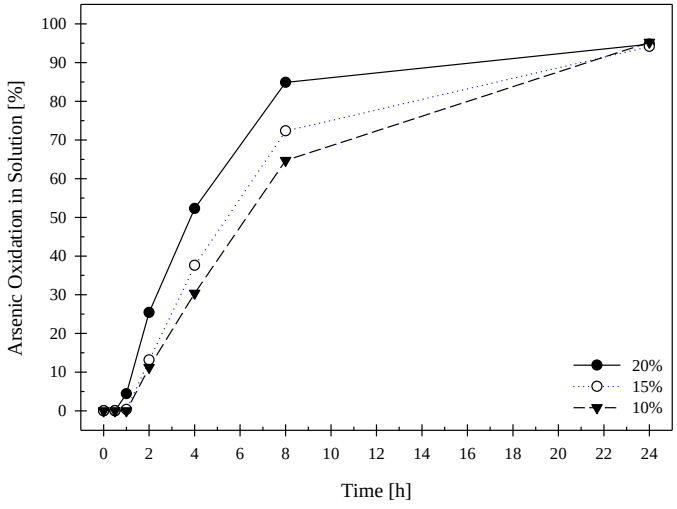

(a)

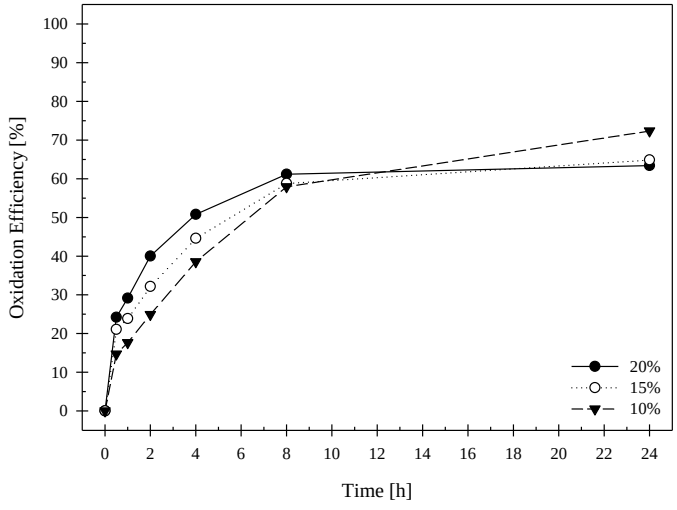

(b)

Figure 5-8: (a) The oxidation efficiency of arsenic in solution with respect to time with carbon pulp density ranging from 10-20% of the total weight of the mixture and (b) the total oxidation efficiency of the system assuming that 50% of the arsenic on the activated carbon surface at a given time is oxidized.

Table 19 shows the final oxidation efficiency of each of the batch tests conducted with varying amounts of activated carbon. Excluding the test with no activated carbon, the oxidation efficiencies ranged

between 94.1-95.2% with no indication that the amount of carbon in the range investigated affects the final oxidation capability of the batch system.

Table 19: Final oxidation efficiency, pH and ORP for tests investigating activated carbon pulp density

% C by Mass on a Dry Basis	Oxidation %	Initial pH	Final pH	Initial ORP [mV]	Final ORP [mV]
0%	0	1.0	1.3	459	417
10%	95.2	1.0	1.4	484	523
15%	94.1	1.1	1.7	465	528
20%	94.7	1.0	1.9	467	517

Table 19 also shows the initial and final pH and ORP of the system, respectively. The initial pH of each test was 1.0 ± 0.1 but the final pH ranged between 1.3-1.9. It is interesting that the larger pH differences occurred in tests with more activated carbon. The test with no activated carbon saw an increase from 1.0 to 1.3 and this shows the baseline for the buffering capacity of the arsenate/arsenite system with little arsenate present. Tests with 10%, 15% and 20% carbon content saw larger decreases in acidity as the amount of activated carbon added was increased. These results support the claims made in the previous section whereby the protons from the sulphuric acid sorb onto the activated carbon surface thereby increasing the pH of the solution. From there the protons may react with surface functional groups or with dissolved oxygen that is adsorbed to the activated carbon to form hydrogen peroxide.

The ORP of each solution containing activated carbon increased from 472 ± 12 mV to 522 ± 12 mV. There was no trend which correlated the amount of activated carbon added to the system and the final ORP value or the difference of potential. Similar to the previous section, the change is likely due to one of two scenarios where the peroxide formed increases the ORP or the ORP is increased once more arsenate is in the system.

The ORP of the batch test with no activated carbon decreased in ORP by 42 mV. The decrease in ORP is perhaps due to the oxygen that had been sparged into the system somehow affecting the reading of the ORP probe. Another scenario is that the decrease in ORP is perhaps due to an error with the ORP probe

as there is no reason for the solution to have changed potential without the introduction of other compounds because if anything, the ORP should have increased due to a slightly more oxygenated solution.

5.2 Effect of Oxygen on Arsenic Oxidation

All batch tests used fresh +16 mesh activated carbon that was stored in room temperature DI water. For all of the tests conducted in this section the pH of the initial arsenite solution was 1 ± 0.1, the initial arsenite concentration was 2 g/L and the amount of activated carbon used was 20% by weight on a dry basis. Batch tests were carried out as described by the procedure in Chapter 3.3.2.

5.2.1 Effect of Varying the Oxygen Flowrate

Four oxygen flowrates were investigated to see how the amount of oxygen introduced into the system would affect the arsenic oxidized in solution. The flowrates tested were 0.1 L/min, 0.2 L/min, 0.3 L/min and 1.0 L/min of industrial grade oxygen. Initial results indicate that the range of oxygen flowrates used does not significantly affect the rate of arsenic oxidation. Figure 5-9 shows the total arsenic in solution over for the duration of each 24 hour test as a function of time.

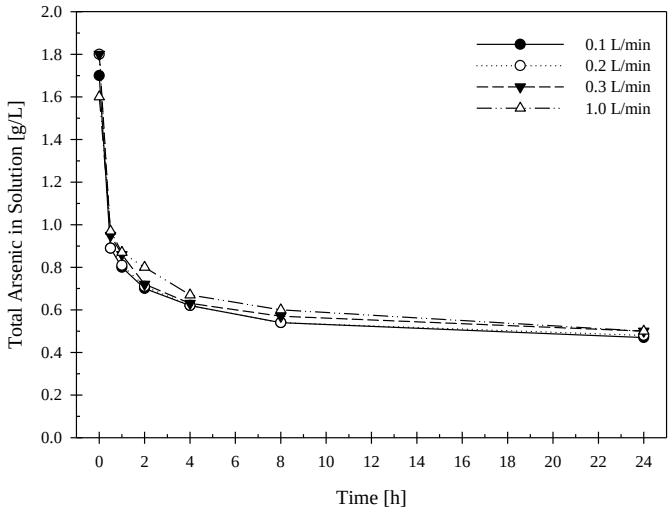

Figure 5-9: Total arsenic concentration in solution as a function of time with varying oxygen flowrates ranging from 0.1-1.0 L/min.

There is no trend evident when looking at the total arsenic in solution. Figure 5-10, which depicts the arsenite in solution as a function of time, provides a deeper understanding of the effect of oxygen in the system and the low level of oxygen required to starve the oxidation and adsorption reactions as there are larger differences early into the test. The curves for the tests conducted at 0.3 L/min and 1.0 L/min follow the same curvature which implies that the arsenic uptake and oxidation, in conjunction with one another, leave the same amount of arsenite in solution. Figure 5-11 illustrates the percentage of arsenic oxidized in solution during the 24 hour test. Even in this graph the curves for 0.3 L/min and 1.0 L/min have similar values which indicates that with an oxygen flowrate of 0.3 L/min the solution reaches its maximum arsenic oxidation capacity so increasing the oxygen flowrate will not significantly increase the oxidation rate.

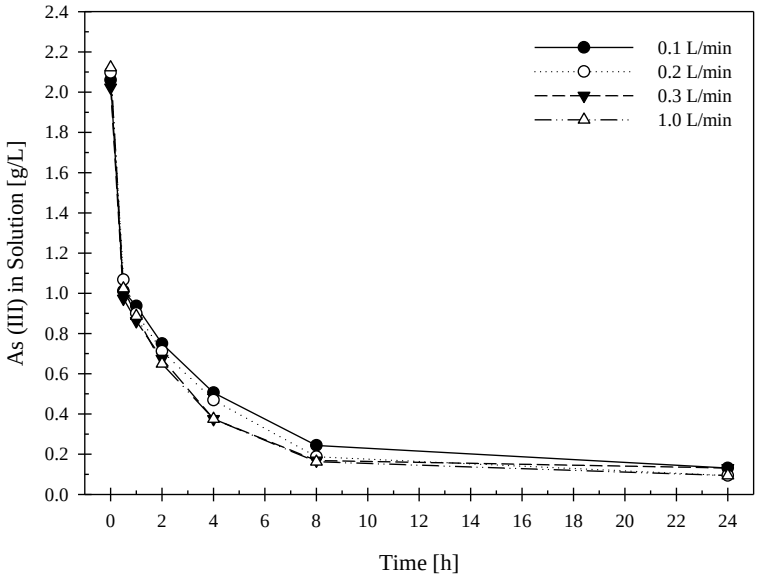

Figure 5-10: As (III) concentration in solution with respect to time with varying oxygen flowrates ranging from 0.1-1.0 L/min.

At the 4 hour time point in Figure 5-10 there appears to be the most widespread data range. The test conducted with 0.1 L/min oxygen has the most arsenite remaining in solution, followed by the test conducted with 0.2 L/min oxygen and then the tests with 0.3 L/min oxygen and 1.0 L/min oxygen. It is in

the range of 0.1 L/min to 0.2 L/min oxygen that there is a glaring difference in both the arsenite remaining in solution and the percent of arsenic oxidized in the solution.

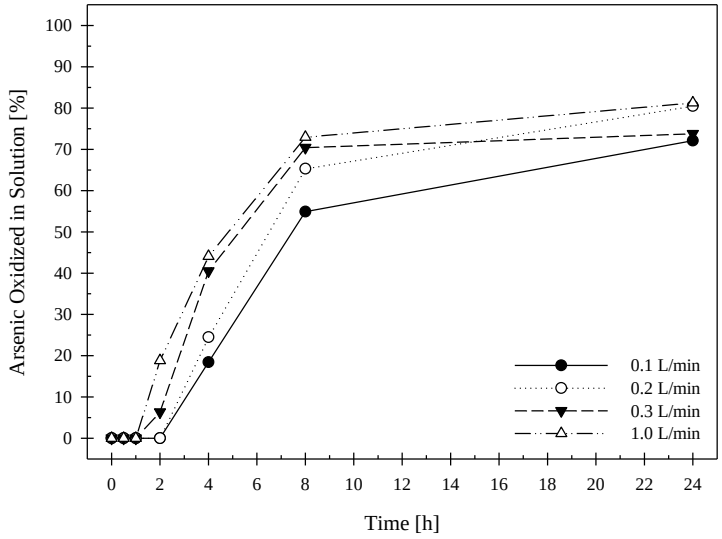

(a)

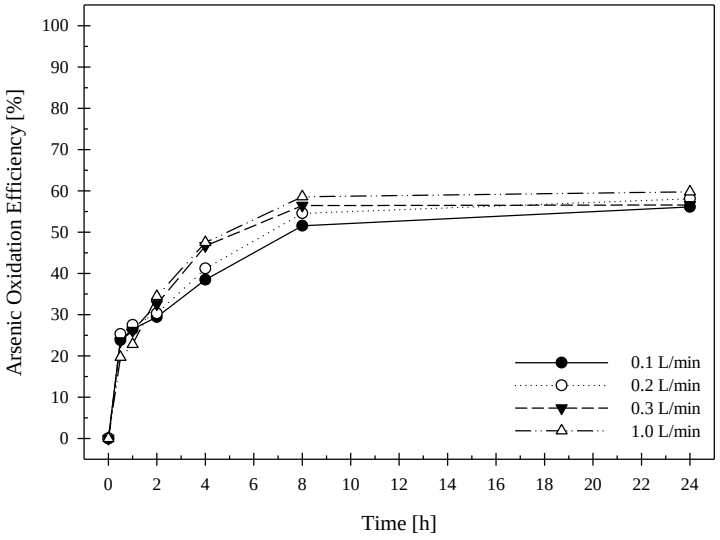

(b)

Figure 5-11: (a) Oxidation efficiency of arsenic oxidized in solution with respect to time for varying oxygen flow rates ranging from 0.1-1.0 L/min and (b) total oxidation efficiency of arsenic assuming that 50% of adsorbed arsenic is in the pentavalent oxidation state.

The arsenite values in Figure 5-10 are generally quite close together so the results presented in Figure 5-11(a) may appear more significant than they are in reality. The data presented in Figure 5-11(b)

illustrates the differences in arsenic oxidation when taking adsorbed arsenic into account. The trend is the same in both figures. More extreme differences in oxygen concentration are required to combat the effect of having very small amounts of arsenic remaining in the solution after a few hours of testing. The next section discusses the results from tests with oxygen and air as the sparged gas.

5.2.2 Effect of Using Air as the Gas Stream

Two tests were initially conducted to investigate how extreme differences in oxygen concentration introduced into the batch system affected the surface chemistry of activated carbon, and in turn the oxidation of arsenic. Industrial oxygen and compressed air were used in their respective tests at a flowrate of 0.2 L/min.

This set of tests yielded interesting results. The total arsenic in solution was affected by the amount of oxygen present. Figure 5-12(a) shows the concentration of arsenic remaining in solution throughout the duration of the tests. From this it is clear that the tests with pure oxygen have less arsenic in solution compared to the test using compressed air. Figure 5-12(b) shows similar data to that in Figure 5-12(a) but shows the relative amount of arsenic adsorbed onto the activated carbon on a percent basis. Both figures clearly illustrate that when oxygen is used there is a higher amount of arsenic adsorbed onto the activated carbon. The adsorption with oxygen is due to the higher oxidation rate of arsenic in solution. Arsenate is formed quicker with more oxygen which subsequently adsorbs onto the activated carbon at a quicker rate that the arsenite still in solution. The relative amount of arsenic in solution is due to the oxidation of arsenic and not just the adsorption because in the test run with air there is nitrogen introduced into the system and nitrogen on the carbon surface significantly increases the sorption capabilities of carbon and anions in solution (Biniak et al., 1997).

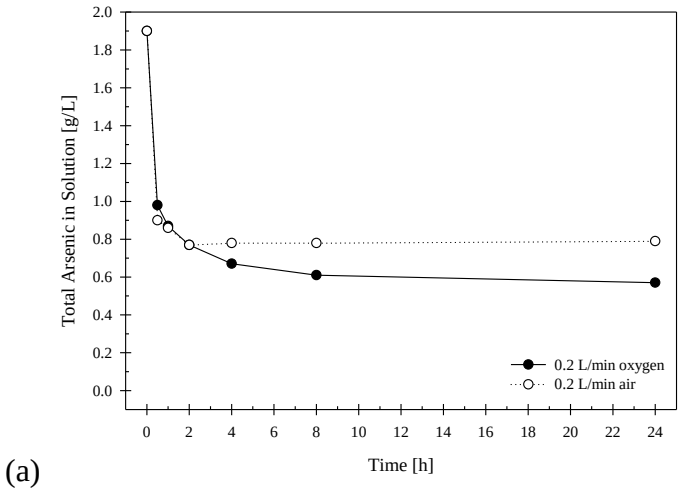

(a)

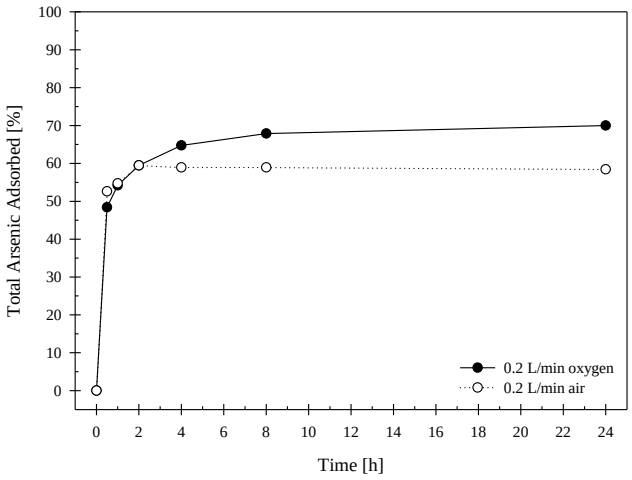

(b)

Figure 5-12: (a) The concentration of total arsenic in solution with respect to time and (b) the relative amount of arsenic adsorbed [%] as a function of time.

Figure 5-13 graphically demonstrates how the arsenite in solution varies over time for the three tests. Interestingly, at 2 hours into the tests the amount of arsenite in solution is different between the gases, whereas the total arsenic in solution at this time is the same across the two gases. This implies that when oxygen is present in larger amounts the oxidation of arsenic is more rapid. This is made evident in Figure 5-14 as the relative percent of arsenic oxidized in solution follows a clear trend whereby the test with

industrial oxygen has the faster initial oxidation rate compared to air (as seen by the relative slopes of the two lines).

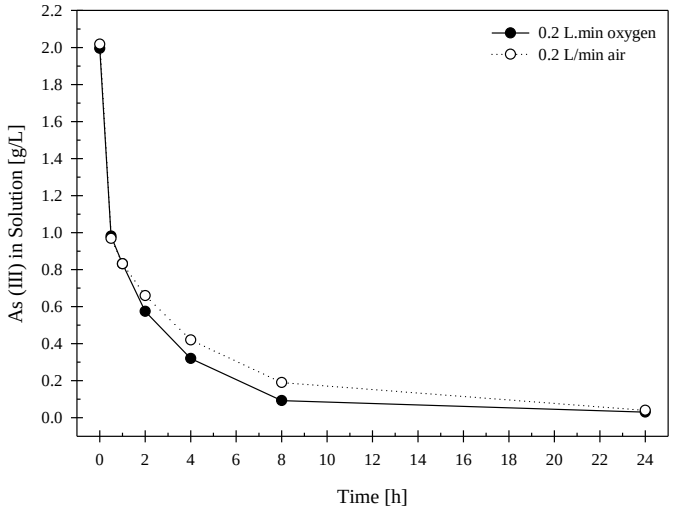

Figure 5-13: As (III) in solution as a function of time for tests using air and oxygen as the gas stream, respectively.

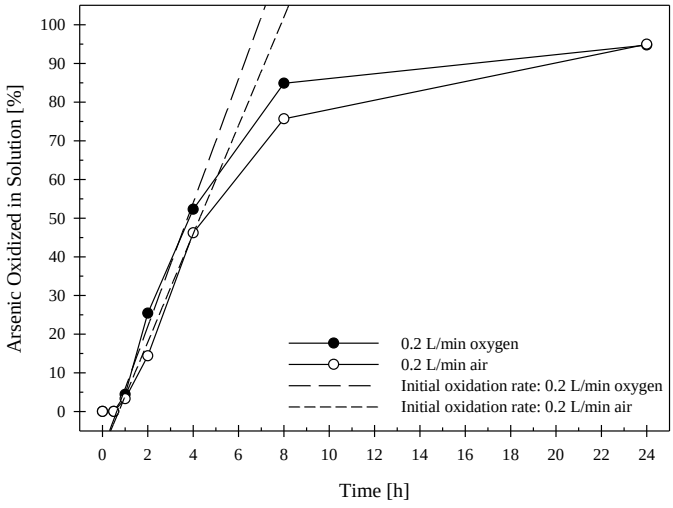

Figure 5-14: Oxidation efficiency of arsenic in solution with respect to time for tests using air and oxygen as the gas stream, respectively.

Figure 5-14 also confirms that activated carbon has a limited capacity to catalyze the oxidation of arsenic without oxygen being continuously added to the system. The final oxidation efficiency of the system,

over the course of 24 hours, is the same for both gases. The oxidation efficiency of arsenic oxidized in solution is maximized by 24 hours. From the research presented in Chapter 4, it is proposed that although there is a limited quantity of arsenic to be oxidized without the presence of oxygen, the presence of oxygen is still necessary because dissolved oxygen is required to create peroxide and form with surface groups of carbon which then oxidize arsenic.

Using air for the industrial and continuous version of this process would yield a more economical process because air from the surrounding area could be used – although cleaning may be required via filters – instead of purchasing or producing industrial grade oxygen. Results in Figure 5-14 show that within 24 hours the nitrogen in air does not make a large difference in a batch test however further investigation is required to draw the same conclusion for a continuous test.

Figure 5-15 and Figure 5-16(a) and (b) show the arsenite concentration in the batch test with respect to time and the percent of arsenic oxidized over time, respectively, to compare three systems: 0.2 L/min oxygen, 0.04 L/min oxygen and 0.2 L/min compressed air.

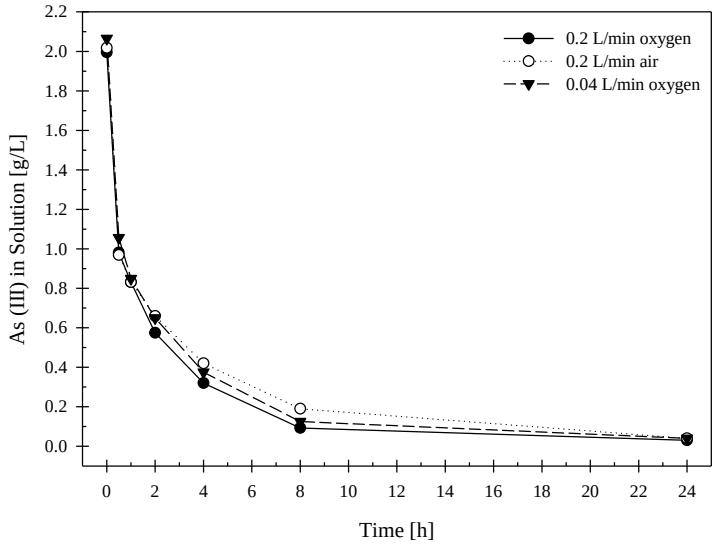

Figure 5-15: As (III) in solution as a function of time; 0.2 L/min air and 0.04 L/min oxygen were compared to determine the effects of nitrogen on the system under investigation.

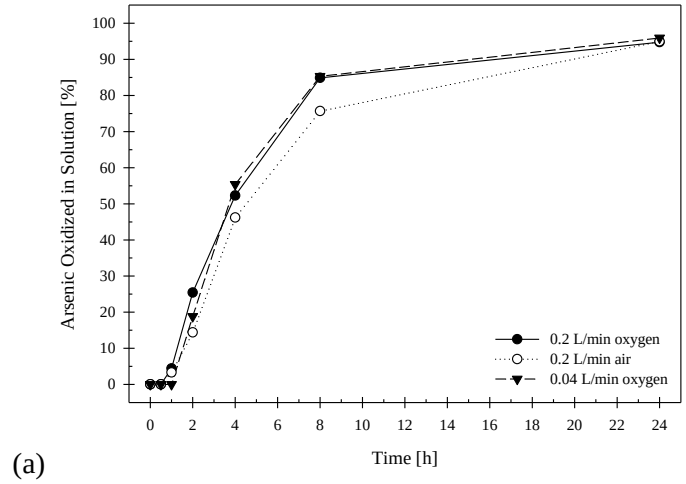

(a)

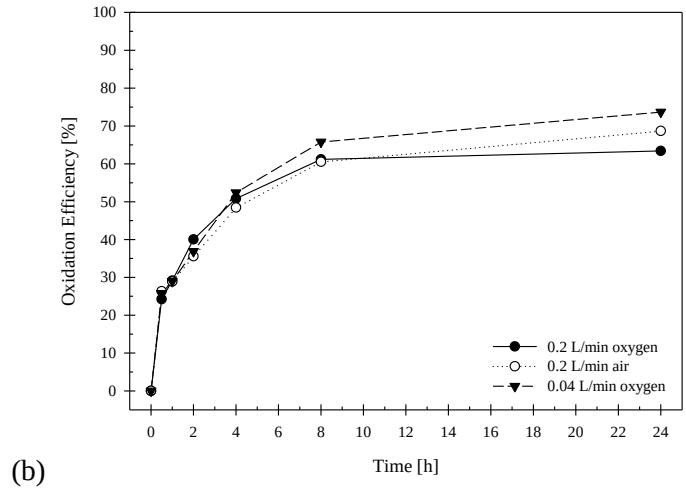

(b)

Figure 5-16: (a) Arsenic oxidation efficiency with respect to time; 0.2 L/min air and 0.04 L/min oxygen were compared to determine the effects of nitrogen on the system under investigation, and (b) the total oxidation of arsenic assuming that 50% of arsenic species on the activated carbon are of the pentavalent oxidation state.

The flowrate of 0.04 L/min oxygen was studied because this flowrate of oxygen adds the same amount of oxygen as the compressed air flowrate of 0.2 L/min since air is approximately 21% oxygen (and the rest is primarily nitrogen). It is clear that the test with 0.04 L/min oxygen more closely follows the curves of the test using 0.2 L/min oxygen. When nitrogen is introduced into the system via air there are consequently nitrogen molecules that take up space within the system. These spaces on or in-between the carbon pores that nitrogen occupies are then no longer able to be used to adsorb or oxidize arsenic. In the

case of batch tests conducted for this work the carbon had an intrinsic ability to oxidize the arsenic in solution to its fullest extent. However, in a continuous test there must constantly be new oxygen introduced into the system for continuous high efficiency arsenic oxidation. If air is used industrially then there are nitrogen molecules being introduced which will passivate, per se, parts of the activated carbon surface and decrease the effectiveness and longevity of the process.

It is interesting that in Figure 5-16(b) the total oxidation of air is higher than that of oxygen at the same gas flowrate. Future studies should be conducted to model how the speciation of arsenic changes over time on the activated carbon surface rather than assuming that 50% of the arsenic adsorbed is arsenate at any given time. This trend is not in accordance with the theories previously mentioned but the results are less heavily weighted as a large assumption was made which may or may not hold true.

5.3 Activated Alumina

Activated carbon is used for a variety of purposes due to its catalytic and adsorbent properties. Activated alumina is not known for being a good catalyst but is a well-established adsorbent material. Many studies have been completed on the use of activated alumina for removing arsenic from contaminated water due to its adsorbent nature (Ghosh & Gupta, 2012; Noyes, 1994; Önnby et al., 2014; Ratnayaka, Brandt, & Johnson, 2009; Singh & Pant, 2004). The PZC of activated alumina is 9.2 (Reyes Bahena, Robledo Cabrera, Lopez Valdivieso, & Herrera Urbina, 2002) which makes it an excellent material for adsorbing the inorganic oxyanions of arsenic. As well, a pH greater than 11.5 is required for arsenic desorption from activated alumina (Ghosh & Gupta, 2012) which makes it an excellent adsorbent for arsenic over a large range of pH. The purpose of this section is to compare the adsorptive properties and oxidative abilities of two adsorbent compounds: activated carbon and activated alumina.

When the activated alumina was mixed with a pH 1.0 arsenite acid solution the activated alumina balls produced fines which made the balls stick together. A higher rpm was needed for this test in order to stir the activated alumina in solution; an rpm of 450 was selected. Also, the gas used for the activated alumina

test was 1.0 L/min of oxygen in order to use the most oxidizing conditions for comparison purposes. The activated carbon batch test used 0.2 L/min oxygen and a stir rate of 200 rpm. Both tests had a solids content of 20% by mass on a dry basis and used a 2 g/L arsenite solution at an initial pH of 1.0 for the activated alumina test and 1.0 for the activated carbon test.

The pH and ORP of the solutions were measured at each sampling time. The pH of the solution with activated carbon initially rose to 1.7 and stayed within a pH range of 1.7-1.9 for the remainder of the test, as seen in Figure 5-17. The pH of the solution with activated alumina, however, kept increasing and did not reach a plateau.

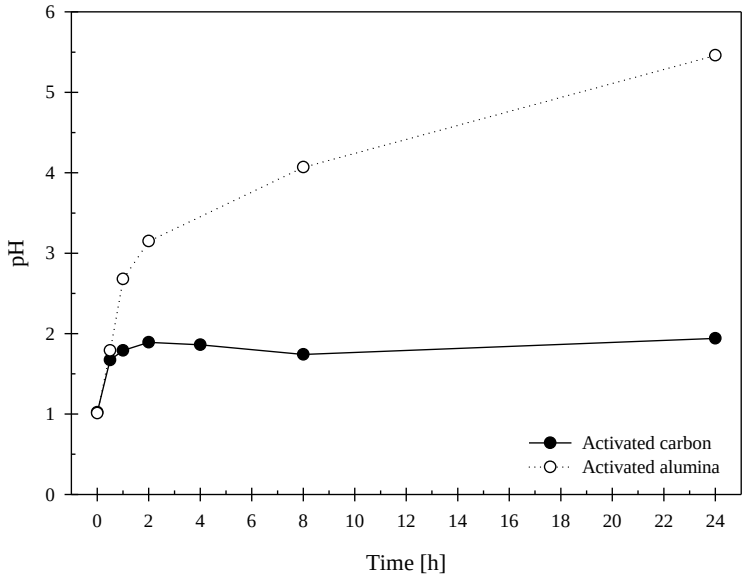

Figure 5-17: pH of the arsenical solution with respect to time for tests using activated carbon and activated alumina, respectively, as the adsorbent/catalyst.

Activated alumina is typically a very stable solid and will not solubilize as the solubility product value (K_{sp}) of aluminum oxide is 10^{-32} (George, Pandit, & Gupta, 2010) but activated alumina may dissolve in highly acidic solutions (Ratnayaka et al., 2009; Valdivieso, Bahena, Song, & Urbina, 2006). The aluminum concentration throughout the test was assayed via ICP analysis to determine if this was the

reason the pH increased or if it was due to the adsorbance of arsenic acid and possibly some protons. Figure 5-18 shows the dissolution of the activated alumina in terms of the concentration of aluminum present in solution with respect to time as well as the corresponding pH. The aluminum in solution is initially negligible but drastically increases to 200 mg/L within 30 minutes of the start of the test (pH is 1.8), and then peaks at 250 mg/L when the pH is 2.7. The increase in pH slows down after 2 hours and the aluminum in solution quickly decreases with a rising pH. At 8 hours the aluminum concentration in solution is 20 mg/L and at 24 hours the concentration is less than 1 ppm (the detection limit). This is in accordance with a study which finds that a system with conditions of a neutral pH at 25 °C will have minimal alumina solubility (Valdivieso et al., 2006).

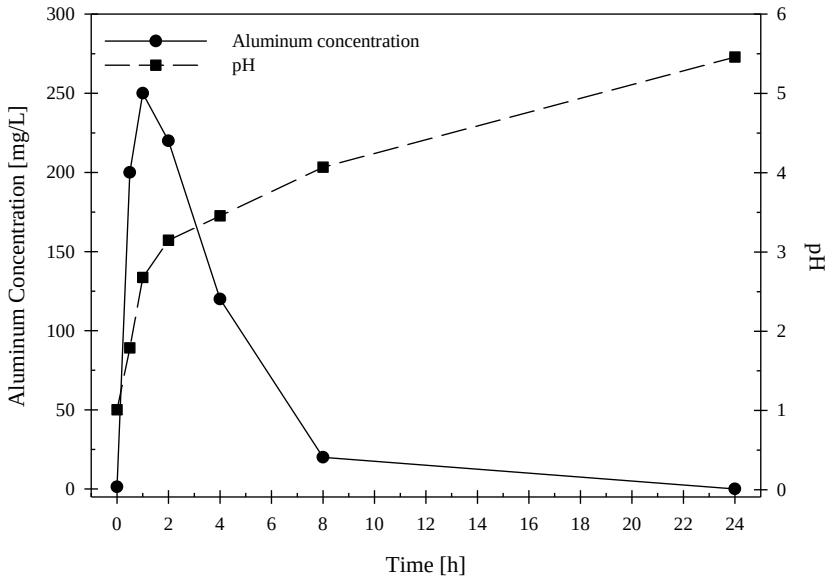

Figure 5-18: Aluminum concentration [mg/L] in solution for the test using activated alumina. The pH of the solution is also included.

Another reason for the drastic increase in pH over the course of the test with activated alumina in comparison with the tests using activated carbon may be seen by looking at a case study where fluoride adsorption onto activated alumina was explored. It is suggested that fluoride, which is an anion, replaces the hydroxide ions on the surface of activated alumina (Reyes Bahena et al., 2002). If this is a similar case

but with arsenic oxyanions adsorbing instead of the fluoride ions then the increase in alkalinity is explained as there are more hydroxide ions in solution as the arsenic is adsorbed onto the alumina.

The ORP of the solution with activated carbon rose by 50 mV to 517 mV which is within the standard final ORP range for tests using activated carbon as a catalyst in the scope of this thesis. Interestingly, the ORP of the solution with activated carbon decreased by 169 mV to a final ORP value of 282 mV. Under these conditions (low ORP and low pH) the dominant arsenic oxidation state would be trivalent in nature, although some pentavalent arsenic could be present. ORP values for this experiment are reported in Table 20.

Table 20: Initial and final ORP for activated carbon with 0.2 L/min O_2 and activated alumina with 1.0 L/min O_2

	Initial ORP [mV]	Final ORP [mV]	Difference [mV]
Activated Carbon	467	517	50
Activated Alumina	451	282	-169

Figure 5-19 illustrates the amount of arsenite remaining in solution over the course of the two tests. It is evident that even though the flowrate of oxygen is 0.8 L/min higher in the activated alumina test compared to the activated carbon test there is still more arsenite present in solution. There are two factors that this figure encompasses: adsorption and oxidation.

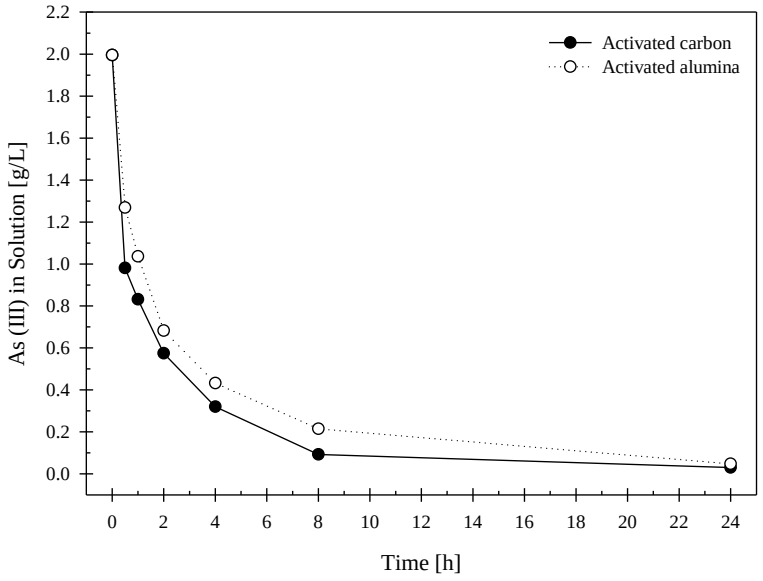

Figure 5-19: As (III) in solution as a function of time for tests using activated carbon and activated alumina, respectively, as the adsorbent/catalyst.

Figure 5-20(a) shows the relative amount of total arsenic adsorbed onto the activated carbon and activated alumina surfaces. It is clear that the forces which bind the arsenic to activated carbon act at a faster pace than the activated alumina, but the activated alumina has a much higher adsorption capacity and therefore surpasses the carbon in terms of the total arsenic adsorbed. Figure 5-20(b) shows that the activated alumina has a much higher capacity to adsorb arsenic compared to activated carbon as the maximum amount of arsenic that the activated carbon can hold is 2.93 mg As/g carbon on a wet basis, whereas the maximum amount that activated alumina can hold is not reached within the 24 hour time period.

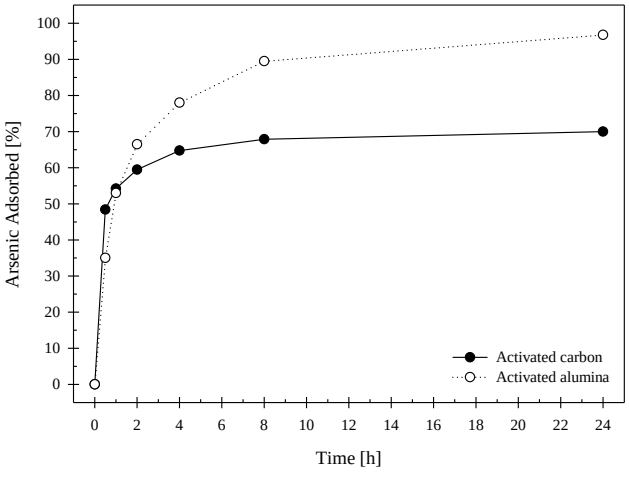

(a)

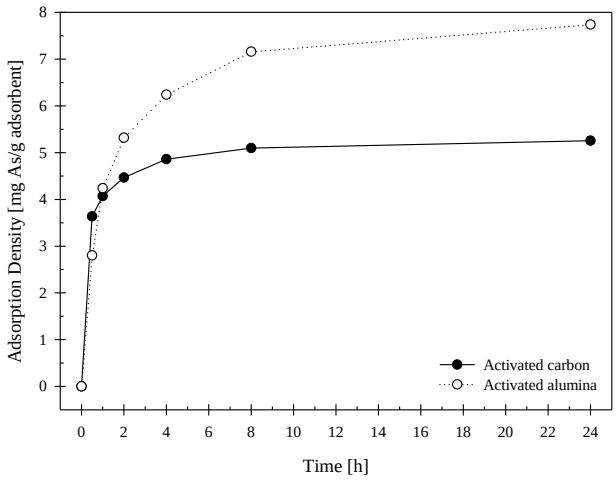

(b)

Figure 5-20: (a) Amount of arsenic adsorbed onto the activated alumina or activated carbon surface as a function of time (b) The amount of arsenic [mg] adsorbed per gram of dry carbon or dry alumina present in the test.

Activated alumina seemingly has little to no ability to oxidize arsenic. Figure 5-21 shows that at 24 hours there is 27% arsenic oxidation in solution in the activated alumina test. However, at that time there is a very small amount of arsenic left in solution so it could be attributed to discrepancies between ICP for total arsenic and titration methods for assaying arsenite. The ICP results indicate that at 24 hours there is 0.065 g/L of arsenic remaining in the solution and the titration results show an arsenite concentration of

0.047 g/L. These results are quite close considering the ICP solution was diluted by 20 times prior to measurement.

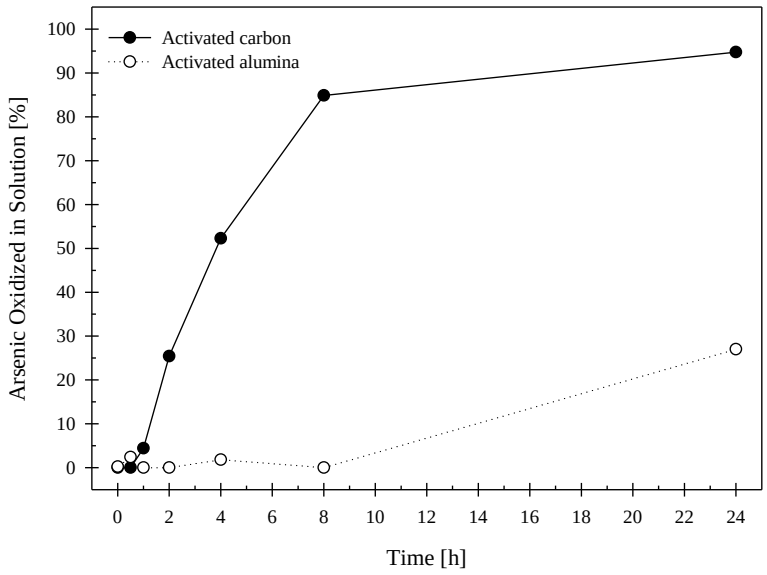

Figure 5-21: Oxidation efficiency of arsenic in solution for tests with activated alumina and activated carbon, respectively.

Conclusions drawn from Figure 5-20 and Figure 5-21 are consistent with literature. No data has been found which postulates that activated alumina and oxygen, alone, has the ability to oxidize arsenic without the addition of supplementary reagents. One study looked at using activated alumina and hydrogen peroxide to oxidize arsenic, but it was found that arsenite would reversibly adsorb onto the activated alumina surface and then hydrogen peroxide would irreversibly oxidize arsenite to arsenate consequentially strengthening the arsenic-activated alumina bond (Önnby et al., 2014).

It is evident that the decrease in arsenite concentration in the solution of the alumina test is due solely to adsorption but the decrease in arsenite concentration in the solution of the activated carbon test is due to both the adsorption of arsenite oxyanions and the oxidation of arsenite to arsenate. The oxidation of arsenic in the solution appears after 50% of the arsenic is adsorbed onto the activated carbon surface, but

a very small (if not negligible) amount of arsenic is oxidized in solution when activated alumina is present after 85% of the arsenic has already been adsorbed.

It is clear that the adsorbent properties do not correspond to catalytic abilities. It has already been discussed that dissolved oxygen plays a role in the oxidation of arsenic in the presence of activated carbon. Dissolved oxygen also exists in the arsenic-oxygen-activated alumina system but still no oxidation occurs. This supports the theory that peroxide in solution, which is created by the activated carbon in-situ, is the oxidant in the arsenic oxidation reaction that is catalyzed by the activated carbon in the system. The peroxide formed on the activated carbon surface is therefore the most significant element in achieving arsenic oxidation. This also means that oxygen, and not air, must be used to maximize the amount of peroxide formed and the oxygen source must be continuously replenished to create hydrogen peroxide.

5.4 Chapter Conclusions

This chapter focused on analyzing batch test experiments to further understand the factors which affect the arsenic oxidation mechanism. Factors investigated include initial arsenite concentration, pulp density of activated carbon, oxygen flowrate, and use of activated alumina as the catalyst/adsorbent.

The amount of arsenic adsorbed follows a logarithmic curve quite well as the r^2 value ranged from about 0.855-0.976. Varying the initial arsenite concentration did not have a large effect on the final pH, ORP or oxidation efficiency of the test.

Tests that were run with different amounts of activated carbon present had no effect on the final oxidation efficiency as the final arsenic oxidation values ranged between 94.1-95.2%. The final pH of the system was higher with increasing carbon pulp density and this is due to protons from sulphuric acid adsorbing onto the activated carbon surface, thereby increasing the pH of the bulk solution. The protons may react with functional groups on the carbon surface to promote the production of hydrogen peroxide.

The effect of oxygen flow rate was investigated but there was not a large difference measured in the pH, ORP or oxidation efficiency. Next, air was used as the gas stream (at 0.2 L/min) and compared against tests using oxygen flowrates of 0.2 L/min and 0.04 L/min, respectively. The test using air as the sparged gas (which consequently introduced nitrogen into the system) had a smaller amount of arsenic adsorbed compared to the test with 0.2 L/min oxygen. This is due to the oxidation of arsenic rather than solely adsorption because nitrogen should actually increase the sorption capacity of activated carbon with respect to anions (Biniak et al., 1997). The batch test using 0.04 L/min oxygen follows the curves of 0.2 L/min oxygen more closely than with using air. Nitrogen molecules that are introduced into the system from air can sorb onto the activated carbon surface and occupy sites that could otherwise adsorb or aid in oxidizing arsenic. Although for a batch test carbon has a limited ability to oxidize arsenic without the introduction of oxygen (see Chapter 4), a continuous test would likely require the constant injection of oxygen into the system in order to maintain the effectiveness of the process.

Lastly, activated alumina was investigated as an alternative catalyst to activated carbon to see if the oxidation was due to a porous surface or the catalytic abilities of a solid. It was concluded that activated alumina does not have the ability to oxidize arsenic but has a higher adsorption capacity compared to activated carbon. In fact, activated alumina has a reducing ability as the ORP for the alumina test was decreased from 541 mV to 282 mV (vs Ag/AgCl) whereas the ORP in the activated carbon test increased from 467-517 mV (vs Ag/AgCl). From the findings it was concluded that it is the functional groups on the activated carbon surface that allow for arsenic oxidation and not the porous nature of the surface.

Chapter 6

A Study on the Effect of Ferrous and Cupric Ions in a Column Test

This section presents and discusses some preliminary continuous column test experiments regarding the effect of using ions to increase the oxidation rate of arsenic as well as using fresh versus recycled activated carbon. More data is required on these topics before drawing final conclusions as this portion of the work presented in the thesis was conducted as an opening to future research on this process.

6.1 Methods

The reagents used were: arsenic trioxide (99.5% on a metals basis from Alfa Aesar), arsenic pentoxide (99.8% on a metals basis from Alfa Aesar), ferrous sulphate heptahydrate (from Fisher Scientific) and cupric sulphate pentahydrate (from Fisher Scientific).

A 2 L Erlenmeyer flask partially filled with DI water was placed on top of a magnetic stir plate and 20 mL of concentrated sulphuric acid was added. Arsenic trioxide powder, As_2O_3, was added to the mixture in a high dosage so that the solution could be diluted in a 5 gallon bucket and have a concentration of 1.8 g/L As (III). The solution in the Erlenmeyer flask was mixed and heated to 75 °C until the arsenic had completely dissolved. The solution was then diluted with water in a large bucket to make 14 L of solution to feed the column. Ferrous sulphate was added to the bucket and stirred via an overhead mixure. Concentrated sulphuric acid was then used to bring the pH down to a pH of 1. For tests requiring copper, two 2 L volumetric flasks were used to prepare 4 L of solution. To these flasks, cupric sulphate was added to meet the experimental parameters. The initial conditions for the two column tests discussed in this chapter are presented in Table 21.

Table 21: Initial conditions for tests containing arsenic, iron and copper

Test	Arsenite [g/L]	Ferrous [g/L]	Cupric [g/L]	pH ± 0.1	ORP [mV]	Activated Carbon State
1	1.8	1.8	0	1.0	327-344	Fresh
2	1.8	1.8	0.5	1.0	360-387	Recycled

6.2 Column Tests Results

6.2.1 Arsenic and Iron with Fresh Carbon

Complete oxidation of arsenic in solution was achieved before 24 hours of column operation; however, the total arsenic leaving the column was less than the arsenic entering the column. This observation is consistent with the results presented at the Conference of Metallurgists in 2014 (Choi et al., 2014b). In the conference proceedings it is mentioned that the initial arsenite concentration exiting the column was as low as 0.1 g/L from an initial concentration of 10 g/L entering the column (Choi et al., 2014b). As well, the system in the proceedings reached steady state in 120 hours but the experiment depicted in Figure 6-1 shows that steady state was not achieved in 144 hours with respect to the arsenic and iron mass balance, as the same trend regarding arsenic can be said for the iron entering and exiting the column. The concentration of total iron and total arsenic leaving the column as a function of time can be seen in Figure 6-1. The column test was in operation for 144 hours (6 days).

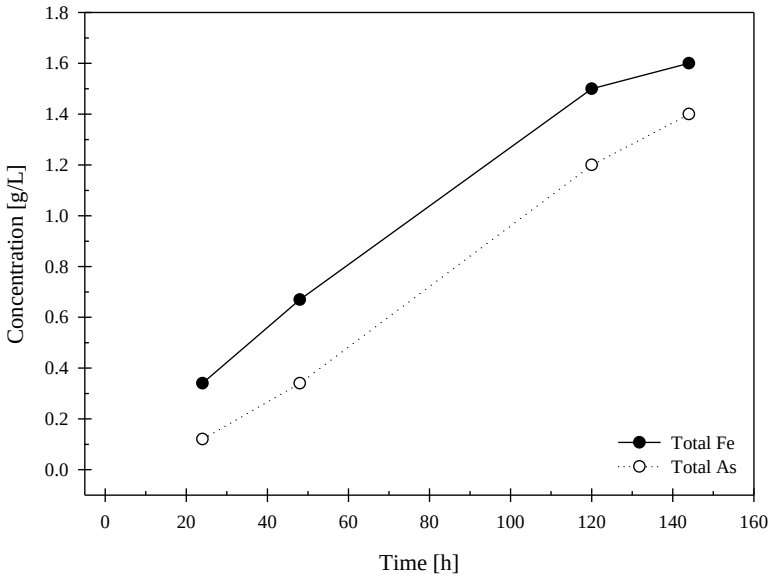

Figure 6-1: Concentration of arsenic and iron at the outlet stream; the solid line represents the concentration of iron at the column outlet and the dashed line represents the concentration of arsenic at the column outlet.

6.2.2 Arsenic, Iron and Copper with Recycled Carbon

The column was flushed with a sulphuric acid solution of less than pH 1 for 24 hours to strip the arsenic and iron that had adsorbed onto the activated carbon. The next test performed in the column contained arsenite, ferrous and cupric ions. As with the first test which only had arsenic and iron introduced into the system, the arsenic and iron were completely oxidized by the time the first sample was taken which was 18 hours. The speciation of copper was not measured or determined. Figure 6-2 displays the concentration of total arsenic, iron and copper in the column effluent for operating times between 18-120 hours.

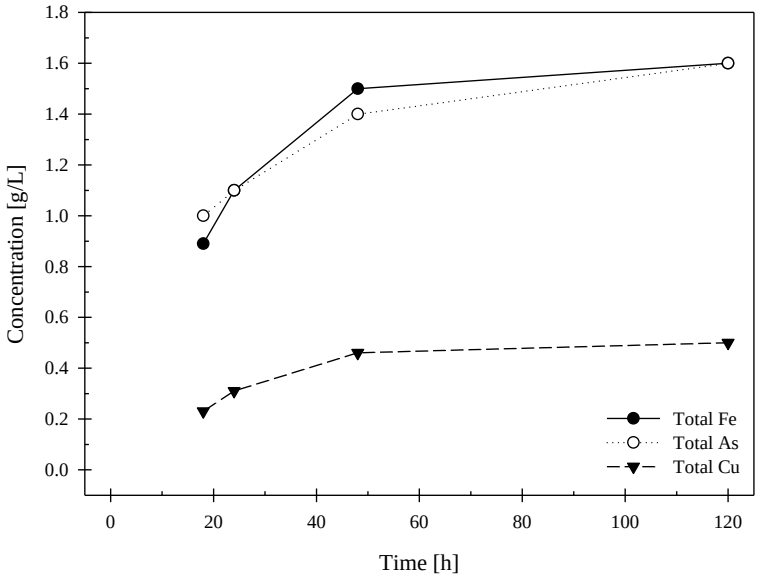

Figure 6-2: Concentration of arsenic, iron and copper at the column outlet stream as a function of operating time.

6.3 Column Test Discussion

Comparing the results from Figure 6-1 and Figure 6-2 yields some interesting observations. Firstly, the arsenic and iron in the first test more rapidly adsorb onto the carbon and are initially present in the effluent stream in low concentrations which gradually rise to just below the reservoir concentrations. In the second test, however, the arsenic and iron first appear at a higher concentrations and take a smaller amount of time to reach the same values in the effluent stream as the first test. The initially higher concentration in the first few samples is likely due to arsenic and iron on the carbon from the previous test

still taking up active sites on the activated carbon which means that more arsenic and iron remain in solution or that the arsenic and iron from the previous test desorb from the carbon to allow for fresher ions to adsorb.

The Barrick patent from 2014 regarding activated-carbon assisted oxidation of arsenic species tested iron in solution and found that the iron was also oxidized and the iron and arsenate consequently formed scorodite (Choi et al., 2014a). It is possible that the reason for the effluent concentrations of arsenic and iron being approximately 300-400 ppm lower than the initial solution is that scorodite crystals or other ferric arsenates maybe be forming on the carbon surface; however, this is highly unlikely due to the extremely acidic pH of the system.

Another interesting observation is that there is consistently more iron in the effluent stream than there is arsenic. Iron sulphate will dissociate into a sulphate ion and an iron cation (ferric or ferrous depending on the oxidation state). If the carbon surface is predominantly positive in the pH range of 0.9-1.1 (test conditions) then the iron cations will be less likely to take a spot on the surface compared to a negatively charged arsenic oxyanion.

Copper appears to reach steady state at a faster rate than the other elements in solution as the concentration of copper in the effluent stream matches the copper in the column reservoir after 48 hours. This is in comparison to the iron and arsenic concentrations which never reach equilibrium within the duration of the two tests. Cupric ions are known to increase the amount arsenic removed from solutions due to two cases: (1) copper reacting with arsenate to form insoluble copper-arsenate precipitates or (2) arsenic adsorbing to activated carbon independently from where the copper is adsorbed (Lorenzen et al., 1995). In this system it is likely the latter of the two cases because there is no copper loss through the column but there is still missing arsenic in the steady-state arsenic mass balance.

Chapter 7

Conclusions and Future Work

The goals for this thesis were to investigate the mechanism of activated carbon-catalyzed arsenic oxidation in the presence of oxygen. It was concluded that activated carbon has an intrinsic catalytic ability to oxidize arsenic in a limited capacity without a supply of oxygen but in order to continue the process oxygen must be introduced into the system.

Hydrogen peroxide is formed on the activated carbon surface from dissolved oxygen in the solution that is in close proximity to the activated carbon. It was determined that it is due to the catalytic ability of activated carbon, and not its adsorbent and porous characteristics, that allows for the expedition of the arsenic mechanism. This was confirmed by comparing the oxidizing abilities and adsorption capacities of two adsorbing materials: activated carbon and activated alumina. The activated alumina did not offer any oxidizing potential but did have a much higher adsorbent capacity.

The oxidation mechanism is partially understood but it is confirmed that the oxidation rate is definitely dependent on the oxygen present and contact with activated carbon. Two mechanisms of arsenic oxidation are proposed and either one may be occurring or both may occur simultaneously:

1) Peroxide is formed on the activated carbon surface. Arsenite ions in close proximity then react with the peroxide and subsequently adsorb onto the activated carbon surface.
2) Peroxide is formed on the activated carbon surface and then reacts with adsorbed arsenite.

Adsorption isotherm models of the arsenic-activated carbon system were analyzed with Freundlich and Langmuir isotherms. It was determined that the Freundlich isotherm model better characterizes the system than the Langmuir isotherm model. The system studied is complex due to peroxide forming, two oxidation states of arsenic and various other ions adsorbing (such as protons). Shake flask experiments showed that there is arsenate present on the carbon surface even if there is none present in solution. The

adsorption shake tests also indicate that arsenate has a slightly higher affinity to adsorb onto the activated carbon surface compared to arsenite. As well, arsenic desorption shake tests indicate that arsenite is more preferentially desorbed from solution. A next step would be to experimentally determine the arsenite and arsenate binding energies with activated carbon.

Batch test experiments produced some interesting results. An increase in carbon present in a batch test yields a higher pH at the end of the 24 hour test due to protons from sulphuric acid adsorbing onto the activated carbon surface. These protons can then react with functional groups to produce hydrogen peroxide. Air was used as the sparged gas and compared to tests using oxygen. The test with air (which introduces nitrogen into the system) had less arsenic adsorb onto the carbon which is not in accordance with literature as nitrogen increases the sorption capacity of carbon to anions (Biniak et al., 1997).

Activated alumina replaced activated carbon in a batch test to investigate if the catalytic abilities of activated carbon are due to the functional groups or due to the porous nature of the surface. It was concluded that activated alumina had no aptitude to oxidize arsenic and therefore it is the functional groups on the carbon surface that promote the oxidative abilities.

There are still many unanswered questions regarding the arsenic oxidation mechanism and there are various experiments and investigations which would deepen the understanding of what is occurring in the system of study. Some future work should include:

- Running 1 L batch tests and completely stripping the arsenic from the activated carbon to determine the speciation of arsenic in the solution and on the activated carbon surface. Running four batch tests in parallel and shutting down after 6, 12, 18 and 24 hours would allow for a complete arsenic balance throughout the test.
- Running continuous tests with a smaller column (to reduce residence time). The column built should have ports throughout the column to take samples as the arsenic acid travels through a bed of activated carbon.

- The lifespan of the activated carbon should be investigated to answer the question as to how long the continuous process can operate with minimal maintenance. Tests can be run with fresh and reused activated carbon and their results compared. Another interesting route this research could take would be to run columns in series to see if it would make a difference when run continuously for a prolonged amount of time.
- Tests with different types of activated carbon should be investigated. Varying the ash content in the carbon will change its adsorptive characteristics and possibly the functional groups.
- Compare how iron, copper, lead and zinc affect oxidation of arsenic and other species that enter the system at a lower oxidation state.

References

Ahumada, E., Lizama, H., Orellana, F., Suarez, C., Huidobro, A., Sepulveda-Escribano, A., & Rodriguez-Reinoso, F. (2002). Catalytic oxidation of Fe(II) by activated carbon in the presence of oxygen. Effect of the surface oxidation degree on the catalytic activity. *Carbon*, *40*, 2827–2834.

Alegria, A. E., Lion, Y., Kondo, T., & Riesz, P. (1989). Sonolysis of aqueous surfactant solutions: probing the interfacial region of cavitation bubbles by spin trapping. *The Journal of Physical Chemistry*, *93*(12), 4908–4913. http://doi.org/10.1021/j100349a046

Barkauskas, J., & Dervinyte, M. (2004). An investigation of the functional groups on the surface of activated carbons. *Journal of the Serbian Chemical Society*, *69*(5), 363–375. http://doi.org/10.2298/JSC0405363B

BASF. (2009). Product Data Sheet: F-200 Activated Alumina For Liquid and Gas Drying. Retrieved from https://www.interraglobal.com/portals/0/pdf/specsheets/basf-f200-activated-alumina.pdf

Basha, C. A., Selvi, S. J., Ramasamy, E., & Chellammal, S. (2008). Removal of arsenic and sulphate from the copper smelting industrial effluent. *Chemical Engineering Journal*, *141*, 89–98. http://doi.org/10.1016/j.cej.2007.10.027

Beers Jr., R. F., & Sizer, I. W. (1952). A spectrophotometric method for measuring the breakdown of hydrogen peroxide by catalase. *The Journal of Biological Chemistry*, 133–140.

Biniak, S., Szymański, G., Siedlewski, J., & Światkoski, A. (1997). The characterization of activated carbons with oxygen and nitrogen surface groups. *Carbon*, *35*(12), 1799–1810. http://doi.org/10.1016/S0008-6223(97)00096-1

Bissen, M., & Frimmel, F. H. (2003a). Arsenic - a review. Part II: Oxidation of arsenic and its removal in water treatment. *Acta Hydrochimica et Hydrobiologica*, *31*(2), 97–107. http://doi.org/10.1002/aheh.200300485

Bissen, M., & Frimmel, F. H. (2003b). Arsenic - a Review . Part I : Occurrence , Toxicity , Speciation , Mobility. *Acta Hydrochimica et Hydrobiologica*, *31*, 9–18.

Bokros, J. C. (1969). Chemistry and Physics of Carbon, Volume 5. In P. C. Walker & M. Dekker (Eds.) (pp. 1–118). New York.

Bonakdarpour, A., Esau, D., Cheng, H., Wang, A., Gyenge, E., & Wilkinson, D. P. (2011). Preparation and electrochemical studies of metal–carbon composite catalysts for small-scale electrosynthesis of H2O2. *Electrochimica Acta*, *56*(25), 9074–9081. http://doi.org/10.1016/j.electacta.2011.06.043

Bora, A. J., Gogoi, S., Baruah, G., & Dutta, R. K. (2016). Utilization of co-existing iron in arsenic removal from groundwater by oxidation-coagulation at optimized pH. *Journal of Environmental Chemical Engineering*, *4*(3), 2683–2691. http://doi.org/10.1016/j.jece.2016.05.012

Brookins, D. G. (1988). *Eh-pH Diagrams for Geochemistry*. Berlin: Springer-Verlag.

Brusciotti, F., & Duby, P. (2007). Cyclic voltammetry study of arsenic in acidic solutions. *Electrochimica Acta*, *52*(24), 6644–6649. http://doi.org/10.1016/j.electacta.2007.04.071

Calgon Carbon Corporation. (2013). Gold Plus Datasheet.

Canada. (2015). Metal Mining Effluent Regulations SOR/2002-222. Retrieved from http://laws-lois.justice.gc.ca

Cariolaro, G. (2015). Applications of Quantum Information. *Quantum Communications*, *303*, 639–663. http://doi.org/10.1007/978-3-319-15600-2

Carlson, J. J., & Kawatra, S. K. (2013). Factors affecting zeta potential of iron oxides. *Mineral Processing and Extractive Metallurgy Review*, *34*, 269–303. http://doi.org/10.1080/08827508.2011.604697

Cheng, H., Hu, Y., Luo, J., Xu, B., & Zhao, J. (2009). Geochemical processes controlling fate and transport of arsenic in acid mine drainage (AMD) and natural systems. *Journal of Hazardous Materials*, *165*(1–3), 13–26. http://doi.org/10.1016/j.jhazmat.2008.10.070

Choi, Y., Ghahremaninezhad, A., & Ahern, N. (2014a). Method for arsenic oxidation and removal from process and waste solutions. United States.

Choi, Y., Ghahremaninezhad, A., & Ahern, N. (2014b). Process for activated carbon-assisted oxidation of arsenic species in process solutions and waste waters. In *COM 2014 - Conference of Metallurgists* (pp. 1–9). Canadian Institute of Mining, Metallurgy and Petroleum.

Chuang, C. L., Fan, M., Xu, M., Brown, R. C., Sung, S., Saha, B., & Huang, C. P. (2005). Adsorption of arsenic(V) by activated carbon prepared from oat hulls. *Chemosphere*, *61*(4), 478–483. http://doi.org/10.1016/j.chemosphere.2005.03.012

Clancy, T. M., Hayes, K. F., & Raskin, L. (2013). Arsenic waste management: A critical review of testing and disposal of arsenic-bearing solid wastes generated during arsenic removal from drinking water. *Environmental Science and Technology*, *47*(19), 10799–10812. http://doi.org/10.1021/es401749b

Cui, J., Du, Y., Xiao, H., Yi, Q., & Du, D. (2014). A new process of continuous three-stage co-precipitation of arsenic with ferrous iron and lime. *Hydrometallurgy*, *146*, 169–174. http://doi.org/10.1016/j.hydromet.2014.03.012

Dai, M. (1994). The Effect of Zeta Potential of Activated Carbon on the Adsorption of Dyes from Aqueous Solution: I. The Adsorption of Cationic Dyes: Methyl Green and Methyl Violet. *Journal of Colloid and Interface Science*, *164*, 223–228.

Demopoulos, G. P. (2014). Arsenic immobilization research advances: past, present and future. In *COM 2014 - Conference of Metallurgists*. Canadian Institute of Mining, Metallurgy and Petroleum.

Doña Rodríguez, J. M., Herrera Melián, J. A., & Pérez Peña, J. (2000). Determination of the Real Surface Area of Pt Electrodes by Hydrogen Adsorption Using Cyclic Voltammetry. *Journal of Chemical Education*, *77*(9), 1195. http://doi.org/10.1021/ed077p1195

Drahota, P., & Filippi, M. (2009). Secondary arsenic minerals in the environment: A review. *Environment International*, *35*(8), 1243–1255. http://doi.org/10.1016/j.envint.2009.07.004

Eguez, H. E., & Cho, E. H. (1987). Adsorption of Arsenic on Activated Charcoal. *Jom*, *39*(7), 38–41. http://doi.org/10.1007/BF03258040

Filippou, D., & Demopoulos, G. P. (1997). Arsenic immobilization by controlled scorodite precipitation. *JOM*, *49*(12), 52–55. http://doi.org/10.1007/s11837-997-0034-3

Filippou, D., St-Germain, P., & Grammatikopoulos, T. (2007). Recovery of Metal Values From Copper - Arsenic Minerals and Other Related Resources. *Mineral Processing and Extractive Metallurgy Review*, *28*(4), 247–298. http://doi.org/10.1080/08827500601013009

Foo, K. Y., & Hameed, B. H. (2010). Insights into the modeling of adsorption isotherm systems. *Chemical Engineering Journal*, *156*(1), 2–10. http://doi.org/10.1016/j.cej.2009.09.013

Fujita, T., Taguchi, R., Kubo, H., Shibata, E., & Nakamura, T. (2009). Immobilization of Arsenic from Novel Synthesized Scorodite—Analysis on Solubility and Stability. *Materials Transactions*, *50*(2), 321–331. http://doi.org/10.2320/matertrans.M-MRA2008844

Gallegos-Garcia, M., Ramírez-Muñiz, K., & Song, S. (2012). Arsenic Removal from Water by Adsorption Using Iron Oxide Minerals as Adsorbents: A Review. *Mineral Processing and Extractive Metallurgy Review*, *33*(5), 301–315. http://doi.org/10.1080/08827508.2011.584219

George, S., Pandit, P., & Gupta, A. B. (2010). Residual aluminium in water defluoridated using activated alumina adsorption - Modeling and simulation studies. *Water Research*, *44*(10), 3055–3064. http://doi.org/10.1016/j.watres.2010.02.028

Ghosh, D., & Gupta, A. (2012). Economic justification and eco-friendly approach for regeneration of spent activated alumina for arsenic contaminated groundwater treatment. *Resources, Conservation and Recycling*, *61*, 118–124. http://doi.org/10.1016/j.resconrec.2012.01.005

Gimeno, P., Bousquet, C., Lassu, N., Maggio, A.-F., Civade, C., Brenier, C., & Lempereur, L. (2015). High-performance liquid chromatography method for the determination of hydrogen peroxide present or released in teeth bleaching kits and hair cosmetic products. *Journal of Pharmaceutical and Biomedical Analysis*, *107*(790), 386–393. http://doi.org/10.1016/j.jpba.2015.01.018

González-Contreras, P., Weijma, J., & Buisman, C. J. N. (2012). Continuous bioscorodite crystallization in CSTRs for arsenic removal and disposal. *Water Research*, *46*(18), 5883–92. http://doi.org/10.1016/j.watres.2012.07.055

Guo, X., Shi, J., Yi, Y., Tian, Q., & Li, D. (2015). Separation and recovery of arsenic from arsenic-bearing dust. *Journal of Environmental Chemical Engineering*, *3*(3), 2236–2242. http://doi.org/10.1016/j.jece.2015.06.028

Gustafsson, J., Mikkola, P., Jokinen, M., & Rosenholm, J. B. (2000). The influence of pH and NaCl on the zeta potential and rheology of anatase dispersions. *Colloids and Surfaces A: Physicochemical and Engineering Aspects*, *175*, 349–359.

Harris, B. (2003). The removal of arsenic from process solutions: theory and industrial practice. In C. Young, A. Alfantazi, C. Anderson, A. James, D. Dreisinger, & B. Harris (Eds.), *Hydrometallurgy 2003 Proceedings* (Vol. 2: Electro, pp. 1889–1902). http://doi.org/10.1002/9781118804407.ch62

Henke, K. R. (2009). Arsenic Thermodynamic Data. In *Arsenic: Environmental Chemistry, Health Threats and Waste Treatment* (pp. 475–493). John Wiley & Sons, Ltd. http://doi.org/10.1002/9780470741122

Jansen, R. J. J., & van Bekkum, H. (1995). XPS of nitrogen-containing functional groups on activated carbon. *Carbon*, *33*(8), 1021–1027. http://doi.org/10.1016/0008-6223(95)00030-H

Johto, H., & Taskinen, P. (2014). Phase diagram of system As2S3-Cu2S-PbS at 773-1173 K. *Canadian Metallurgical Quarterly*, *53*(3), 362–366. http://doi.org/10.1179/1879139514Y.0000000133

Kanthale, P., Ashokkumar, M., & Grieser, F. (2008). Sonoluminescence, sonochemistry (H2O2 yield) and bubble dynamics: Frequency and power effects. *Ultrasonics Sonochemistry*, *15*, 143–150. http://doi.org/10.1016/j.ultsonch.2007.03.003

Kelebek, S., Salman, T., & Smith, G. W. (1982). An Electrokinetic Study of Three Coals. *Canadian Metallurgical Quarterly*, *2*, 205–209.

Khuntia, S., Majumder, S. K., & Ghosh, P. (2014). Oxidation of As(III) to As(V) using ozone microbubbles. *Chemosphere*, *97*, 120–124. http://doi.org/10.1016/j.chemosphere.2013.10.046

Klassen, N. V., Marchington, D., & Mcgowan, H. C. E. (1994). H2O2 determination by the I3- method and by KMnO4 titration. *Analytical Chemistry*, *66*(18), 2921–2925. http://doi.org/10.1021/ac00090a020

Lamb, A. B., & Elder, L. W. J. (1931). The electromotive activation of oxygen. *Journal of the American Chemical Society*, *53*(1904), 137–163.

Laskowski, J. (2001). *Developments in Mineral Processing Volume 14: Coal Flotation and Fine Coal Utilization*. (D. W. Fuerstenau, Ed.). Amsterdam: Elsevier Science B.V.

Lattanzi, P., Da Pelo, S., Musu, E., Atzei, D., Elsener, B., Fantauzzi, M., & Rossi, A. (2008). Enargite oxidation: A review. *Earth-Science Reviews*, *86*(1–4), 62–88. http://doi.org/10.1016/j.earscirev.2007.07.006

Leist, M., Casey, R. J., & Caridi, D. (2000). The management of arsenic wastes: Problems and prospects. *Journal of Hazardous Materials*, *76*(1), 125–138. http://doi.org/10.1016/S0304-3894(00)00188-6

Lengke, M. F., Sanpawanitchakit, C., & Tempel, R. N. (2009). The oxidation and dissolution of arsenic-bearing sulfides. *Canadian Mineralogist*, *47*(3), 593–613. http://doi.org/10.3749/canmin.47.3.593

Long, G., Peng, Y., & Bradshaw, D. (2012). A review of copper-arsenic mineral removal from copper concentrates. *Minerals Engineering*, *36–38*, 179–186. http://doi.org/10.1016/j.mineng.2012.03.032

Lorenzen, L., van Deventer, J. S. J., & Landi, W. M. (1995). Factors affecting the mechanism of the adsorption of arsenic species on activated carbon. *Minerals Engineering*, *8*(4–5), 557–569. http://doi.org/10.1016/0892-6875(95)00017-K

Mandal, B. K., & Suzuki, K. T. (2002). Arsenic round the world: A review. *Talanta*, *58*(1), 201–235. http://doi.org/10.1016/S0039-9140(02)00268-0

Marcus, T. C. E., David, M., Yaacob, M., Salim, M. H., Asmi, A. I., Idrus, S. M., & Buntat, Z. (2015). Alternative Wavelength for linearity preservation of Beer-Lambert Law in ozone concentration measurement. *Microwave and Optical Technology Letters*, *57*(4), 1013–1016. http://doi.org/10.1002/mop

Marsden, J. O., & House, C. I. (2006). *Chemistry of Gold Extraction (2nd Edition)*. Society for Mining, Metallurgy, and Exploration (SME).

Martinson, C. A., & Reddy, K. J. (2009). Adsorption of arsenic(III) and arsenic(V) by cupric oxide nanoparticles. *Journal of Colloid and Interface Science*, *336*(2), 406–411. http://doi.org/10.1016/j.jcis.2009.04.075

McDougall, G. J., & Hancock, R. D. (1981). Gold complexes and activated carbon - A literature review. *Gold Bulletin*, *14*(4), 138–153. http://doi.org/10.1007/BF03216558

Miller, P., & Brown, A. (2005). Bacterial oxidation of refractory gold concentrates. In M. D. Adams & B. A. Wills (Eds.), *Developments in Mineral Processing* (pp. 371–402). Elsevier B.V.

Molnár, L., Virčíkova, E., & Lech, P. (1994). Experimental study of As(III) oxidation by hydrogen peroxide. *Hydrometallurgy*, *35*(1), 1–9. http://doi.org/10.1016/0304-386X(94)90013-2

Moon, D. H., Dermatas, D., & Menounou, N. (2004). Arsenic immobilization by calcium-arsenic precipitates in lime treated soils. *Science of the Total Environment*, *330*(1–3), 171–185. http://doi.org/10.1016/j.scitotenv.2004.03.016

Ng, J. C., Wang, J., & Shraim, A. (2003). A global health problem caused by arsenic from natural sources. *Chemosphere*, *52*(9), 1353–1359. http://doi.org/10.1016/S0045-6535(03)00470-3

Nishimura, T., & Umetsu, Y. (2001). Oxidative precipitation of arsenic (III) with manganese (II) and iron (II) in dilute acidic solution by ozone. *Hydrometallurgy*, *62*(2), 83–92. Retrieved from http://linkinghub.elsevier.com/retrieve/pii/S0304386X01001888

Nogueira, R. F. P., Oliveira, M. C., & Paterlini, W. C. (2005). Simple and fast spectrophotometric determination of H2O2 in photo-Fenton reactions using metavanadate. *Talanta*, *66*(1), 86–91. http://doi.org/10.1016/j.talanta.2004.10.001

Noyes, R. (1994). *Unit Operations in Environmental Engineering*. Noyes Publications.

Önnby, L., Kumar, P. S., Sigfridsson, K. G. V., Wendt, O. F., Carlson, S., & Kirsebom, H. (2014). Improved arsenic(III) adsorption by Al2O3 nanoparticles and H2O2: Evidence of oxidation to arsenic(V) from X-ray absorption spectroscopy. *Chemosphere*, *113*, 151–157. http://doi.org/10.1016/j.chemosphere.2014.04.097

Opio, F. K. (2013). *Investigation of Fe(III)-As(III) bearing phases and their potential for arsenic disposal*.

Payne, K. B., & Abdel-Fattah, T. M. (2005). Adsorption of Arsenate and Arsenite by Iron-Treated Activated Carbon and Zeolites: Effects of pH, Temperature, and Ionic Strength. *Journal of Environmental Science and Health*, *40*(August), 723–749. http://doi.org/10.1081/ESE-200048254

Peacey, J. G., Gupta, M. Z., & Ford, K. (2010). Review of process options to treat enargite concentrates. In *Proceedings of Copper, Copper-Cobre 2010* (pp. 1035–1050).

Ratnayaka, D. D., Brandt, M. J., & Johnson, M. (2009). *Water Supply* (6th ed.). Elsevier Ltd.

Rennie, R. (2016). *A Dictionary of Chemistry*. Oxford University Press.

Reyes Bahena, J. L., Robledo Cabrera, A., Lopez Valdivieso, A., & Herrera Urbina, R. (2002). Fluoride adsorption onto alpha-Al2O3 and its effect on the zeta potential at the alumina-aqeous electrolyte interface. *Separation Science and Technology*, *37*(8), 1973–1987.

Ritcey, G. M. (2005). Tailings management in gold plants. *Hydrometallurgy*, *78*(1–2 SPEC. ISS.), 3–20. http://doi.org/10.1016/j.hydromet.2005.01.001

Riveros, P. A., Dutrizac, J. E., & Spencer, P. (2001). Arsenic Disposal Practices in the Metallurgical Industry. *Canadian Metallurgical Quarterly*, *40*(4), 395–420. http://doi.org/10.1179/000844301794388263

Robins, R. G., & Jayaweera, L. D. (1992). Arsenic in Gold Processing. *Mineral Processing and Extractive Metallurgy Review*, *9*(1), 255–271. http://doi.org/10.1080/08827509208952710

Ruthven, D. M. (2001). Adsorption, Fundamentals. In *Kirk-Othmer Encyclopedia of Chemical Technology* (Vol. 1, pp. 582–617). John Wiley & Sons, Inc.

Safarzadeh, M. S., Moats, M. S., & Miller, J. D. (2012). An Update to "Recent Trends in the Processing of Enargite Concentrates." *Mineral Processing and Extractive Metallurgy Review*, (2009), 121016112728008. http://doi.org/10.1080/08827508.2012.725683

Schoonen, M. A. A., Harrington, A. D., Laffers, R., & Strongin, D. R. (2010). Role of hydrogen peroxide and hydroxyl radical in pyrite oxidation by molecular oxygen. *Geochimica et Cosmochimica Acta*, *74*(17), 4971–4987. http://doi.org/10.1016/j.gca.2010.05.028

Singh, T. S., & Pant, K. K. (2004). Equilibrium, kinetics and thermodynamic studies for adsorption of As(III) on activated alumina. *Separation and Purification Technology*, *36*(2), 139–147. http://doi.org/10.1016/S1383-5866(03)00209-0

Smedley, P. L., & Kinniburgh, D. G. (2002). A review of the source, behaviour and distribution of arsenic in natural waters. *Applied Geochemistry*, *17*(5), 517–568. http://doi.org/10.1016/S0883-2927(02)00018-5

U.S. Environmental Protection Agency, T. (1992). *Toxicity Chracteristic Leaching Procedure (Method 1311)*.

Valdivieso, A. L., Bahena, J. L. R., Song, S., & Urbina, R. H. (2006). Temperature effect on the zeta potential and fluoride adsorption at the α-Al2O3/aqueous solution interface. *Journal of Colloid and Interface Science*, *298*, 1–5. http://doi.org/10.1016/j.jcis.2005.11.060

van Aswegen, P., van Niekerk, J., & Olivier, W. (2007). The BIOX ™ Process for the Treatment of Refractory. In D. E. Rawlings & D. B. Johnson (Eds.), *Biomining* (pp. 1–33). Springer Berlin Heidelberg.

van Weert, G., & Droppert, D. J. (1994). Aqueous processing of arsenic trioxide to crystalline scorodite. *JOM*, *46*(6), 36–38. http://doi.org/10.1007/BF03220716

Vaughan, D. J. (2006). Arsenic. *Elements*, *2*(2), 71–75. http://doi.org/10.2113/gselements.2.2.71

Vidic, R. D., & Suidan, M. T. (1991). Role of dissolved oxygen on the adsorptive capacity of activated carbon for synthetic and natural organic matter. *Environmental Science & Technology*, *25*(9), 1612–1618. http://doi.org/10.1021/es00021a013

Wei, Z., & Somasundaran, P. (2004). Cyclic voltammetric study of arsenic reduction and oxidation in hydrochloric acid using a Pt RDE. *Journal of Applied Electrochemistry*, *34*(2), 241–244. http://doi.org/10.1023/B:JACH.0000010005.59717.44

Yang, B., Zhang, G. L., Deng, W., & Ma, J. (2013). Review of Arsenic Pollution and Treatment Progress in Nonferrous Metallurgy Industry. *Advanced Materials Research*, *634–638*, 3239–3243. http://doi.org/10.4028/www.scientific.net/AMR.634-638.3239

Zhang, D., Yuan, Z., Wang, S., Jia, Y., & Demopoulos, G. P. (2015). Incorporation of arsenic into gypsum: Relevant to arsenic removal and immobilization process in hydrometallurgical industry. *Journal of Hazardous Materials*, *300*, 272–280. http://doi.org/10.1016/j.jhazmat.2015.07.015

Zhang, W., Singh, P., & Muir, D. M. (2000). SO2/O2 as an oxidant in hydrometallurgy. *Minerals Engineering*, *13*(13), 1319–1328.

Zhu, Y. N., Zhang, X. H., Xie, Q. L., Wang, D. Q., & Cheng, G. W. (2006). Solubility and stability of calcium arsenates at 25°C. *Water, Air, and Soil Pollution*, *169*(1–4), 221–238. http://doi.org/10.1007/s11270-006-2099-y